ASD-TDR-63-454

(UNCLASSIFIED)

LUNAR ALIGHTMENT SYSTEMS INVESTIGATION

TECHNICAL DOCUMENTARY REPORT ASD-TDR-63-454

JUNE 1963

Flight Dynamics Laboratory
Aeronautical Systems Division
Air Force Systems Command
Wright-Patterson Air Force Base, Ohio

Project No. 1369, Task No. 136903

OCT 8 1963

NOTICES

FOREWORD

The research work in this report was performed by American Machine & Foundry Company, Stamford, Connecticut, for the Flight Dynamics Laboratory, Directorate of Aeromechanics, Deputy Commander/Technology, Aeronautical Systems Division, Wright-Patterson Air Force Base, under AF Contract No. AF33(657)-8197. This research is part of a continuing effort to obtain design philosophies and techniques for reliable, minimum weight extraterrestrial launching and alighting systems for aerospace vehicles, which is part of the Air Force Systems Command's Applied Research Program 750A, the Mechanics of Flight. The Project Nr. is 1369 "Mechanical Subsystems for Aerospace Vehicles", and the Task Nr. is 136903 "Launching and Alighting Systems for Ground Contact". Mr. Wallace C. Buzzard of the Flight Dynamics Laboratory was the Project Engineer. The research was conducted from February 1962 to May 1963 by Messrs. Andrew B. Burns and James A. Plascyk.

Specific technical contributions to the work described in this report were also made by Messrs. H. T. Bossung, F. DiFlora and S. M. Levin of the American Machine and Foundry Company. Mr. Buzzard of the Flight Dynamics Laboratory made many helpful criticisms and suggestions and, in particular, contributed the material on scaling principles contained in this report.

ABSTRACT

Mission parameters are estimated for a manned lunar alight-
ment. Undercarriage concepts are developed which provide for alight-
ment on unprepared lunar surfaces and provide the necessary support
for subsequent launch from the lunar surface. A novel concept is
described which places steel honeycomb energy absorption elements at
the ends of four self-aligning strut mechanisms. The self-aligning
feature, which is applicable to any number of surface contactors, re-
sults in an alightment system whose bulk and weight are a small frac-
tion of the comparable quantities for systems using fixed undercarriages.
It has been found that the incorporation of auxiliary launch engines in the
alightment system to utilize salvaged alightment energy or chemical
fuels offers no advantage. Analytical background material is reported
and an experimental program which verified the feasibility of the self-
aligning feature is described.

PUBLICATION REVIEW

This report has been reviewed and is approved.

FOR THE DIRECTOR

T. J. BAKER
Assistant for R&T
Vehicle Equipment Division
AF Flight Dynamics Laboratory

ASD-TDR-63-454

TABLE OF CONTENTS

APPENDICES

LIST OF ILLUSTRATIONS

LIST OF TABLES

I. INTRODUCTION AND SUMMARY

1.1 SCOPE

This report presents the findings established in a concept study for lunar alightment and launch. The specific technical objectives of the program may be summarized as follows:

1) Establish alightment system concepts which provide for the alightment of manned aerospace vehicles on unprepared lunar surfaces. The undercarriage must include provisions for subsequent launch support.

2) Establish design parameters for missions which are to be undertaken subsequent to the first manned lunar alightment.

3) Conduct tests necessary to verify feasibility of unusual features of proposed alightment system configurations.

The three principal facets of a lunar alightment system are the energy absorbers which absorb the kinetic energy of the vehicle at alightment, the surface contactors which engage the lunar surface and cause the energy absorbers to be actuated, and the undercarriage structure which transmits the deceleration loads to the energy absorbers and/or the vehicle itself. These several facets of the problem were studied independently and collectively and from the results of these efforts, a preferred alightment system concept was developed. This concept is described briefly in the following paragraphs. Detailed discussion of the technical problem, including the establishment of mission parameters and stability criteria, is contained in subsequent sections of this report.

A detailed description and an evaluation of an experimental program are indicated in Section 10 of this report. A number of appendices are included which offer detailed analytical developments or incidental descriptive information.

1.2 PRINCIPAL CONCLUSIONS

1.2.1 Mission Parameters

The mission parameters established in this study are listed in Table 1. It may be expected that several years will elapse before this

Manuscript released by the authors 6 May 1963, for publication as an ASD Technical Documentary Report.

mission is finalized. In that interval, considerable advancement may be fairly anticipated in the state of knowledge of the lunar environment and of lunar alighting vehicle characteristics. Since the "efficiency" of the alightment system is of tremendous importance to a space mission, mission parameters have been established in this study on the basis of those values which will "most probably" apply at the time this mission is finalized.

In establishing the mission parameters, it has been assumed that vehicle aiming capability permits alightment in a favorable region of the moon's surface and that vehicle maneuvering capability permits the avoidance of serious local obstacles such as crevices.

1.2.2 Launch Support

It has been concluded that for this mission, no advantage is gained from the employment of non-rocket auxiliary launch engines or mechanisms which salvage alightment energy. There is also no need for hold down for lunar launch nor is there any need for carrying the alightment system with the vehicle at launch.

It has been assumed that a nominal vertical attitude of the vehicle is best for both lunar alightment and lunar launch. It has been concluded that it is far simpler and more reliable to provide that the vehicle does not upset at alightment than it is to provide means for coping with upset.

1.2.3 Preferred Alightment System Configuration

For the mission parameters established in this study, the most attractive alightment system configuration is one in which four individual Mar-Aging steel honeycomb energy absorption elements are located at the ends of a system of four self-aligning strut mechanisms which are spaced equally about the periphery of the vehicle. To each of the energy absorption elements is attached a load distributing surface contactor which contacts the lunar surface at a horizontal radius of approximately fourteen feet. Figure 15 indicates general system proportions. Each of the strut mechanisms is a parallelogram which permits the surface contactor to be axially realigned to accommodate sloping or irregular surfaces without tilting of the vehicle or unequal distribution of the alightment load among the four energy absorption elements. Each of the strut mechanisms includes a self-energizing lock mechanism which fixes the strut structure when alignment has been accomplished. Each lock is actuated by a trip line which is differentially connected to every other lock. The differential arrangement provides that all the brake trip lines go taut simultaneously

2

when the sum total of all four surface contactor displacements reaches a pre-established value. This value is sufficient to insure that all contactors engage the lunar surface under the most aggravating design conditions. Once actuated, the locks remain energized irrespective of the status of the lock trip lines. The overall weight of this alightment system is approximately two percent of the total vehicle alightment weight.

The novel feature of the preferred alightment system configuration is its self-aligning quality which provides dramatic reductions in the weight and envelope of the undercarriage. For the established mission parameters, introduction of the self-aligning quality to a fixed tripod alightment system reduces its lateral spread by a factor of 2-1/4 and its weight by a factor of 4. The self-aligning quality also affords good load distribution among any number of surface contactors, readily permitting the use of four surface contactors instead of three. For the established mission, this reduces alightment system weight by an additional factor of 2.

The physical proportions of a fixed tripod configuration and self-aligning tripod and quadripod configurations of comparable performance capabilities are indicated in Figures 13, 14, and 15, respectively. Variations on these systems and there components are discussed more fully in following sections of this report.

1.3 EXPERIMENTAL VERIFICATION

A one-twelfth scale model alightment vehicle with a self-aligning quadripod undercarriage was fabricated and subjected to drop tests on a sloping surface to verify the efficacy of the self-aligning quality. Horizontal vehicle velocity was simulated by horizontal motion of the sloping surface. The feasibility of using a self-aligning undercarriage for a lunar alightment system was confirmed by the test results.

1.4 FUTURE STUDY REQUIREMENTS

The general approach to the lunar alightment problem covered in this report has been reviewed with the objective of identifying those areas in which the need for specific study and development can be seen. Recommendations for future study are presented and discussed.

2. DESIGN CRITERIA

2.1 PHILOSOPHY

There is a strong tendency to establish criteria in accordance with the worst conceivable conditions. There is also reason to expect that by the time of the mission to which this study is directed, better information will be available in several respects, including information gained from earlier unmanned and manned lunar alightments. Since the "efficiency" of a system is of tremendous importance to a space mission, the results of this study will have maximum effectiveness if they are based on the conditions which will "most probably" apply at the time detail designs are finalized. This philosophy has been considered in establishing criteria for this study.

A number of specific design criteria have been established for this study and are summarized in Table 1.. Since the current state of the art does not permit these quantities to be established with precision, the specified values should be understood to indicate the emphasis or "focus" of attention in the study. In some instances, it is felt that the ultimate criteria may be expected at this time, to fall within a range of values wherein variation within the range can have a significant bearing on alightment system design. These ranges are indicated in the table where appropriate. Their significance is discussed in Section 9.

2.2 MISSION PARAMETERS

2.2.1 Vehicle Description

The vehicle description assumed for this study is a composite of the descriptions of manned lunar vehicles found in references 24, 26, and 35. A summary of the current manned and unmanned space vehicles that are designed or under consideration, by NASA, is presented in Table 2. By way of further confirming the plausibility of vehicle alighting weights, the calculations of Appendix XV were performed. Based on a conservative value for impulse of 200 seconds (intended to reflect the weight of the whole propulsion stage) a lunar escape vehicle could be launched from the moon surface with a total vehicle weight equal to 3.4 times the escape vehicle weight. Reference 35 indicates potential Apollo capsule weights from 15 to 30 earth tons. When the mission are compared, this range of values does not seem inconsistent with the 1-1/2 earth ton weight of the Mercury capsule. The assumed alighting weight values are based on the foregoing.

4

Table 1 Mission Parameters				
Category	Quality	Units	Nominal Values	Potential Values
Vehicle Description	Diameter	feet	20	15 to 20
	Height	feet	70	50 to 90
	C. G. Height to Overall Height Ratio	---	50	35 to 65
	Lunar Alighting Weight	earth tons	50	25 to 100
Maximum Alighting Conditions	Vertical Velocity	fps	35	
	Horizontal Velocity	fps	3. 5	
	Spin Velocity	deg/sec	1/4	
	Tilt Velocity	deg/sec	1/4	
	Tilt Magnitude	degrees	1	to 3
	Allowable Deceleration	earth g's	10	
Lunar Geology	Surface Slope	degrees	3	to 5
	Maximum Obstacle Height	feet	1	
	Surface Bearing Strength	psi	200	50 to 1000
	Dust Overlay Thickness	inches	6	0 to 12
Atmospheric Exposure	Atmospheric Pressure	earth atm's	10^{-13}	
	Solar Radiation	$BTU/hr/ft^2$	425	
	Particle Radiation	---	*	
	Electromagnetic Rad.	---	*	
	Prelaunch Exposure Time (for Launch from Earth Orbit)	earth days	14	
	Maximum Flight Exposure Time	earth days	3	
	Lunar Surface Exposure Time	earth days	14	42
* Inconsequential effect on lunar alightment system.				

Table 2 Summary of Proposed Space Vehicles		
Space Vehicle	Mission	Approximate Max. Weight - lbs.
Mercury	1 man, earth orbit	2,900
Gemini	2 man, earth orbit	6,000
Apollo A	3 man, earth orbit	35,000
Apollo B	3 man, lunar orbit	61,000
Apollo C	3 man, lunar landing	215,000
Ranger 2	Non-manned, hard lunar impact	730
Surveyor A	Non-manned, soft lunar impact	2,500
Surveyor B	Non-manned, lunar orbit	2,500
Prospector	Non-manned, soft lunar impact	2,500

There appears to be no particular reason for attempting to carry from the lunar surface the substantial weights of the fuel tanks and engines used to accomplish deceleration preparatory to lunar surface alightment. It is therefore considered probable that salvage of these items will be unnecessary and they may be used to contribute to the absorption of impact energy if practical.

2.2.2 Maximum Alighting Conditions

The maximum vertical and horizontal velocities are based on the suggestion of the ASD Project Engineer and are considered by this organization to be conservative values.

The spin and tilt velocities are conservatively estimated on the basis of the orientation stability achieved in the Mercury orbital flights as reported in reference 28 and various elements of the popular press.

Equipment fragility appears to be the deciding factor in establishing allowable deceleration rates at impact. According to references 9 and 23, the relatively small impact velocity change assumed for this study can be tolerated by humans at deceleration rates of 50 or 100 earth g's. Considering that the sustained vehicle acceleration rates for manned space flight are limited to the order of 8 earth g's gradually applied (as in the Mercury program), there is no reason, discounting impact, for designing the vehicle's equipment to withstand much more than 8 earth g's. Since 20 g design has been standard practice for aircraft equipment for some time and allowing for the fact that sudden application of a load increases its effect, the figure of 10 earth g's appears to offer a reasonable basis for peak allowable deceleration at alightment impact. It should be borne in mind that the vehicle structure and/or on-board equipment can experience momentary accelerations of up to 20 g as a result of the sudden application of a nominal 10 g decelerating load.

2.2.3 Lunar Geology

References 15, 17, and 25 deal in whole or in part with lunar geology. There are various degrees of consistency and contradiction among the sources concerning various details of the lunar geology. The values indicated in Table 1 are felt to represent a consensus of prevailing opinions and are felt to be reasonable values in the light of the missions considered in this study.

2.2.4 Atmospheric Exposure

The ratio indicated for lunar to earth atmospheric pressure represents a popular estimate (reference 17). Since a variation by a factor of 1000 either way would probably not perceptibly affect the alighting studies, there appears to be no point in refining the estimate.

The exposure duration values are more or less casual estimates since the indicated order of magnitudes had no influence on the alightment system configurations.

2.3 GENERAL DESIGN CONSIDERATIONS

2.3.1 Design Loading for Supporting Structure

The actual vertical load in the supporting structure should be expected to exceed the equivalent static deceleration load owing to the sudden application of the decelerating load and the influence of the actual mass and elasticity of the structure. This load amplification would vary from unity at the outer extremity of the supporting structure to a value conceivably as high as 2 at the inner extremity of the supporting structure. The value selected for the design load is not necessarily the best value for ultimate design purposes, but it is considered suitable for making comparisons between various alightment concepts. To account for the effects of horizontal and spin velocity of the vehicle at alightment, horizontal design loads have been established at 20 percent of vertical design load in the radial direction and 10 percent of the vertical design load in the tangential direction. In the design of an actual lunar alightment system, the dynamic loads appearing in various portions of the structure should be carefully evaluated.

The nominal design loads are illustrated graphically in Figure 1. The radial and tangential loads are assumed to act concurrently with the vertical load but not concurrently with each other.

In summary:

Vertical Load (P_V) 11 g

Radial Load (P_R) (.2)(11g)

Tangential Load (P_T) (.1)(11g)

8
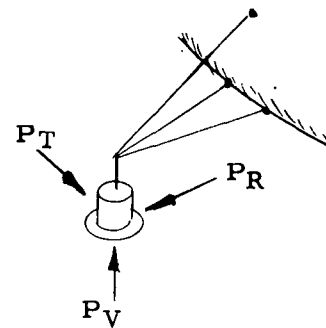
Figure 1. Strut Design Load Diagram

2.3.2 Allowable Lateral Motion

It is necessary to limit the lateral motion of the surface contactor during alightment so as not to cause excessive side forces which might significantly affect the performance of the energy absorber (see Figure 2). A nominal value of four inches has been (somewhat intuitively) selected as the limiting value for the horizontal contactor motion associated with the alignment action during alightment.
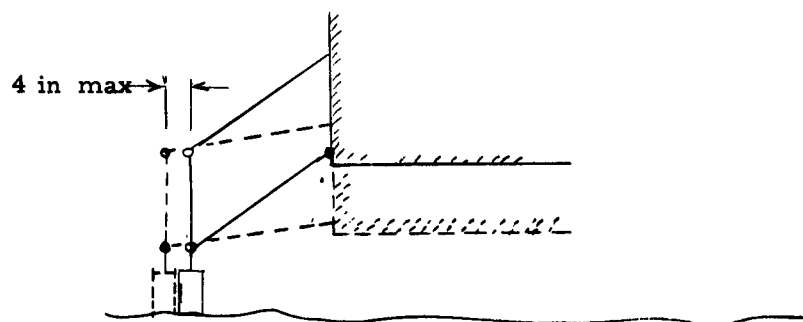
Figure 2   Allowable Lateral Contactor Motion

2.3.3 Clearance Requirements

It is necessary that the landing support system be designed so that no portion of the unit or vehicle will be damaged due to the lunar surface having a contour of a three-degree slope plus a scattering of one foot obstacles. It is assumed that for a tripod landing system, the obstacle may appear under one or two surface contactors when the vehicle alights on a three-degree slope. It is assumed that for a quadripod landing system, the obstacle may appear under one, two adjacent, or two opposite surface contactors when the vehicle alights on a three-degree slope. Figure 3 gives the required clearance profile to preclude any interference between vehicle and obstacle.
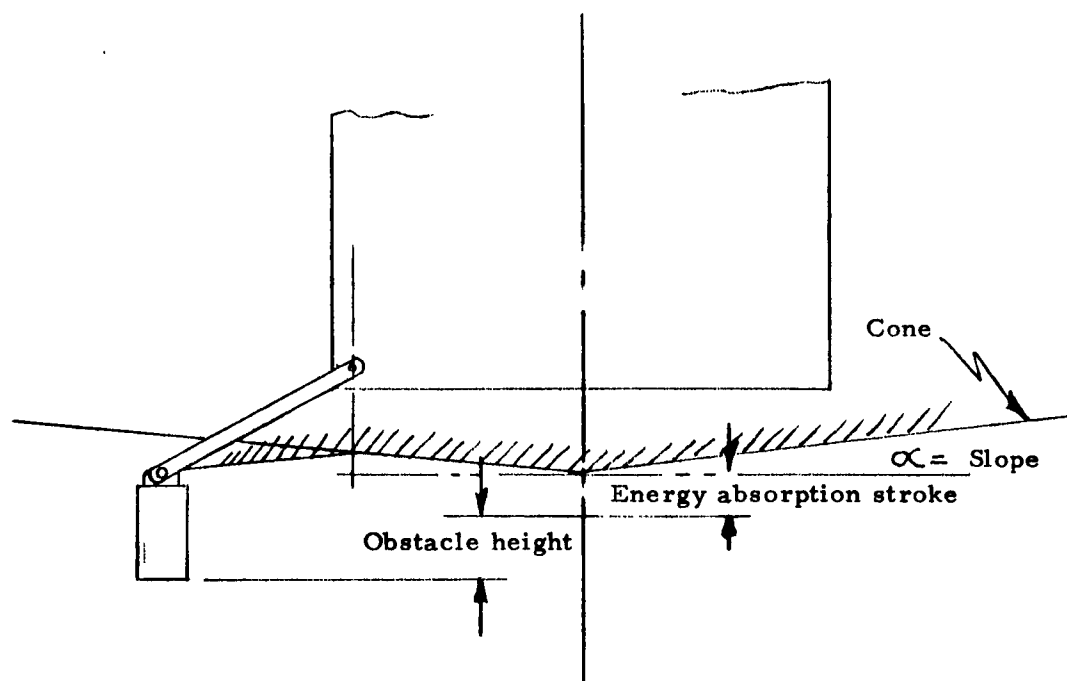
Figure 3 Clearance Profile

3. STRUCTURAL MATERIALS

Alloys of steel, aluminum, magnesium and titanium were evaluated for structural use. For this application, the strength per unit weight was considered the most important criteria. Promising alloys of each of these materials have been considered. A comparison of properties at room temperature is listed in Table 3.

Table 3. Metal Properties					
Material	Yield Strength (lb/in^2)	Modulus of Elasticity (lb/in^2)	Density (lb/in^2)	Strenght/wt Ratio $\left(\dfrac{lb/in^2}{lb/in^3}\right)$	Stiffness/wt. Ratio $\left(\dfrac{lb/in^2}{lb/in^3}\right)$
Steel (1)A 1S14130	176,000	29×10^6	0.283	6.2×10^5	102×10^6
(2) 18NiCoMo (300) Mar-Aging Steel	300,000	27.5×10^6	0.289	10.6×10^5	95.1×10^6
Aluminum - Alloy 7178	80,000	10.3×10^6	0.101	7.93×10^5	102×10^6
Magnesium - Alloy ZK 60 A	38,000	6.5×10^6	0.0659	5.78×10^5	98.7×10^6
Titanium - Alloy 99 Ti	70,000	15.5×10^6	0.164	4.27×10^5	94.5×10^6

The above table shows the comparison of two basic properties, the strength and elasticity. These two quantities are not the only considerations but will serve to show which materials can be discounted with a minimum consideration. For this application, these two properties are of prime importance. The two most applicable materials from these considerations can be seen to be the 18 NiCoMo(300) and Aluminum Alloy 7178. The steel shows the greatest strength-to-weight value and the aluminum is stiffer for a given weight. This particular steel has low ductility, but by proper heat treating and adjusting of the alloys, a more ductile material can be achieved at the expense of some loss in strength.

Since compression members tend to be the heavier members of a structure, and since the stiffness of a material is more significant than strength in determining the size of long compression members, Aluminum Alloy 7178 has been selected as the basis for establishing weight comparisons of the various structural configurations. It is probable that some benefit could be obtained with hybrid designs which, for tension and short compression members, exploit the more favorable strength to weight ratio of steel. The Maraging Steel has been selected for consideration in such items as the surface contactor, where strength is more critical.

The yield stress values discussed above must be modified to account for environmental temperature extremes and for variations in raw material production. The value reported for the aluminum alloy was obtained from MIL-HDBK-5, March 1959, which indicates that this value for yield stress will be met or exceeded by 90 per cent of the material supplied by the producers as a result of statistical studies conducted over a period of time. For this type of program where cost is not the prime consideration, it is felt that selective testing could produce even stronger samples but certainly a 90 per cent guarantee would require little testing to obtain a sample at least as strong as the tabulated value.

The temperature consideration will depend upon the evaluation of the radiation heat transfer to or from the components in question while operating near the surface of the moon. This is a complex problem depending on the solar heat flux, the surface radiating properties of the materials in question and the shape factor of the unit in question. It is felt that the reflecting characteristics of the vehicle, being primarily clean metallic surfaces, will be the same or better than that of the moon in regard to the infrared spectrum. Therefore, there is little reason to suspect that the vehicle will experience greater temperatures than the lunar surface which is known to be no greater than +260°F. Since the strength of the material increases at lower temperatures, the lower extreme of -240°F will not be a problem.

It is not anticipated that there will be any difficulty with the rocket exhaust. The assumption is that the system will be designed so that there will be no direct impingement of the jet on the landing system components. The radiative heat transfer to the alightment system will also be insignificant due to the small temperature difference which will probably exist between the structure and the exhaust gases. If the maximum temperature of the structure were assumed to be that of the lunar surface, or +260°F, and if isentropic flow of the exhaust gases through the nozzle occurred, then the exhaust gases issuing from the nozzle exit would be at the same temperature (260°F) at a mach number of approximately 6.0. The combustion chamber total temperature was assumed to be at about 5000°F from information available in reference 14. The exit Mach number for rockets designed for lunar

landings is anticipated to be above Mach 10, for which the exhaust gas temperature would be less than the estimated maximum structure temperature. Further, the emissivity of the exhaust gases will be very low since only the water vapor and incandescent particles will act as sources of radiant energy.

Therefore, it is not expected that the temperature of the material will rise appreciably above 260°F. A value of 300°F will be assumed for safety. At this temperature, the aluminum alloy selected experiences a reduction of 22 per cent which reduces the allowable strength to 62,500 psi. A rounded-off value of 60,000 psi has been selected as a tensile strength design criteria for this study. A stress value equal to 60 per cent of the yield strength has been selected for shear strength.

The Mar-Aging steel exhibits low ductility and it was considered desirable to derate the yield strength appreciably to allow for this effect in addition to the temperature effect. It was felt that a value of 175,000 psi would be safe for design purposes. The shear strength of this material was considered to be 60 per cent of the yield which results in an allowable shear stress of 105,000 psi.

The high strength aluminum alloys (such as 7178) are difficult or impossible to weld and hence the structure will have to joined by other means. If welding were necessary, a weldable material could be bolted to the high strength material. The aluminum alloys which can be welded are of much lower strength.

The Mar-Aging steels seem to offer no appreciable problems associated with welding. A controlled environment and care must be taken when welding but success has been achieved with this method of fabrication.

Sublimation is not a significant factor in any of the material selections discussed above since the duration of exposure and operating temperatures established in the design criteria are not extreme in this respect.

4. ENERGY ABSORBERS

4.1 SUMMARY AND CONCLUSIONS

The most attractive energy absorption medium evaluated in this study is a nickel alloy steel honeycomb structure. This medium which absorbs energy in axial compression, has a specific energy capacity in the order of 25,000 ft-lb/lb, comparable to that of the lightest energy absorption devices developed to date. It has excellent force uniformity with efficiencies (ratio of average to peak force) in excess of 90% attainable. Its flexible form and compact size permit the energy absorption elements to be directly mounted on the outer extremities of the under-carriage structure eliminating the need for mechanisms to transmit loads to remote energy absorption elements.

Nominal characteristics of a number of potential energy absorption media are listed in Table 4. The specific energy capacities for simple metal bars are based on commonly published values for ultimate strength and elongation at rupture and are listed primarily for reference. In a typical test specimen, "failure" occurs when a localized region of the material suffers gross strain (necks down), but most of the material has been subjected to only moderate strain when "disconnected" as a result of rupture. Mechanisms which permit the introduction of a gross strain in a large proportion of a metal element before rupture disables the energy absorption action, permit substantial improvements over the specific energy capacities of simple metal bars. The hexagonal cell honeycomb structure is an example of such a mechanism. Another example of such a mechanism is the "Invertube", which absorbs energy by turning a metal tube inside out. Specific energy capacities of 14,000 ft-lb/lb have been experimentally obtained with mild steel.

An alternate approach to increasing the specific energy capacity of metal is the "frangible tube" in which a metal tube is forced over an expending mandrel to successively cause rupture of short axial sections of the tube. Specific energy capacities of up to 30,000 ft-lb/lb are claimed for this device.

Relationships for evaluating the proportions of bulk energy absorption media (including honeycomb structures) required to attain specific performance characteristics are developed in Appendix V.

It has been found that for the high capacity absorbers, the weight of

14

			Table 4.	Characteristics of Potential Energy Absorbers			
Member	Material	Manner of Loading	Efficiency $\frac{ft\text{-}lb}{lb}$	Efficiency $\frac{ft\text{-}lb}{ft^3}$	Usable Stroke % of Total Length	% Rebound	References
Bar	Steel (ASTM A7)	Tension or Compression	2700		20	Neglig.	Appendix III
Bar	Aluminum (2024)	Tension or Compression	3200		15	Neglig.	Appendix III
Cylindrical Shell	Aluminum (2024 T-3)	Compression parallel to axis. Deflects by local buckling.	3000		80	Neglig.	7
Invertube	Aluminum (3003)	Compression parallel to axis. Deflects by turning inside-out.	10,000		To 200 (Not counting mandrel)	Neglig.	19
Invertube	Steel	Compression parallel to axis. Deflects by turning inside-out.	14,000		To 200 (Not counting mandrel)	Neglig.	19
Cylindrical Shell and Trapped Air	Aluminum (2024 T-3)	Compression parellel to axis. Deflects by local buckling.	10,000		80	Neglig.	7
Cylindrical Shell and Trapped Helium	Aluminum (2024 T-3)	Compression parallel to axis. Deflects by local buckling.	13,700		80	Neglig.	7
Frangible Tube	Steel	Compression	30,000		100	Neglig.	10
Honeycomb	Alum. (Hexcel 4 Mil 5052)	Compression parallel to cell.	11,000	88,000	75	Neglig.	7, 22
Honeycomb	Steel	Compression parallel to cell axes.	25,000 to 30,000		80	Neglig.	22
Honeycomb	Paper	Compression	3500		70	8	34
Air Bag (Vertical Cylinder)	Fabric Bag	Compression parallel to cylinder axis.	7900			Large unless bleed is used to deflate.	7
Block	Balsa	Compression parallel to grain.	24,000	144,000	80	Neglig.	8
Block	Styrofoam T-22	Compression	2500	3750	60	35	8, 34
Block	Styrofoam HD-2	Compression	4000	18,000	50	24	8, 34
Hydraulic Cylinder		Compression or Tension	3000		Less than 50 (comp)	Neglig.	Appendix VI
Coulomb Friction Type	Aluminum	Various	37,000			Neglig.	Appendix IV
Coulomb Friction Type	Steel	Various	44,000			Neglig.	Appendix IV

15

the actual energy absorption element constitutes a small part of the total alightment system weight and other qualities of the absorption media assume correspondingly increased significance.

Various aspects of potential energy absorber types are discussed in the following paragraphs.

4.2 MAR-AGING STEEL HONEYCOMB

4.2.1 General Performance Characteristics

Hexagonal cell, honeycomb structure has been found to be attractive as an energy abosrber when subjected to axial compression. The findings reported here are primarily those established during the course of a program being conducted at Jet Propulsion Laboratory (JPL), Pasadena, California. This study has dealt in general with the performance of metal energy absorbers in the space environment. A number of types were surveyed and particular attention was then given to the development of metal honeycombs which were found to have attractive characteristics. The results of an early portion of the program were covered in Reference 22. Subsequent efforts have not yet been covered in published reports. The related information reported herein has been obtained in communication with Mr. Russell McFarland who is associated with the JPL program. The principal relevant findings of the study are discussed in the following paragraphs.

a) A theoretical approach to the evaluation of the compression characteristics of metal honeycombs was established (Reference 22). Aluminum honeycomb data collected by several agencies was reviewed and generally supported the theoretical approach.

b) A Mar-Aging steel (A-L 18 NiCoMo (300) by Allegheny Ludlum Steel Corporation) was evaluated both theoretically and empirically and found to be particularly attractive. This material has a tension yield strength of 258, 000 psi and an elongation of 3 to 4 percent. Honeycombs of the Mar-Aged steel have been found to have specific energy absorption capacities of 24 to 27 thousand ft-lb/lb, based on compressions of 75 or 80 percent. JPL has tested specimens to this degree statically and has conducted dynamic tests with compressions up to 30 percent.

c) Titanium and Aluminum alloys have been considered for the honeycomb structure. Titanium was found to be unsatisfactory because of its poor ability to carry "biaxial" stress and aluminum alloys have a limited

specific energy capacity in the order of 10,000 ft-lb/lb.

d) The highest specific energy capacity for a hexagonal cell structure is obtained with a value of 0.030 to 0.033 for the ratio of cell wall thickness to the dimension across the flats of the hexagon. The influence of this ratio is discussed in some detail in reference 22.

e) JPL used 3/4 inch "diameter" cells and welded construction in their empirical program. Bonded construction, which is suitable for some aluminum configurations, is not strong enough to permit full utilization of the extra shear strength of steel.

f) Honeycombs formed of round tube arrays offer ten to fifteen percent better specific energy capacity than the hexagonal configuration but it is felt that the fabrication problems with the tube arrays are much more involved and that category has not been given much attention.

g) With the exception of an initial spike the deflection force is very uniform. Further, the force compression history is essentially unaffected by removal of the compression force and since the "spike" energy is considerably less than the 5% of the total energy capacity of a specimen, the spike effect can be readily removed by slight precompression of the core, providing subsequent energy absorption at very high efficiency, estimated to be well over 90 percent. Rebound energy is not more than a few percent of the energy capacity.

h) For direct axial loading, aspect ratios (height to diameter) for honeycomb cores can be as high as ten to one without introducing buckling problems. Consideration of observations reported in a Radioplane test program (reference 14) suggest that aspect ratios as much as 2 could be utilized for the established design problem without having the vertical energy absorption characteristics seriously affected by lateral loads. Further study in this area would be particularly desirably, but it should be noted that the recommended absorber configuration readily permits the incorporation of independent lateral restraints.

i) It is felt that honeycomb core sections should be at least four cells wide in any direction to insure that the effect of unsupported cell walls does not serious affect the performance of the honeycomb.

4.2.2 Preferred Honeycomb Absorber Configuration

Two basic alightment system configurations have been established

in this study; the tripod and the quadripod (see Section 7). A honeycomb energy absorption element design has been established for each of these. The principal difference between the two designs is that the capacity of the tripod element is one-third the vehicle's alightment energy while the capacity of the quadripod element is only one-fourth that energy.

Circular cross sections with vertical axes have been chosen for the absorber elements since the symmetry of that shape offers equal resistance to lateral loading from any direction.

Values for the stroke, height and total area of the energy absorber elements have been established in Appendix V. Appropriate proportions and material choice for tubular arrays of hexagonal cell honeycombs are indicated in Figure 4 and Table 5 for both the tripod element and the quadripod element.

Table 5. Energy Absorber Proportions			
Quantity	Units	Tripod	Quadripod
Outer diameter	in.	18	18
Inner diameter	in.	10.0	12.5
Cross-sectional area	in.^{2}	175	132
Length	in.	32	32
Minor cell diameter	in.	0.5	0.5
Thickness parameter, t/s	---	0.013	0.013
Thickness of cell wall	in.	0.0065	0.0065
Weight	lb.	55	42
Energy Capacity	ft.lb.	644,000	482,000
Crushing pressure	psi	1710	1710

Fabrication of the honeycomb core in a 32-inch length may pose certain problems, owing to the fact that welded construction is indicated and the half-inch cell diameter seriously limits the proportions of the structure which supports the welding electrodes. However, it is completely feasible to fabricate the honeycomb core in shorter lengths which can be stacked and bonded to form

18

1/2"

Axial Length 32"

0.0065" Mar-Aging Steel

Tensile Yield $\approx$ 250,000 psi

5.0"

←Tripod
configuration
(approx. crushing
force = 300,000 lb.)

Quadripod configuration
(approx. crushing
force = 230,000 lb.)

6.2"

9"
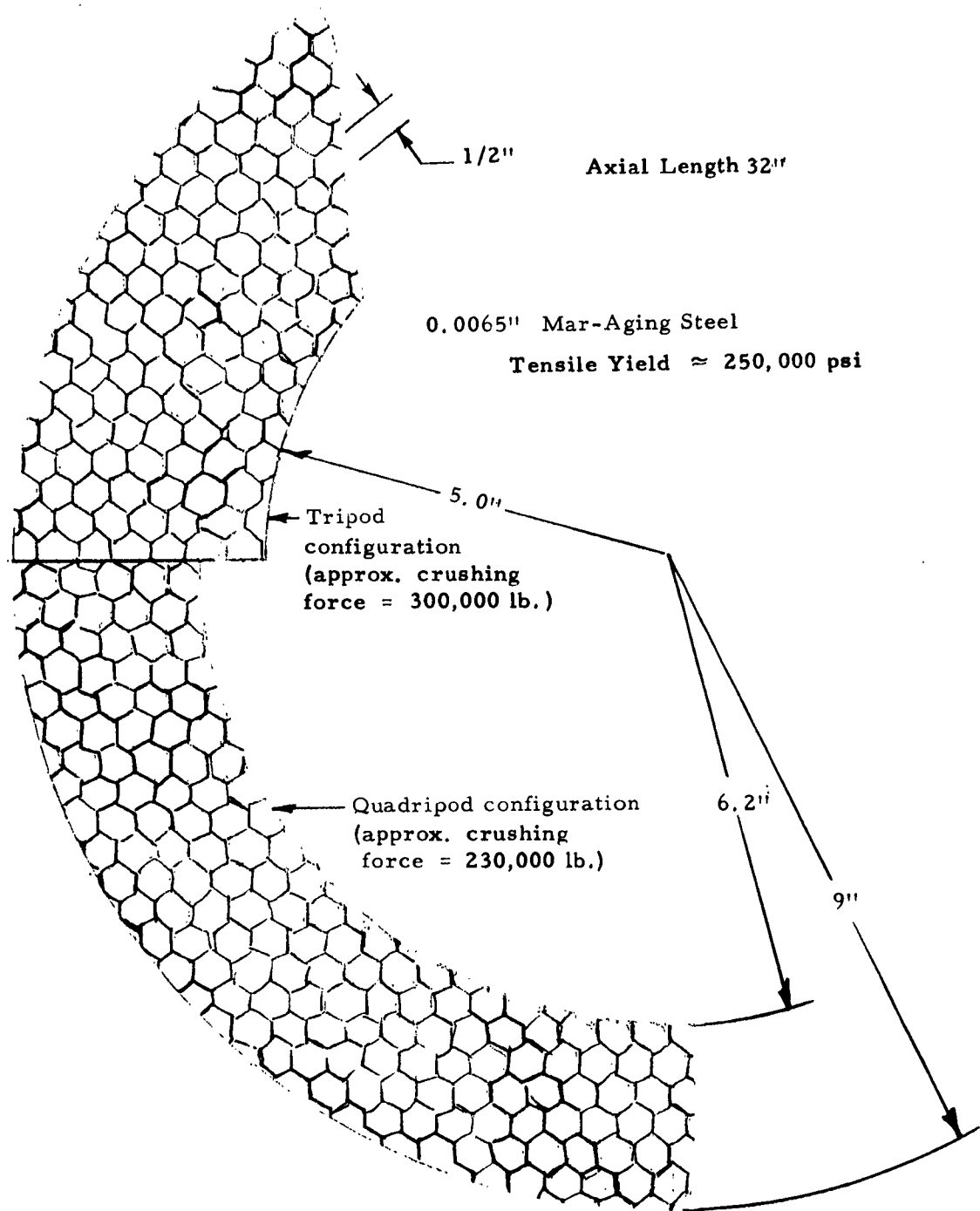
Figure 4. Cross Section of Honeycomb Absorber

a longer section. Potential methods for achieving the tubular shape for the honeycomb core include the following:

1) Bending a flat slab of the required thickness into a tubular shape.

2) Forming a core of concentric arrays of cells whose diameter varies with radius.

3) Cutting a tubular section from a conventional rectangular section.

4) Approximating a tubular shape with a polygon formed of several straight sections of conventional core construction.

If the unit was bent from a flat slab, there would be induced in the structure bending stresses which might affect its performance. Some testing would have to be conducted to assess this effect.

Restrictions on lunar surface contact pressure required the use of a relatively large surface contact area as discussed in Section 5. Increasing the area of the energy absorption element can facilitate the design of surface contactors. The specific energy capacity and the required cross-sectional area of a honeycomb absorber element are both dependent upon the ratio of cell wall thickness to cell diameter, and the optimum ratio for one quality is not necessarily the optimum ratio for the other. For the ultimate application the design of the energy absorption element and the lunar surface contactor should be treated as a single problem with the proportions of the two elements being optimized on an integrated basis.

4.3   ALTERNATE ENERGY ABSORPTION SCHEMES

The energy absorption arrangement emphasized in this study is a direct acting type with the unit located at the extremities of the strut. Alternate schemes are also available whereby the absorber is located in a region remote from the surface contactor.

The advantages of such a remote acting system are:

1) The direction of force application can be controlled accurately.

2) The stroke applied to the energy absorber can be altered compared to that applied to the vehicle.

3) The energy absorber can be used in tension as well as compression.

4) The absorber can be used as a component of the alignment system (see Section 7) thereby effecting a weight savings due to the absorber's serving a dual purpose.

The main disadvantage associated with the use of a remote system is the requirement for a mechanism to transmit the deceleration load to the energy absorption element. In the case of the self-aligning quadripod configuration described in Section 7, remote actuation of the energy absorber would require that the alignment stroke be doubled.

4.4 BALSA

The information available on balsa (Reference 38) has indicated values for specific energy capacity ranging from 16,000 to 24,000 ft-lb/lb. Weights used in the evaluation of these capacities did not include the material necessary for lateral support. The balsa has a tendency to split or splinter when crushed without this lateral support. Consequently, the values reported are more than likely higher than readily obtainable. More accurate testing would be desirable to determine the true range of capacities. The density of the balsa is in the same order of magnitude as the steel honeycomb and hence there would be a similar necessity of a surface contactor to distribute the load. In order to minimize the possibility of buckling, the absorber would probably have to be tubular. This would then necessitate the addition of support around the inside and outside surfaces. This would increase the weight of the absorber over that of the solid unit and consequently the specific energy capacity will further drop.

4.5 INVERTUBE

The Invertube is an energy absorption device which offers controlled straining of each element of its material under the application of an axial force to the tube. The rolling action of the tube during the energy absorption stroke causes a flexure of each element of the tube into and out of the roll in addition to a circumferential strain of the element due to an increase in the diameter of the tube as the roll action occurs (see Figure 5).
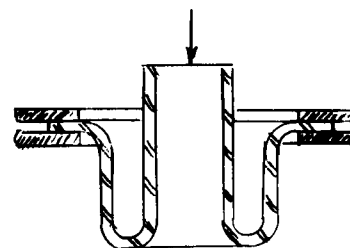
Figure 5. Invertube

The results of an empirical evaluation of this device are reported in reference 19, by Mr. C. K. Kroell of the Research Laboratories of the General Motors Corp., Warren, Mich.

By evaluating the energy under the curve of Figure 4 of reference 19, the specific energy capacity of an aluminum tube was found to be about 9,000 ft-lb/lb. Values of 14,000 ft-lb/lb have been achieved with mild steel. The following additional points to the Invertube development program were established in communication with Mr. Kroell:

a) Difficulty was encountered when stainless steel and copper were used for the tube. The tube could not be rolled and it is speculated that the lack of ductility is responsible in the case of stainless and a work hardening condition in the case of copper:

b) The alignment of the vertical load is very critical since as much as 5° offset could destroy the rolling mechanism and cause failure. Mr. Kroell utilized à loading member supported by an Oilite bearing to provide alignment.

c) The weight of the pusher tube must be considered when evaluating energy capacity. The weight of the clamping attachment must also be considered. This weight can be minimized by welding the tube to the existing structure, which has proven quite satisfactory during test.

d) The roll radius of the tube depends on the material and dimensions of the tube and is little affected by the manner of clamping.

e) The Invertube provides excellent control of the deceleration forces since it has a relatively flat force-deflection curve as opposed to the spikes exhibited in the force-deflection curves of tubes which collapse because of a buckling failure.

4.6   COULOMB FRICTION

The feasibility of utilizing coulomb friction to absorb impact energy was investigated. Relatively high specific energy capacities can be realized with this type mechanism but it has poor force efficiency (see Section 10.4.3) and in uncontrolled environments its performance characteristics are much less predictable than those of deformable metallic types. There is almost no information in the literature concerning the variation of friction coefficients with velocity and with the external temperature and vacuum conditions encountered in the lunar environment.

22

Further, the specific energy capacities established in this study are ideal values which do not reflect the weight of supporting and actuating elements.

The specific energy capacity values listed in Table 4 for coulomb friction are based on the assumption of a multiple disc energy absorber in which discs are stacked axially and alternately keyed to a stator and a rotor. The discs are considered to act as a heat sink which attains an almost uniform temperature distribution. The calculations, with pertinent assumptions, are presented in Appendix IV.

4.7 ALTERNATE ENERGY ABSORPTION MEDIA

Other energy absorption materials and devices covered in this investigation are listed below:

1) Frangible tube

2) Crushable tube

3) U-Mount

4) Hydraulic cylinder

5) Fabric air bag

With the exception of the frangible tube, the specific energy capacity of these devices are relatively low and offer little competition to the steel honeycomb.

Reference 13, a survey of energy absorption devices for space applications published in December, 1961, refers to a study in which a frangible tube system appreciably outweighed an aluminum honeycomb of comparable performance, and specific energy capacity values for aluminum honeycomb are generally reported not more than 11,000 ft-lb/lb. Reference 10 reports, however, that the results of unpublished work have indicated capacities in the order of 30,000 ft-lb/lb for frangible tube systems. This value is approximately 20 percent better than the values attainable with steel honeycomb but for the established design criteria, the resulting weight advantage is not more than 15 pounds for the whole system. In addition, there is a good possibility that this weight advantage would be lost in the surface contactor design. There is also the danger of shrapnel from the tube piercing components on the underside of the vehicle. In view

of these considerations, and the lack of readily available information, evaluation of this type energy absorber was not pursued further in this study.

The cylindrical shell derives its energy absorbing capability from a buckling failure of the walls. The specific energy capacity of this device is relatively small, about 3000 ft-lb/lb for aluminum, and further, the force deflection curve is irregular exhibiting a repetitive spike pattern. An increase in the capacity of this device can be effected by trapping a gas in the cylinder. The reliability of such a device would be low due to the possibility of puncture by a meteorite and the resultant loss in capability of the system to effect a safe landing.

The U-mount is basically a bar of metal bent in half. This is a simple device which has been successfully used for shock mitigation where weight has not been of prime concern. Since this device behaves in a manner similar to a cantilever beam, only a portion of the material would be strained plastically. It is doubtful, therefore, whether the energy capacity would be anywhere near that of the steel honeycomb or the frangible tube. The elastic characteristics of U-mounts are discussed in references 4 and 5.

Hydraulic cylinders were given particular attention in this study in connection with an evaluation of their use as auxiliary engines which would assist the vehicle's main engines for launch from the lunar surface. Even with the advantage of having a dual function, they were found to compare unfavorably with other available types of energy absorbers. They are discussed in further detail in Section 8.

Fabric air bags have capacities of from 7000 to 8000 ft-lb/lb if properly designed but would have considerable rebound and an undesirable force deflection curve unless bleed is used. In order to obtain a constant deceleration rate it would be necessary to incorporate a constant pressure bleed which requires the use of a variable area orifice. Such design complexities tend to reduce reliability and increase weight. The air bag offers little lateral stability which would leave a need for incorporating additional structure to react the effects of horizontal velocity. The danger of puncture, either by meteorites or sharp objects on the lunar surface, is a factor which would also tend to reduce reliability. There is one advantage, not pertinent to the mission of the vehicle under study, and that is the ability of the air bag to be stowed in a small package. Another advantage would be a reduction in weight due to elimination of the surface contactor. If the air bag could be designed to have a footprint of sufficient area to keep contact pressures low and with sufficient lateral stability, either inherent

24

or by utilization of supporting structure, and be lighter than the combination of absorber and surface contactor presently recommended, then of course the air bag would be desirable. Presently, though, there is not sufficient evidence nor information available to support the choice of such a design in this study. The calculation of Appendix II shows that the specific energy capacity of air itself is potentially very high, It can be concluded therefore, that the bulk of the weight of a fabric air bag energy absorber is accounted ior by the bag and associated mechanism and structure.

5. SURFACE CONTACTOR

5.1 SUMMARY

A large lunar surface contact area is indicated by the low bearing strength specification indicated in Section 2. The structure required to transmit the load from the lunar surface to the relatively small area of the recommended steel honeycomb energy absorption element outweighs that element by several times and efficient surface contactor design accordingly has a substantial influence on the overall success of a complete alightment system. The quadripod and tripod concepts require individual surface contactor diameters of 42 and 48 inches respectively.

Similar contactor designs have been established for both the quadripod and tripod concepts and are indicated in Figure 6. The design is based on the use of Mar-Aging, nickel Alloy Steel derated from a nominal Tensile yield strength of 250,000 psi to a working value of 175,000 psi to account for the effects of the extreme temperature environment. The designs are felt to represent practical possibilities but are not necessarily optimum in weight. The contactors are specifically designed to accommodate the preferred steel honeycomb energy absorbers.

5.2 DESIGN CRITERIA

The basic shape of the surface contactor is circular (see Figure 6) to provide equal strength in all radial directions to resist loads which may be applied from any lateral direction. The vertical load is applied over an area smaller than that of the contactor and an appreciable bending moment is induced in the circular plate. A relatively thick heavy plate would be required to resist the bending loads and therefore a much thinner plate was designed and reinforced with ribs. The portion of the surface contactor immediately beneath the absorber was made thicker than the portion extending beyond the absorber to resist the higher pressures. The thinner outside plate served as the lower flange of the rib and an upper flange was added which resisted the bending loads caused by the landing pressure from the lunar surface. A relatively thin web was designed to resist shear loads in the rib. The ribs were made triangular in shape which eliminated inactive material in the regions where the shear loads and bending moments were small.

In order to resist the shear and bending loads, the ribs were backed-up by a central tube topped off by a rim thicker than the walls. The thinner tube wall serves to react the shear from the ribs and the thicker rim reacts

FOR QUADRIPOD CONCEPT

MAR-AGED STEEL
HONEYCOMB

18"

12.5"

HT. OF ENERGY
ABSORBER
36"

1/16 SUPPORT TUBE

21/32

1/4

7

1/16

42

3/16

SECT AA
2:1 Scale

1/16

1/32

1 1/2" (16 RIBS)

1"

SCALE 1:16
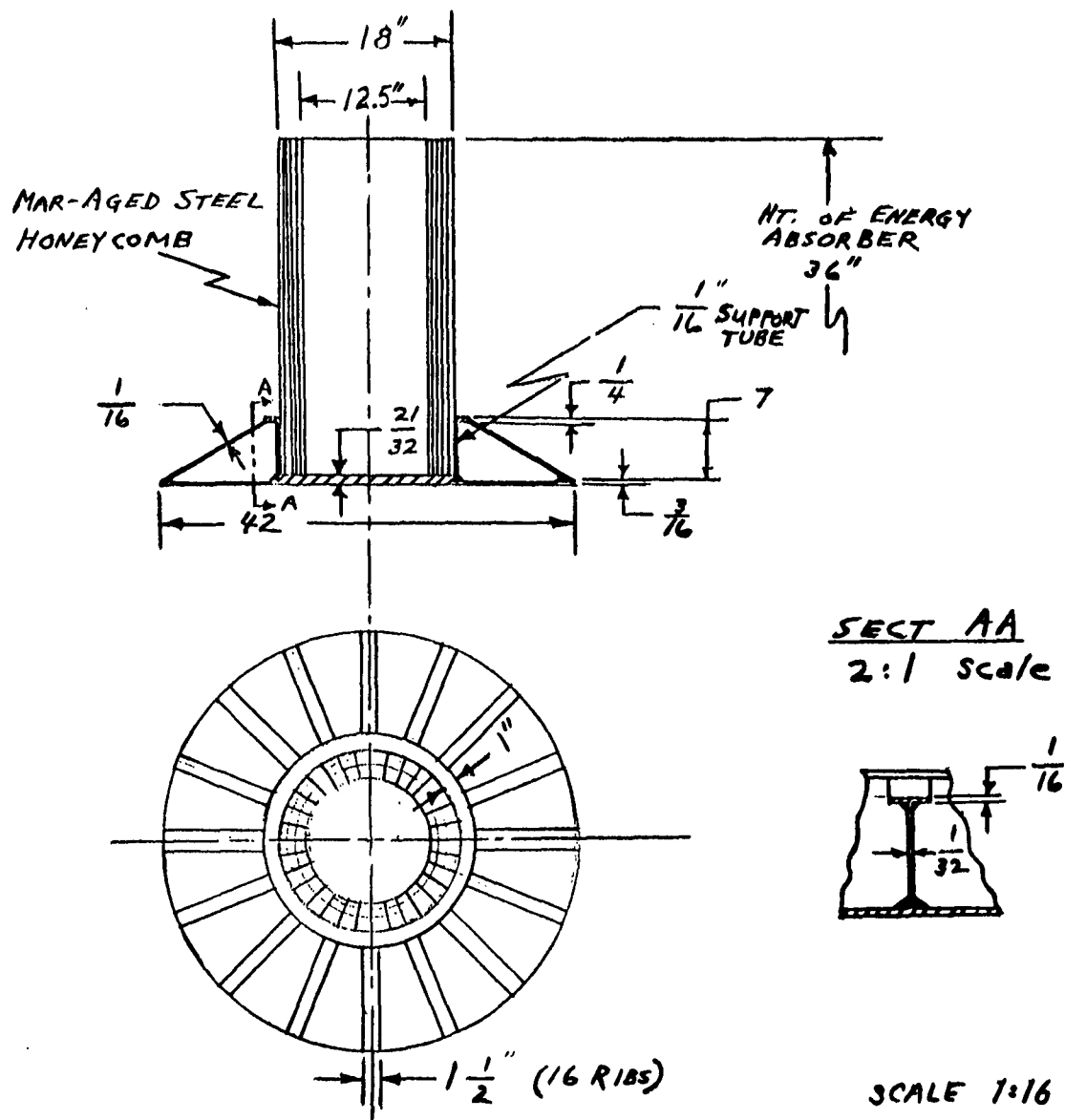
FOR TRIPOD CONCEPT: Same as for quadripod concept except:
Bottom Plate - 48 in O. D. by 5/16 in and 29/32 in thicknesses.
Energy Absorber bore - 10.0 in.

Figure 6. Surface Contactor Design

27

the compressive loads from the upper flange of the ribs. Dimensions for both the tripod and quadripod configuration are indicated in Figure 6. Details of the stress analysis for this design are presented in Appendix VIII.

There is also required a means of attaching the absorber and surface contactor assembly to the vehicle and to provide a structure to transmit the load into the supporting structure. An end cap has been designed for this function. It consists of a solid circular plate, the same diameter as the O. D. of the absorber (18") and approximately half the thickness of the central bottom plate of the surface contactor. In order to reduce weight the plate is ribbed in much the same manner as the surface contactor. The ribs are attached to the square strut protruding down from the supporting structure at the central portion of the cap. A circular hub protrudes down from the bottom of the cap into the absorber bore. This hub, which is a short ring, serves to stiffen the cap and also positions the cap laterally on the top of the absorber. There are several means of attaching the cap to the absorber to secure the absorber-surface contactor assembly to the vehicle. Since the forces acting to pull the assembly from the cap will be only the weight of the assembly plus the deceleration caused by the retrorockets, it is not anticipated that the attachment will have to be very substantial. Bonding the cap to the honeycomb would more than likely suffice. There are other possibilities available such as welding, or tying the cap to the surface contactor by cables which of course would become slack upon compression.

A weight optimization study of the surface contactor design was made but due to the limited time available, a complete optimization study could not be accomplished. Since the surface contactor comprises approximately one quarter of the total system weight, it is felt that further significant weight savings could be achieved by a more rigorous optimization study.

28

6. STABILITY CRITERIA

6.1 SUMMARY AND CONCLUSIONS

Of the several mission parameters established in Section 2, four have a direct and significant effect on the disposition of the vehicle to upset at lunar touchdown. They are the horizontal velocity and tilt magnitude of the vehicle at touchdown and the slope magnitude and presence of obstacles on the lunar touchdown surface. Stability analyses have been established which reflect these parameters and which form the basis for establishing the horizontal undercarriage "reach" dimensions considered in this study. Reach is defined as the minimum horizontal distance from the center of the vehicle to the straight line connecting two adjacent surface contactors. The analyses, which cover both fixed and self-aligning undercarriages (see Section 7), are developed in Appendix IX. The minimum reach for the fixed tripod and quadripod configurations has been found to be 22 and 18 feet, respectively. For self-aligning undercarriages, the required value of reach is essentially independent of the number of surface contactors and has been found to be 9.7 feet.

6.2 BASIC STABILITY CRITERIA

A vehicle cannot be driven to upset during a lunar alightment action if the potential energy level of the vehicle at incipient upset exceeds the total (kinetic and potential) energy of the vehicle at any time prior to upset. This principal has been exploited to establish the minimum horizontal reach required to preclude upset in the established lunar alightment mission. Specifically, the reach of the vehicle must provide that its center of mass is lifted a discreet distance against a local gravity field as a result of any tipping action occurring during a lunar alightment. The total lift distance, from initial contact status to incipient upset status, must result in an increase in potential energy of the vehicle equal to or greater than the horizontal kinetic energy of the vehicle at touchdown. The potential C. G. lift distance of a vehicle with rigid undercarriage alighting on a level surface is illustrated in Figure 7.

6.3 DEVELOPMENT OF SELF-ALIGNING UNDERCARRIAGE CONCEPT

As a vehicle with a rigid undercarriage alights, with a vertical attitude, on a non-level surface, the first motion which ensues after the initial contact results in a net downward motion of the C. G. as the vehicle pivots about the surface contactor (s) which first engaged the lunar surface. This action
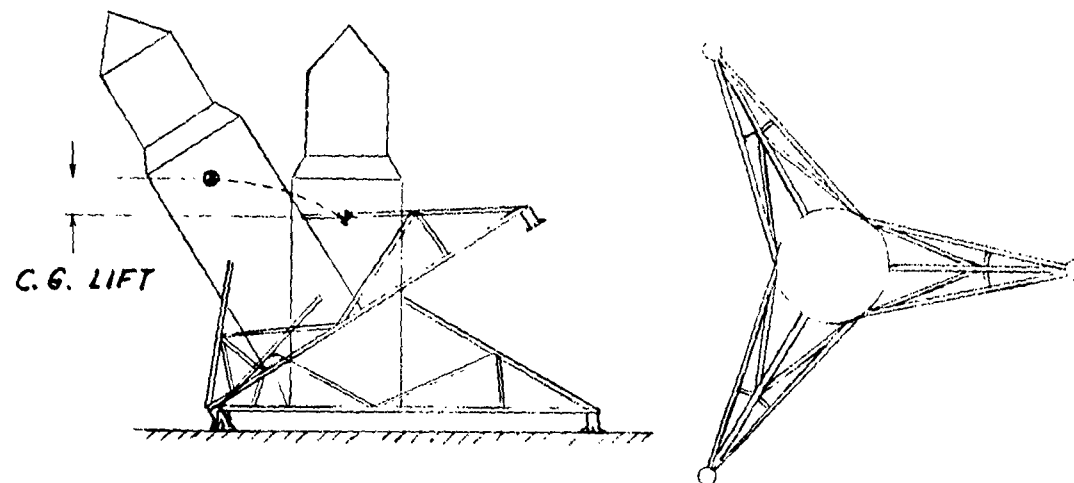
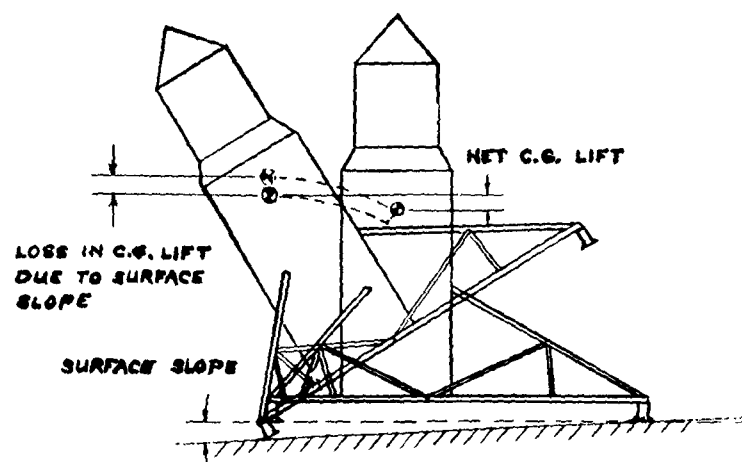Figure 7. C. G. Lift During Upset on Level Surface

Figure 8. C. G. Lift During Upset on Non-Level Surface

reduces the net C. G. lift distance as illustrated in Figure 8. This effect of the surface slope can be neutralized if the surface contactors are allowed to align with the lunar surface before energy absorption commences as illustrated in Figure 9.

A potential mechanism which could serve as an alignable supporting structure is the parallelogram linkage illustrated in Figure 10. Each surface contactor would be supported on such a mechanism which is equipped with a telescoping diagonal which can be locked to render the structure rigid when surface alignment has been accomplished. A familiar example of an effective self-energizing lock is the common military belt buckle pictured in Figure 11. The two ends of the belt correspond to the two elements of a telescoping diagonal of the type illustrated in Figures 31 and 32. If the telescoping diagonal is so oriented that the "buckle end" is the outer element, axial motion of the surface contactor is directly related to motion of the locking pin relative to the vehicle. If the several locking pins are "differentially" connected by a single continuous trip line (see Figure 12) which, in the approach status, has a fixed amount of slack, the sum of the several lock motions, relative to the vehicle, will be specifically limited by the amount of the trip line slack, although the relative motions of the individual locks are independent of each other. Accordingly, the several surface contactors in such an alightment system can be aligned with complete independence of each other with the exception that the sum of the several contactor motions is approximately a constant. When that total motion has been accomplished in an alightment action, the slack will be eliminated from the trip line and all the locking pins will be simultaneously actuated, causing the entire surface contactor supporting structure to be locked in the position which accomodates the slope and irregularities of the alightment surface. No alightment loads are felt in the trip line, since the locks are self-energizing.

Several variations of the self-energizing lock concept are indicated in Figure 16. Mechanical principles pertinent to two types of self-energizing locks are developed in Appendix XII.

The fixed tripod undercarriage proportions required to prevent upset for the established mission parameters are indicated in Figure 13. Figure 14 illustrates the dramatic reduction in undercarriage proportions provided for the same mission parameters by the incorporation of the self-aligning feature described in these paragraphs.

It may be noted that while the load distribution qualities of the tripod configuration have special merit for rigid undercarriage systems, the

31

SURFACE
SLOPE

INITIAL CONTACT STATUS

ALIGNED STATUS
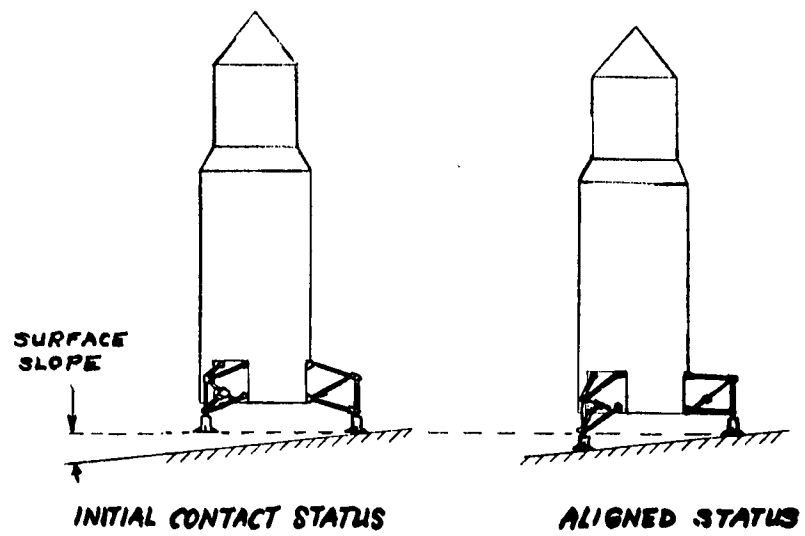
Figure 9. Alignment of Surface Contactors

VEHICLE
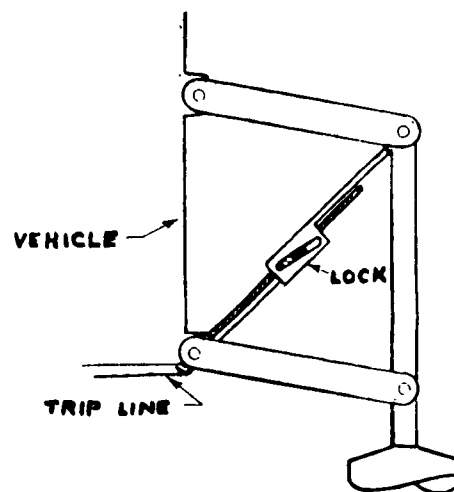
LOCK

TRIP LINE

Figure 10. Parallelogram Supporting Structure
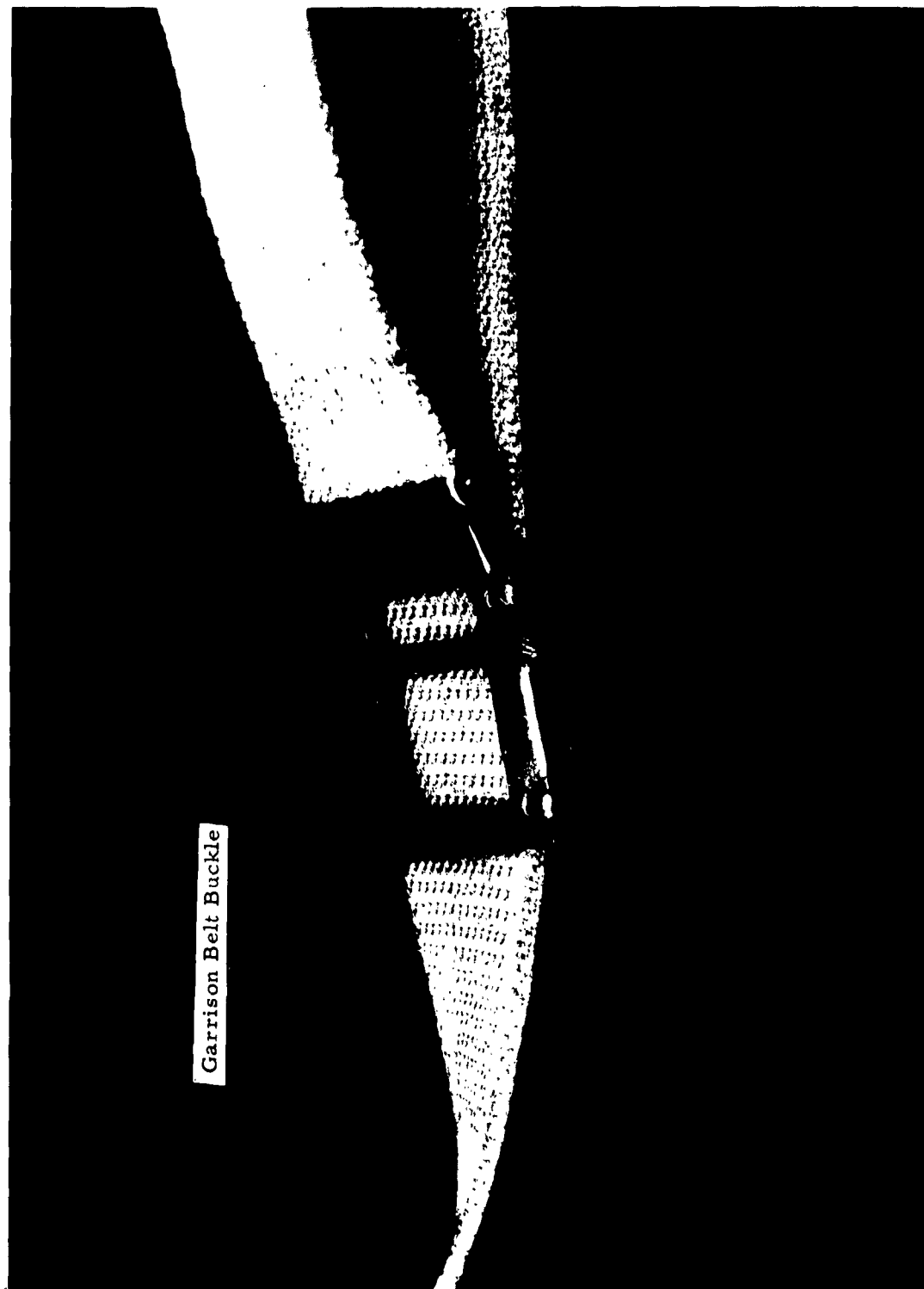
Garrison Belt Buckle

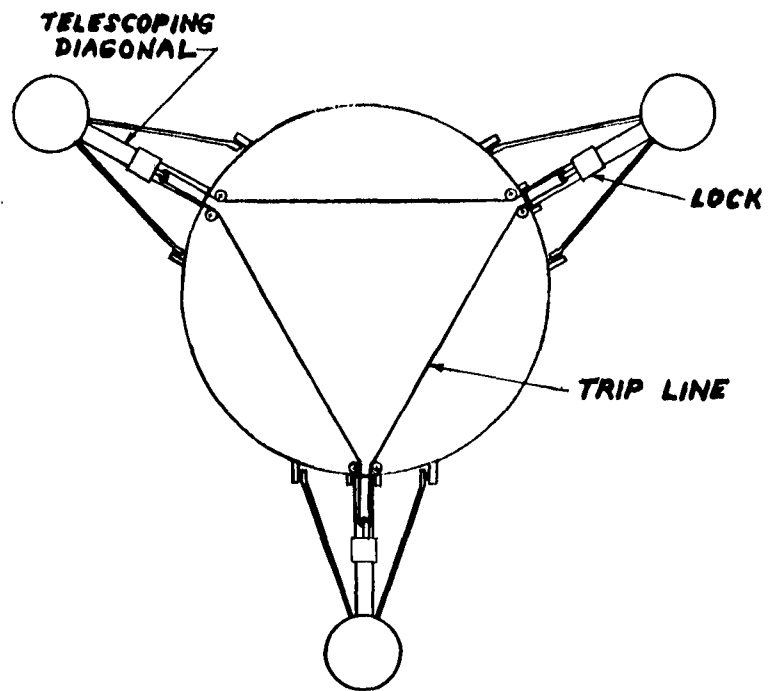Figure 11. Familiar Application of Self-Energizing Lock

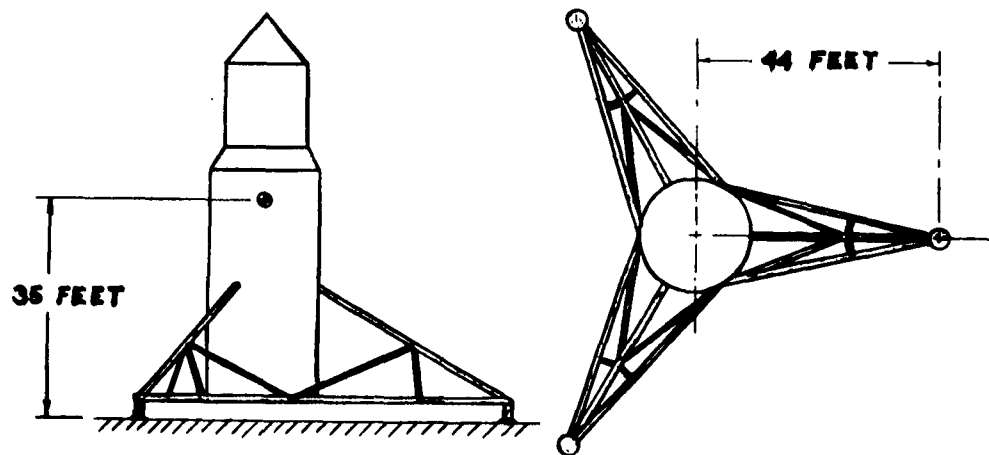Figure 12. Lock Trip Line Arrangement
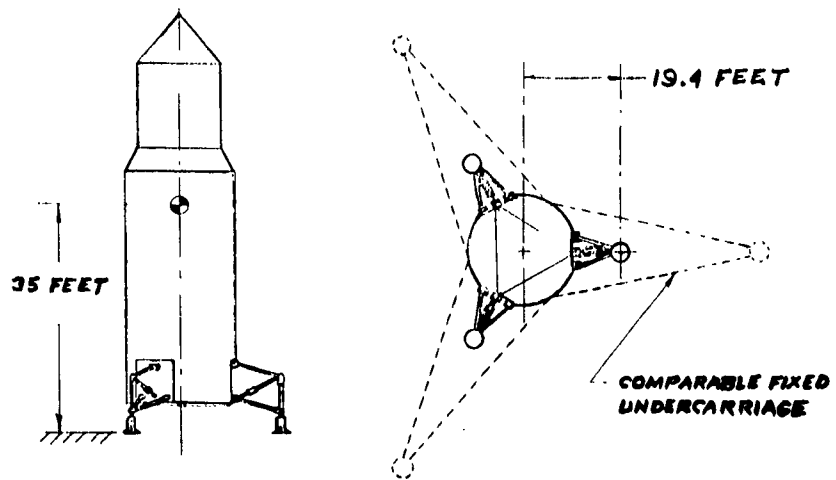

Figure 13. Fixed Tripod Concept
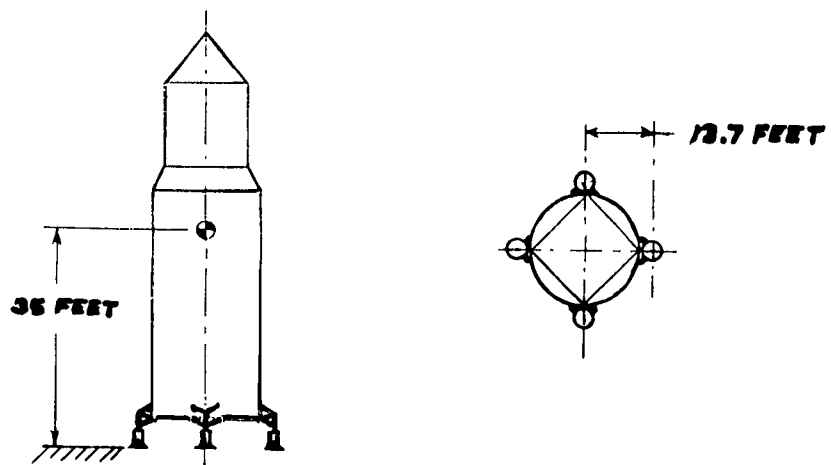
Figure 14. Self-Aligning Tripod Concept

Figure 15. Self-Aligning Quadripod Concept

self-aligning feature provides good load distribution qualities for any number of surface contactors permitting, for the same mission parameters, the optimized quadripod concept depicted in Figure 15.

6.4   GENERAL ALIGHTMENT CONDITIONS

Several assumptions regarding the upsetting motion have been made in the analyses. These assumptions are discussed in the following paragraphs.

It is assumed that the total upsetting motion occurs after the vertical velocity has been completely arrested, with the horizontal vehicle velocity essentially equal to the value prevailing at initial contact. By way of establishing the reasonable quality of this assumption, a comparison can be made of the approximate times which would elapse during the vertical and horizontal kinetic energy absorption phases of an alightment action. At a nominal deceleration rate of 10 g, the vertical alightment velocity will be arrested in approximately one-tenth second. Appendix X makes use of an "inverted pendulum" model to establish a time-displacement relationship for the case where there is just enough horizontal kinetic energy to cause upset. The time required to absorb 90% of the horizontal energy exceeds the vertical deceleration time by a factor of more than twenty-five, confirming the assumption that the vertical deceleration has a negligible influence on the upsetting tendencies. It follows that the local gravity field in which the upsetting action occurs is one lunar gravity.

Appendix XI establishes order of magnitude values for the vehicle tilt magnitude and velocity which would result from a "reasonable" variation between the several energy absorber deceleration forces of a given alightment system and confirms that this factor does not significantly affect the problem.

It has been assumed that deflections and alignment motions of the energy absorber are sufficiently small to justify the assumption that the vehicle's reach and effective c.g. height are constant. A calculation of Appendix IX shows a variation of one foot from nominal c.g. height causes a variation of only one-seventh foot in required reach.

The analyses also reflect the conservative assumptions that the surface contactors are restrained from sliding as tipping occurs and that the lunar surface obstacles are encountered under such surface contactors as to most aggravate the effect of the lunar surface slope.

36
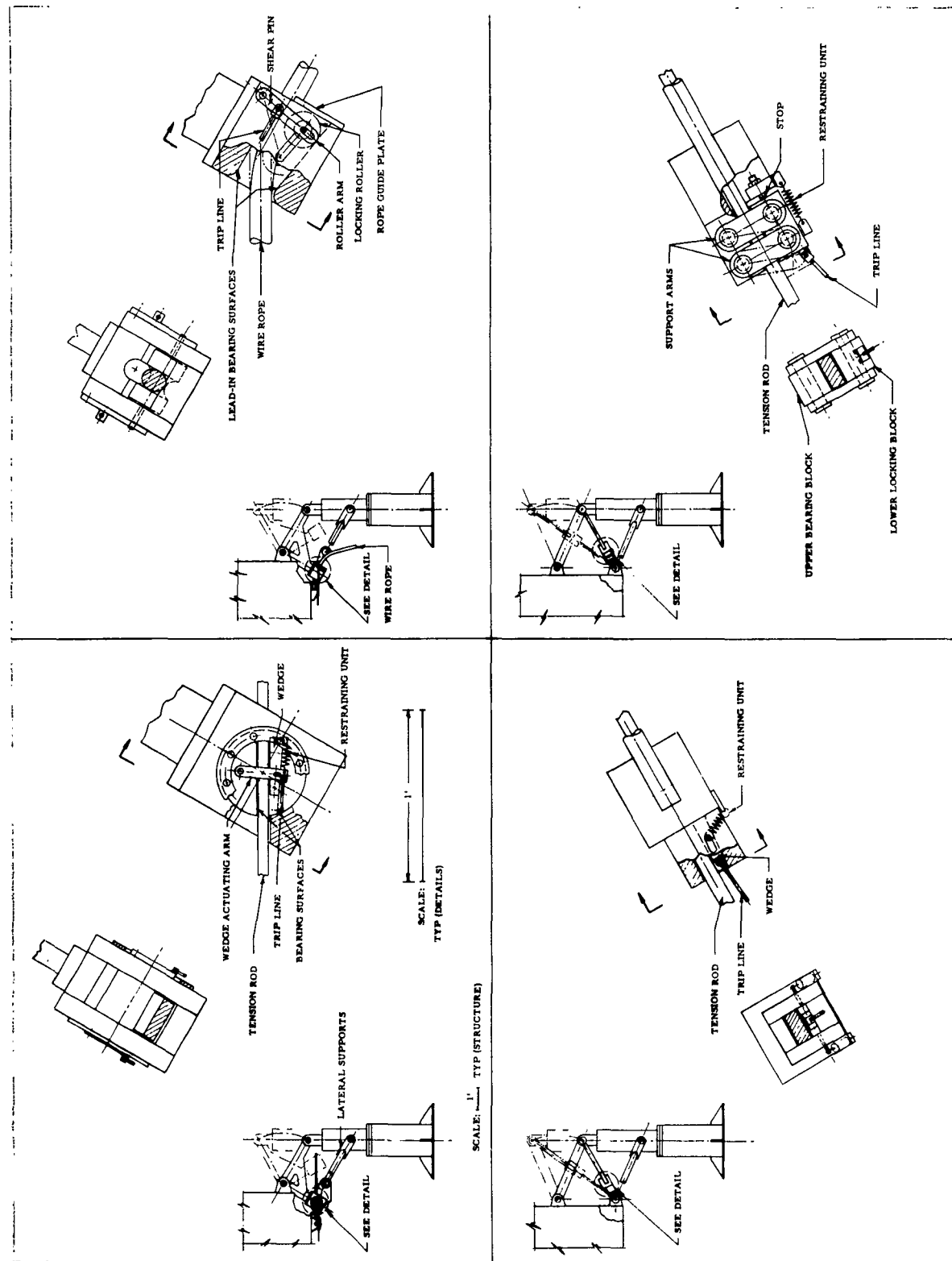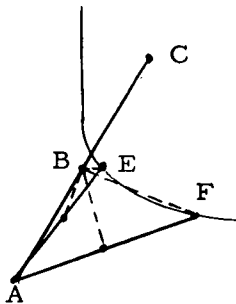
Figure 16 Self-Energizing Lock Concepts

7. UNDERCARRIAGE STRUCTURE

7.1 PRINCIPAL CONCLUSIONS

Calculations have been performed to establish approximate weight values for the fixed tripod undercarriage concept and for the tripod and quadripod self-aligning undercarriage concepts. The schematic configurations on which the calculations were based and the resulting undercarriage structure weights are listed in Tables 7 and 8. The structure weight found for the self-aligning tripod concept is in the order of one-fifth that found for the comparable rigid tripod, and the weight for the self-aligning quadripod is in turn in the order of one-half the value found for the self-aligning tripod concept. The net values of alightment system weight are summarized in Table 6.

Table 6. Comparison of Alightment System Proportions			
Concept	Fixed Tripod	Self-Aligning Tripod	Self-Aligning Quadripod
Horizontal Radius to Contactor (ft)	44	18.2	12.8
Horizontal Reach (ft)	22	9.1	9.1
Structure Weight (lb)	9,640	1920	770
Energy Absorber Weight (lb)	55	55	42
Surface Contactor Weight (lb)	744	744	450
Total Alightment System Weight (lb)	10,400	2720	1260

Table 7. Structure Weights For Fixed Tripod Undercarriage					
Strut Diagram	Member	Dimension			Weight (lb.)
		Length (ft)	Diam. (in.)	Wall (in.)	
	AB	24.4	12	1	994
	BC	24.4	11	1/2	488
	AE	45.5	10-1/2	1/2	865
	AF	45.5	10-1/2	1/2	865
	Total Weight, 1 Strut				3212 lb.
	Total Weight, 3 Struts				9640 lb.

7.2 GENERAL CONSIDERATIONS

The evaluation for the self-aligning concepts are based on the use of parallelogram mechanisms to accomodate the axial alignment requirements. The parallelogram has been selected over the potentially lighter cantilever structure to eliminate change in orientation and variation in horizontal position of the energy absorber element during axial alightment. The axial alignment stroke magnitudes required for the self-aligning systems were calculated as indicated in Appendix XIII and are equal to 28 and 39 inches for the quadripod and tripod configuration, respectively.

It may be noted from Table 6 that the horizontal reach of the self-aligning concepts evaluated is approximately one-half foot less than the value established in Section 6 for these concepts. This latter value of reach was established on the basis of "point" contact of the surface contactor and takes no account of the stability provided by the substantial area of the indicated surface contactors. It is felt that some increase in reach may be assigned to this factor and refining the structure weight calculations (which are actually based on earlier information) to incorporate larger reach dimensions would not enhance their precision as applied to an ultimate alightment system configuration. The weight of the self-energizing locks has been found to be negligible.

Careful efforts to optimize structure design are considered beyond the scope of this study. A sample weight calculation is included in Appendix XIV.

Table 8. Structure Weights for Self-Aligning Undercarriages
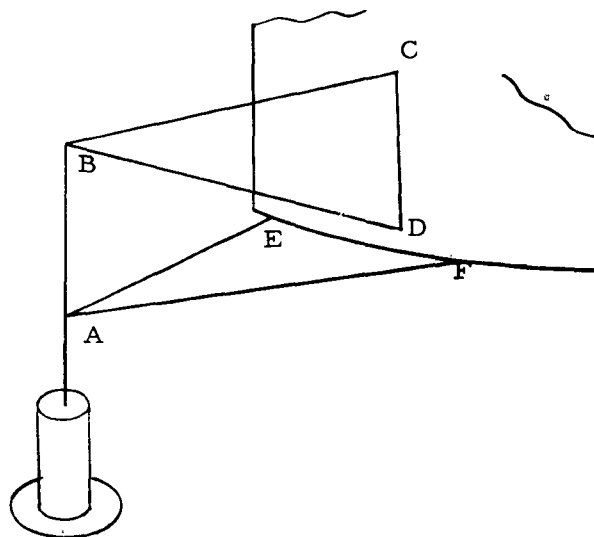
Tripod Configuration				
Member	Length (ft)	Tube Size	Wall Tk's (in)	Weight (lb)
BD	10.17	9" O.D.	3/8	127
AB	6.00	9" Square	3/4	180
BC	8.52	8" O.D.	1/2	121
CD	6.00	6" O.D.	1/4	33
AE	9.41	7" O.D.	3/8	89
AF	9.41	7" O.D.	3/8	89
			Total	639
			Total 3 legs =	1920 lb.

Quadripod Configuration				
BD	3.90	5-1/4" O.D.	7/16	31
AB	4.25	12" Square	3/8	90
BC	2.78	5" O.D.	7/16	21
CD	2.78	5-1/4" O.D.	5/16	16
AE	3.93	5" O.D.	1/4	17
AF	3.93	5" O.D.	1/4	17
			Total	192
			Total 4 legs =	770 lb.

8.   LAUNCH CONSIDERATIONS

8.1 SALVAGE OF ALIGHTING ENERGY

Efforts to utilize the energy absorbed in alightment to assist sub-
sequent launching are not justified.   The energy associated with a given
velocity is proportional to the square of the velocity.   The energy required
for lunar launching is equal to the kinetic energy at the lunar escape velo-
city.   The ratio of alightment energy to launching energy is equal to the
square of the ratio of the alightment impact velocity and the lunar escape
velocity.   For the assumed conditions this ratio is in the order of 1/50,000.
Consider for example, a vehicle requiring 100,000 earth pounds of fuel for
lunar takeoff.   Salvage of the alightment energy would reduce this fuel re-
quirement by the order of two earth pounds, an insignificant portion of the
weight of the devices which would be required to accomplish the energy
salvage.

8.2   ASSISTED TAKE-OFF

It has been concluded that special auxiliary launch engines are not
justified by the fuel savings associated with their use.   Ideally speaking,
a positive drive auxiliary engine shows considerable advantage over the
rocket engine for the first portion of flight of a lunar vehicle from the
moon's surface.   The mechanical efficiency of the rocket engine does not
reach that of the positive drive engine until the vehicle speed is equal to
one-half the rocket exhaust velocity.   By way of evaluating the use of
auxiliary launch engines, consider the positive drive engine which consists
of several hydraulic cylinders which might be used in absorbing the energy
of alightment.   The logical launch energy capacity of such an engine is equal
to the alightment energy capacity.   Assuming the use of liquid hydrogen and
oxygen for fuel and the nominal parameters of Section 2, such an engine
would use approximately 330 pounds less fuel than the rocket engine would
use for the same purpose (see Appendix VII).

A simplified estimate of the weight of three (equally spaced) cylinders
which could serve as the positive drive engine, indicates a total cylinder weight
of more than 500 pounds based on a cylinder working pressure and stress value
of 5000 psi and 60,000 psi, respectively.   These cylinders might be used to
absorb the alightment impact energy, but another 75 pounds of hydraulic fluid
would be required, meaning that the alightment system weight exceeded the
fuel savings weight by more than 200 pounds.   The details of this analysis
are presented in Appendix VII.   The selection of 60,000 psi as a working
stress in this study is based on a factor of 2 to account for the load doubling
due to the sudden application of the load and an additional safety factor of 1-1/2

on an ultimate strength of 180,000 psi (e.g., 4130). The overall weight comparisons for a quadripod configuration would be essentially the same as for the tripod configuration discussed above.

It should be borne in mind that no·consideration has been given in the foregoing discussion to the feasibility of designing pressure control valves or orifices which can adequately regulate the pressure during the alightment impact stroke. Each of the three cylinders used for the alighting system of a 50 ton vehicle would have to handle a peak orifice flow rate in the order of 10,000 gallons per minute. The weight of these devices and associated plumbing has not been accounted for. Coupled with these negative considerations is the problem of reliability associated with delayed rocket engine ignition, and, where independent charges are used in three or more cylinders, the problem of simultaneous ignition of these charges exists.

8.3 THE NEED FOR AN ERECTION SYSTEM

A vehicle erection system should not be required. Such a system is not justified unless it can be established that there is a reasonable possibility that the vehicle may be upset at alightment and that after such an upset the vehicle possesses a launch and return capability. To accommodate the latter postulate, the design would have to include a controlled energy absorber system capable of preventing catastrophic damage as a result of the upset and this system would have to account for upset in any of the probable directions of occurrence. Further, the high radial decelerations would impose a whole new set of design restrictions on the vehicle's structure, equipment and crew support accommodations. It is felt that the weight attendant to these special features could be better devoted to insuring that the vehicle does not upset at alightment.

8.4 LAUNCH PREPARATION NEEDS

It is assumed that there is no need for vehicle hold-down in the lunar launch program. Hold-down is ordinarily required to insure that thrust builds up to a value sufficient to provide a good value of vertical acceleration before extraneous influences can act to upset the vehicle. There seems no reason to presume that the lunar launch vehicle will have the low thrust to takeoff weight ratio common to large earth launched vehicles and further, the earth's major upsetting influence, (wind and weather) is not a problem on the moon's surface.

9. EFFECTS OF VARYING DESIGN CRITERIA

9.1 GENERAL CONSIDERATIONS

The conclusions developed in this study are based on the application of the nominal values indicated for the several design criteria in Table 1, Section 2. Since the design criteria cannot be established with great precision at this time, it is well to consider the effects on alightment system design, of variations in these design crtieria, particularly in the case of those parameters for which a range of values is indicated in Table 1. The effects of variations in a number of these parameters are discussed in the following paragraphs, presuming in each instance that all other parameters remain unchanged.

9.2 VEHICLE PARAMETERS

It has been assumed in this study, that the alightment system can be attached directly to the lunar vehicle at its periphery and that the weight of the vehicle structure required to support the alightment system attachment points was not part of the alightment system weight. To the extent that this assumption is applicable, the indicated variations in vehicle diameter would have a noticeable effect on alightment system weight, since the required length of alignment mechanism "reach" is directly affected. Reducing the vehicle diameter from 20 feet to 15 feet could increase the weight of the recommended quadripod alightment system by half. Increasing the diameter to 25 feet would tend to reduce the advantage which the self-aligning quadripod configuration exhibits over the self-aligning tripod configuration but would not qualitatively alter any of the conclusions presented in this report. The weight of the alignment mechanism structure would vary approximately as the square of its radial length, but the weights of other portions of the alightment system would not be significantly affected by variations in structure length. For the preferred self-aligning quadripod configuration, the structure weight accounts for about half the total alightment system weight.

There is a possibility that special structure would need to be incorporated within the vehicle specifically for support of the alightment system attachment points and the weight of such structure would be properly chargable to the alightment system. In this event, it may be concluded that variations within the indicated range of diameters would not substantially affect overall alightment system weight.

Variation in vehicle height would be significant only to the effect that it varies the height to the center of gravity. The effects of variation in the center of gravity height can be deduced from the equations of Appendix IX which deals with the reach required to establish satisfactory stability. For the self-aligning quadripod configuration, a 2 percent increase in vehicle height requires an increase of approximately 1 percent in the horizontal reach.

With the exception of the surface contactor, the weight of the alightment system components varies directly with alightment loads which in turn varies directly with vehicle alightment weight. For the surface contactor design concept established in this study (which is subject to refinement) the surface contactor weight would vary approximately as the three halves power of the vehicle alightment weight, but for the indicated range of values this latter factor does not materially alter the alightment system weight to vehicle weight ratio established for the quadripod configuration.

9.3 ALIGHTMENT CONDITIONS

Vertical alightment energy is proportional to the square of the vertical vehicle velocity. The stroke and weight of the energy absorption element is directly proportional to the alightment energy, and the weight of other components tends to vary in the same degree except where increased stroke length introduces buckling problems.

The required reach of the vehicle's alightment system varies approximately in proportion to the horizontal alightment velocity and the alightment system weight varies accordingly (see discussion of self-aligning system, Appendix IX).

Increasing the tilt of the vehicle at touchdown has the same effect as a proportionate increase in horizontal velocity.

The horizontal velocity of the surface contactors associated with the specified spin and tilt velocities are each less than one twentieth of the indicated horizontal alightment velocity and it may be concluded that large variations in the spin and tilt velocities from the values of Table 1 would be inconsequential.

Decreasing the maximum allowable deceleration reduces the vertical alightment loads proportionately, but the minimum stroke length increases proportionately and the lateral stability of the energy absorber becomes more significant.

44

9.4 LUNAR GEOLOGY

The self-aligning alightment system is affected by variations in lunar surface slope in that the slope directly effects the required value of the alignment stroke. Increasing the surface slope from 3° to 5° would require a total increase of about 10 inches for the self-aligning quadripod configuration. Variation in the maximum obstacle height affects the required alignment stroke length directly. The effect of variations in these two parameters on rigid undercarriage systems may be determined in accordance with the relationships presented in Appendix IX.

The real function of the surface contactor design is to distribute the energy absorber crushing load from an operating pressure of several thousand psi to pressure levels compatible with the bearing strength of the lunar surface. For the nominal design value, the surface contactor weight represents a large portion of the total weight of the self-aligning configuration. For the indicated contactor design concept, contactor weight would vary in approximately inverse proportion to the lunar surface bearing strength. It is probable that a more efficient surface contactor design concept could be established, perhaps incorporating honeycomb structures in the surface plate. If the surface bearing strength were to go as low as 50 psi, the surface contactor problem should be given special design attention.

10. EXPERIMENTAL VERIFICATION

10.1 SUMMARY AND CONCLUSIONS

An experimental program was conducted with the principal objective of verifying the feasibility of incorporating in a lunar alightment system, the self-aligning qualities proposed for the system in this study. To this end, a one-twelfth scale model vehicle utilizing a self-aligning quadripod undercarriage was fabricated and subjected to controlled drop tests simulating the alightment conditions delineated in Section 2. Feasibility of the self-aligning concept was confirmed. To the extent that test precision permitted, the tests results supported the quantitative propositions embodied in the lunar alightment system recommendations developed in this study.

The general test approach, the test apparatus and the test results are described in the following paragraphs of this section.

10.2 TEST APPROACH

10.2.1 Detail Test Objectives

The approach selected to verify the feasibility of the proposed lunar alightment system concept consists of subjecting a scale model of the lunar vehicle, fitted with a functioning self-aligning undercarriage, to a vertical alightment under conditions simulating the actual alightment conditions and environment predicted in Section 2 of this report. The detail test objectives include demonstrating that the vehicle alightment attitude is insensitive to variations (within design limits) of the simulated lunar surface conditions, and that vehicle proportions are such that the vehicle does not upset under simulated lunar alightment conditions, but does upset when the alightment conditions are appreciably aggravated.

10.2.2 Test Scaling

Owing to the substantial proportions of the established vehicle parameters, it is essential that experiments conducted in this study make use of reduced physical scale. A one-twelfth scale on all linear dimensions (one model inch equals one real foot) and a one-to-one scale for time and density was found suitable for the purposes of this study. This scaling provided a manageable six-foot vehicle model and a nominal test deceleration less than 1 g. This latter quality is essential to the pulley system test concept selected since decelerations in excess of 1 g would cause slack in the supporting flexible lines (chains).

46

10.2.3 Scaling Principles

The Buckingham Pi Theorem states that in any equation involving n physical quantities, and if these quantities are measured in terms of m fundamental units, then the equation may be reduced to another equation involving n-m dimensionless products. The dimensionless products are denoted by π_i. An equation of the form A = f (B, C, D, E, ...) can also be expressed as $0 = \emptyset$ (A, B, C, D, E, ...). These variables can be grouped into dimensionless products and the equation written as $0 = \emptyset$ (π_1, π_2, π_3, ...) or $\pi_1 = f$ (π_2, π_3 .....).

The above dimensionless products could represent the general equation for the prototype. The general equation for the model could then be written as $0 = \emptyset$ (π_{1m}, π_{2m}, π_{3m}, ...) or $\pi_{1m} = f$ (π_{2m}, π_{3m}, ...). The prediction equation is formulated by dividing the general equation for the prototype by the general equation of the model. This would then be written as:

$$\frac{\pi_1}{\pi_{1m}} = \frac{f(\pi_2, \ \pi_3 \ \cdots \ \pi_i}{f(\pi_{2m}, \ \pi_{3m} \ \cdots \pi_{im})}$$

If the design conditions for a true model are all satisfied ($\pi_{im} = \pi_i$), the functions are equal and $\pi_1 = \pi_{1m}$ and $\pi_2 = \pi_{2m}$. Furthermore, in the scaling process, identity of one of more non-dimensional parameters, such as Cauchy's Number, Froude's Number, Reynold's Number, etc., must be realized. In the lunar landing situation the Froude's Number (Inertia Force/Gravity Force or $(\text{Velocity})^2$/(Gravity) (Length) of the model should be the same as for the prototype.

10.2.4 Test Gravity Field

The selected scale requires that the test gravity field be one-twelfth the actual gravity field to be simulated, in this case lunar gravity. Since lunar gravity is, in turn, approximately one sixth of earth gravity, the required test gravity field is one twelfth of one sixth of earth gravity, or 1/72 of local gravity. The means chosen to establish the test gravity field consists of a pulley and ballast system which supports the vehicle model with a slightly unbalanced counterweight, the unbalance being so established that when otherwise unrestrained, the vehicle model falls with an acceleration of 1/72 earth gravity (i.e., scaled lunar gravity). Equations for establishing the proper value of unbalance, accounting for all the connected mass, are developed in Appendix XVI.

10.2.5 Simulating Vertical Velocity

In the established test gravity field, a drop height of approximately 10 feet would be required to cause the desired vertical touchdown velocity, discounting any friction losses. This imposes an overhead clearance requirement for the test apparatus which exceeds the limitations of many laboratory spaces. A method for reducing the required drop height utilizes a compound ballast arrangement which increases the net unbalance which operates during the first portion of a drop motion. A secondary ballast is automatically removed from its support before the drop motion is completed to establish the desired gravity field at touchdown. This ballasting approach is illustrated in Figure 17.

10.2.6 Simulating Horizontal Velocity

Establishing a precise horizontal motion of the vehicle model during a test drop is a difficult problem. A more direct means for simulating the horizontal alightment velocity of the vehicle consists of dropping the vehicle model at zero horizontal velocity (with respect to ground) onto a platform which is moving at the simulated horizontal touchdown velocity during the alightment action. Since, in an actual lunar alightment, the horizontal velocity of the vehicle will ultimately be arrested, the test suspension must permit the vehicle to assume the horizontal velocity of the drop platform without appreciable restraint. The drop platform must have a capacity for being tilted to simulate the effects of lunar surface slope and obstacles.

48

10.3 TEST APPARATUS

10.3.1 Test Rig

The test vehicle is supported by a double chain and pulley system with the required weight unbalance achieved by means of a ballast as discussed in Section 10.2. An endless chain was used to minimize the change in weight between the vehicle and ballast suspension. The only difference in weight will be due to the lack of symmetry of the chain suspension as the vehicle drops. Friction drag was minimized by mounting the pulleys on ball bearings. Figures 26 and 27 show various views of the rigging and Figure 17 indicates over-all dimensions.

The compound ballast used to obtain the required weight unbalance and the proper touchdown velocity is shown in Figures 17 and 35. The secondary ballast also serves to actuate a micro-switch that starts the motor driving the landing platform to provide the horizontal velocity. The switch is actuated at the proper time to assure that the landing platform is moving at a uniform speed and will be directly under the vehicle at touchdown.

The landing platform is mounted on a cart and pulled by a chain connected to a gear motor as shown in Figure 18. Over-all dimensions of the landing cart are indicated in Figures 18 and 19. The effect of surface slope and obstacle height is simulated by hinging one end of the landing platform. The proper angle is obtained by inserting blocks under the raised end of the platform as indicated in Figure 19.

In order to provide complete freedom of movement in the direction of the horizontal travel, the vehicle was suspended from a bar secured at either end to the suspension chains.

A trolley free to move along this bar supports a rod attached to the vehicle as shown in Figure 28. The rod is connected to the vehicle by means of a spherical bushing which permits freedom of rotation in any vertical plane. Nominally the rod is secured at the c. g. of the vehicle to eliminate any couple associated with an offset when tipping of the vehicle occurs. Figure 34 shows the details of this attachment.

10.3.2 Test Vehicle

The test vehicle is fabricated from two fiber barrels which are reinforced at the top and bottom. Approximate scale is indicated by the figure of the man in Figure 26. Under the influence of gravity, a support structure engages the spherical bushing by which the vehicle is supported vertically.

Accelerometers are mounted on this support structure as shown in Figure 34. The spherical bushing engages a nut which bears against the support structure (see Figure 20). Lateral adjustment of the bushing position is provided by three rods which connect the nut to thumb screws attached through the side of the vehicle. Figure 20 shows an elevation of the vehicle.

Slots were provided in the top of the vehicle structure to provide clearance for the suspension rod during the tipping motion. These slots can be seen in Figure 35.

The alignment system comprises four struts. Each strut includes an energy absorber supported by two "A-frame" members and a two piece extendible diagonal as shown in Figures 31 and 32. The over-all dimensions of the strut are presented in Figure 21 and a detail of the "A-frame" support arm is shown in Figure 24. Each diagonal includes a self-energizing lock which can be actuated by tautening a common trip line which interconnects the locks of all four diagonals (see Figures 32 and 33). Figure 25 is a detail of the diagonal end fitting.

The energy absorber used in this test was not the crushable honeycomb proposed in the original design but was a friction type to facilitate repeated test usage. A detail view of this energy absorber is presented in Figure 23.

The self-energizing lock operates on the same principal as the common garrison belt buckle illustrated in Figure 11. A disassembly of the lock is shown in Figure 32 and over-all dimensions are indicated in Figure 22. The lock consists of a roller mounted in a yoke. The roller rides between two surfaces of the housing, one of which is at an angle to the other and serves to wedge the roller in a locked position. The trip line exerts the initial pull on the yoke to wedge the roller in place. Premature engagement is prevented by a spring mounted on the housing and pressing against the yoke.

The trip line is a continuous line interconnecting all four brakes. Proper action of the trip line depends upon relatively friction free operation. Figure 33 indicates the trip line configuration in a pre-alightment attitude of the landing system whereby all surface contactors are in their lowest position. This is the slack line type differential discussed in Section 6.3.

50

10.4   TEST RESULTS

10.4.1   Drop Tests

Table 9 presents data collected in drop tests performed under varying conditions of velocity, vehicle attitude, and surface slope.

Definition of Symbols:

V_v = Vertical velocity

V_h = Horizontal velocity

α = Surface slope

β = Vehicle tilt (positive in direction of upset)
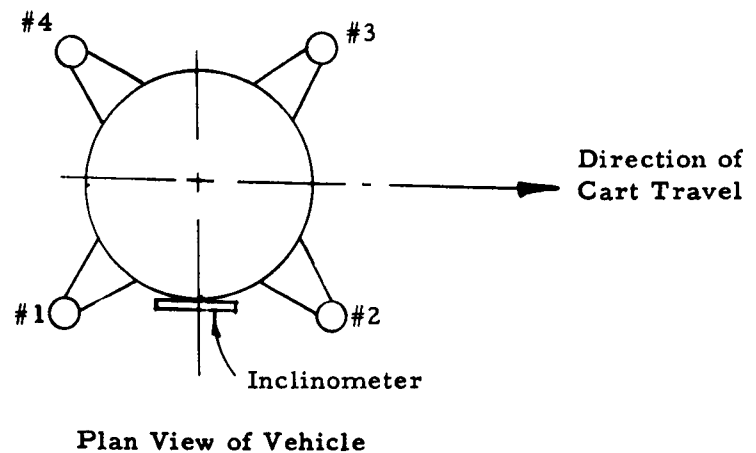
Strut Identification

Plan View of Vehicle

			Vehicle Tilt (Degrees)			Stroke (Inches)				Average Stroke (Inches)
Run No.	V_h ($\frac{in.}{sec.}$)	α (Deg.)	At Contact	Max	Final	#1	#2	#3	#4	
1	3.6	0	0	$2\frac{1}{2}$	$1\frac{1}{2}$	$4\frac{4}{16}$	$4\frac{3}{16}$	$4\frac{3}{16}$	$4\frac{10}{16}$	$4\frac{5}{16}$
2	3.6	6.2	0	4	$1\frac{1}{2}$	$3\frac{13}{16}$	$4\frac{10}{16}$	$3\frac{10}{16}$	$4\frac{5}{16}$	$4\frac{2}{16}$
3	0	0	0	$-\frac{1}{2}$	$-\frac{1}{2}$	$4\frac{4}{16}$	$4\frac{9}{16}$	$4\frac{6}{16}$	$4\frac{3}{16}$	$4\frac{6}{16}$
4	0	6.2	0	$1\frac{1}{2}$	$\frac{1}{2}$	$4\frac{1}{16}$	$4\frac{2}{16}$	$4\frac{2}{16}$	$4\frac{4}{16}$	$4\frac{3}{16}$
5	3.6	6.2	2	15	6	$4\frac{1}{16}$	$4\frac{1}{16}$	$3\frac{8}{16}$	$4\frac{5}{16}$	$4\frac{1}{16}$
6	3.6	6.2	3	Upset	-	-	-	-	-	-

Table 9. Test Data

$V_v = 35$ in/sec. for all runs

10.4.2 Accelerometer Recordings of Drop Tests

Records were taken of the two accelerometer readings during each of the drop tests described in the previous paragraphs. A typical record is presented in Figure 36. Certain of the factors which bear on the acclerometer readings are discussed in the following paragraphs.

The lowest channel on the record is the output of a 50 cps (20 millisecond period) audio oscillator, impressed for the purpose of establishing a time scale. The signal record immediately above is derived from the actuation of a microswitch which is actuated once in each 5.0 inches of vehicle drop travel.

The second record from the top is the signal from the horizontally oriented accelerometer. Based on its relation to the "5 inch" signal, it has been deduced that the first appreciable signal on the horizontal record marks the initial engagement or "touchdown" of the alightment system.

The top record is the signal from the vertically oriented accelerometer. The steady oscillation which appears on the vertical acceleration record throughout the dropping motion can be deduced to be associated with the "polygon" effect of the suspension chain sprocket, since the number of cycles of oscillation in a given period corresponds to the number of teeth engaged on a sprocket in the same period.

The longer period oscillation, which appears on the vertical acceleration just before touchdown, results from oscillations of the secondary ballast which is picked up suddenly when the vehicle is about 2-1/2 feet from touchdown position.

By comparison with the displacement and horizontal acceleration signals, it can be deduced that the first appreciable signal which can be observed on the vertical acceleration record is associated with touchdown. Commencement of energy absorber action is characterized by the sharp spike on the vertical acceleration record which goes well over 4 g in the case illustrated. It should be noted that test vehicle decelerations in excess of 1 g theoretically cause the suspension chain to develop slack, which fact of itself could act to induce appreciable vertical acceleration influence on the vehicle.

10.4.3 Miscellaneous Observations

Certain observations made during the test preparation phase of the experimental verification program contribute insight into the degree to which the significant variables were controlled and may be helpful in any planning which may be undertaken in connection with further testing in future programs. The following notes are applicable.

The friction of the pulley bearings as delivered was extremely high. Bearing seals were removed, grease was washed out, and bearings were relubricated with light oil. Resulting combined friction of pulley system measured in terms of chain pull at slow speed under nominal system load was in the order of 3/4 pounds. (Removal of vehicle and ballast accounting for about two-thirds of the pulley supported weight, cut the pulley system friction approximately in half.) A small vibrator was clamped to the pulley support system and at first operation of the vibrator resulted in a reduction of 3 to 4 ounces in the pulley system friction. Later, when record tests were about to be conducted, the vibrator operation was found to have a negligible effect on pulley system friction which then averaged about 10 ounces which compares to a nominal test unbalance of 18 ounces. Since vibrator operation did have a substantial effect on the reading of the vertical accelerometer, its use was abandoned.

It was found that even with ball bearings, the frictional resistance of the trolley caused a noticable tilting of the vehicle suspension rod as the test vehicle was carried along on the moving platform. An effort was made to neutralize this frictional resistance by tilting the "trapeze" bar by one inch in 48 inches, in the sense which aided trolley travel. The degree of tilt was such that starting friction was sufficient to prevent travel of the vehicle, but running friction is lower and not sufficient to impede motion.

During the test preparation, each of the energy absorbers was set to about 15 pounds slip force (at low slip speed) and preliminary drops onto the test platform at low vertical velocity were made. Under these conditions, the average absorber stroke was less than a half inch and the vehicle rebounded from 3 to 5 inches. Dropping the vehicle onto the concrete floor instead of the test platform had no noticable effect on the rebound characteristics, confirming that the test platform elasticity was not significant with these velocities and forces.

The slip force of each of the energy absorbers was reduced from the above value to provide an energy absorption stroke of approximately 2-1/4 inches at nominal vertical test velocity (35 inches per second). The resulting slip force at each of the energy absorbers measured about 7 pounds (at low slip speed) although the average stopping force over the full 2-1/4 inch stroke can be readily reduced to be approximately 13 pounds on the basis of the dissipated kinetic energy. With this setting of the energy absorbers, the vehicle rebounded two to three inches when dropped at nominal vertical test velocity. Stiffening of the vehicle structure by the addition of two 1 x 4 pine cross members located in the region of the energy absorber attachment plates had no significant effect on the rebound characteristics. Since the rebound action could have a considerable effect on the alightment performance, it was felt necessary to modify the system to preclude the occurrence of significant rebound. This was accomplished by extending the absorption stroke to approximately 4-1/4 inches.

10.5   EVALUATION OF EXPERIMENTAL OBSERVATIONS

The complete success of the self-aligning action of the alightment system was attested by visual observation during the tests and by the generally consistent decelerator stroke readings listed in Table 9. The low values indicated for final vehicle tilt (β) in runs 1 through 4, also support that conclusion. The higher final vehicle tilt reading of run 5 is due in part to the unsymmetrical location of the vehicle c.g. associated with the initial vehicle tilt. This latter effect was probably aggravated by the poor low-velocity performance characteristics of the energy absorbers used in the test. It is interesting to note that during the test preparation phase, the

vehicle model was accidentally dropped the full test drop height onto a tilted platform without any connected ballast. The estimated impact energy was fifteen times nominal but although slight model damage was sustained, the model withstood the impact without perceptible tilting.

An attempt has been made to establish a quantitative correlation between the stability analysis methods used in this study and the observed value of initial vehicle tilt required to cause upset of the test model (see Appendix XVII). Good correspondence was not attained between the horizontal kinetic energy of the test model (9 in-oz) and the increase in system potential energy (19 in-oz) which occurs as the model displaces from an initial tilt of 3 degrees to upset position, but problems associated with system friction could readily account for this poor correlation. If the effect of the friction in the overhead pulleys is introduced it causes a substantial increase in the work done on the system by "lift" of the vehicle which would suggest that an appreciably greater initial tilt should have been required to cause upset. However, the cant introduced into the "trapeze" bar to neutralize the bearing friction encountered in the trolley has a counter effect, since motion of the trolley in the direction of ground (platform) motion causes the ballast to be lowered for a given vehicle model position, thereby decreasing the total potential energy of the system. Calculations of Appendix XVII indicate that if the rolling coefficient of friction of the trolley were only half the cant of the trapeze bar (which was actually set to neutralize static friction), a trolley motion of only five inches would be required to balance the system energy equations using the data collected in the test. In short, the observed test data is not inconsistent with the prediction methods used in this study, but neither does it provide quantitative justification for those prediction methods.

11. RECOMMENDATIONS FOR FUTURE STUDY

11.1 INTRODUCTION

There were a number of areas treated in this study which could clearly benefit from more detailed study and experimentation. Principal areas are discussed in the following paragraphs.

11.2 ENERGY ABSORBER - SURFACE CONTACTOR CONSIDERATIONS

For the preferred alightment system described in Section 1.2.3, the specific configuration of the honeycomb energy absorption element was found to have a significant effect upon the design of the surface contactor. However, the latter item outweighs the energy absorption element by a factor of 10 and it appears that some compromise of the "efficiency" of the absorber might permit a significant reduction in the weight of the surface contactor. In any event, the combination of absorber and contactor, which accounts for a third of the self-aligning quadripod alightment system weight, should be studied as a unit with the view to establishing an optimum design. Since the bearing strength of the lunar surface has a substantial influence on the design of the surface contactor, there may be some merit in conducting design studies for two or three ranges of bearing strength.

It would be well that refined studies of the absorber-contactor give consideration to the problem of eccentric engagement of local obstacles. In particular, attention should be given to the question of whether it is better to allow the contactor or the energy absorber to deform to accomodate obstacles encountered off the center of the surface contactor area. The value of mechanical guides to restrain the honeycomb absorber element from horizontal or irregular vertical deformation deserves consideration.

For the purpose of further study of the mechanics of alightment, there is a need to establish the effect on vertical energy absorption characteristics of simultaneous horizontal loading, and to assess the horizontal reach afforded by the finite radius of the surface contactors.

11.3 THE MECHANICS OF ALIGHTMENT

It would be useful to develop a mathematical model which would be utilized to establish computer studies for a more thorough evaluation of the performance capabilities of fixed and self-aligning alightment systems,

56

and to permit the establishment of more complete specifications for various features of the alightment systems. The mathematical model should reflect the vertical and horizontal energy absorber characteristics, the deceleration stroke length and the pertinent elasticity characteristics of the vehicle and undercarriage structure. In addition, it should include the influence of the axial and radial surface contactor motion associated with alignment of the contactors with the lunar surface, and the several pertinent alightment conditions such as vehicle alightment velocities and attitudes and surface slope and other surface impediments. The desirability of establishing a low limit for vertical velocity to enhance stability should be considered. Because of the "plastic" deformation characteristics of desirable types of energy absorbers, the analog computer is probably better suited for this problem than the digital computer.

The study of alightment mechanics should include evaluation of the load amplification associated with the elastic response of the vehicle and structure to the fairly sudden application of the deceleration load. Response motion histories should be established for the vehicle to permit more complete specification of the mounting environment for equipment on board the vehicle.

11.4   UNDERCARRIAGE STRUCTURE

Only a minimal effort was made in this study to optimize undercarriage structure design. Further study of such structure would be desirable, particularly with regard to establishing and evaluating various concepts for providing the required alignment stroke. Stroking requirements for remote energy absorption could be considered to permit a more precise evaluation of that approach.

11.5   EMPIRICAL PROGRAMS

When more thorough analytical predictions of the performance of pertinent alightment system concepts have been accomplished there would be value in empirical programs to establish quantitative confirmation of the performance of such concepts. Particular care should be taken to establishing a test set up with sufficient precision and freedom from friction to permit satisfactory quantitative data collection. Some difficulties encountered in this respect are discussed in Section 10.4.3.

12. REFERENCES

The various publications cited in the text of this report are identified in the following list. Certain additional publications are listed which are not specifically cited in this report but which are considered helpful as background material.

1.   Ali, Ahmin and Benson, Leonard R., "Cushioning for Air Drop, Part IX, Bibliography of Literature Pertaining to the Absorption of Impact Energy," University of Texas, June 9, 1957.

2.   Beltran, A. A., et al; "Annotated Bibliography of Lunar Properties, Geology, Vehicles, and Bases. Part II Vehicles, Trajectories, and Landings," December 1961, 296 pp. AD 271 033.

3.   Bjork, R. L. and Gazley, C. Jr., "Estimated Damage to Space Vehicles by Meteoroids," USAF Project Rand Res. Memo Rm 2332, February 20, 1959.

4.   Burns, A. B., "Guide for the Selection and Application of Shock Mounts for Shipboard Equipment," BuShips Contract No. NObs-78963, AMF, September 1, 1961.

5.   Burns, A. B. and Plascyk, J. A., "Design of Deformable Foundations," BuShips Contract No. NObs-78963, AMF, March 30, 1962.

6.   Buzzard, Wallace C., "Future Design Concepts for Lunar Landings," ASD, Technical Memorandum ASRMDD-TM-62-69, December, 1962.

7.   Coppa, Anthony, P.,; "Collapsible Shell Structure for Lunar Landings," G. E., Philadelphia, Pa., American Rocket Society, October 9-15, 1961, (N. Y. Coliseum).

8.   Daigle, D. and Lanborg, J.; "Evaluation of Certain Crushable Materials," Jet Propulsion Laboratory, Tech. Report No. 32-120, January 13, 1961.

9.   Eiband, M. A., "Human Tolerance and Rapidly Applied Accelerations: A Summary of the Literature," NASA Memo 5-19-59E, 1959.

10.   Esgar, Jack B., "Survey of Energy-Absorption Devices for Soft Landing of Space Vehicles," TN D-1308, NASA, June, 1962.

11. Esgar, J. and Morgan, W.; "Analytical Study of Soft Landings on Gas Filled Bags, 1960, NASA TR R-75.

12. Evans, G. R., "Lunar Probes and Landing, an Annotated Bibliography," Lockheed Aircraft Corp., Sunnyvale, California, Report No. SB-61-24.

13. Fisher, Lloyd, Jr., "Landing Impact Dissipation Systems" December, 1961, NASA TN D975.

14. Flora, C. L., "Impact Deceleration Systems Applicable to Lunar Landing Vehicles," 9-21-60, Radioplane Div., of Northrop Corp.

15. Green, J., "Geophysics as Applied to Lunar Exploration (Final Report)," Aero-Space Laboratories, North American Aviation, Inc., 30 June 1960.

16. Jaffe, Leonard D., and Rittenhouse, John B., "Behavior of Materials in Space Environment," ARS Journal, March 1962, pg. 320.

17. Kiess, C., and Lassovzsky, K., "The Known Physical Characteristics of the Moon and Planets," July, 1958, AF 18(600)-1770, ASTIA Doc. No. AD 115-617.

18. Kriegsman, Bernard A., and Reiss, Martin H., "Terminal Guidance and Control Techniques for Soft Lunar Landings," ARS Journal, March 1962, pg. 401.

19. Kroell, C. K., "A Simple, Efficient, One-Shot Energy Absorber," Part III Bul. #30 Shock, Vibration and Associated Environments, February, 1962, Off. of Sec. of Defense.

20. Lad, Robert A., "A Survey of the Materials Problems Resulting from the Low Pressure and Radiation Environment in Space," NASA TN (Proposed), 1960.

21. Levings, N. Jr., "Launching and Alightment Systems for Aero-Space Vehicles," WADD Technical Report 60-857, May 1961.

22. McFarland, R. K., Jr., "A Limit Analysis of the Collapse of Hexagonal Cell Structures Under Axial Load," Technical Report No. 32-186, December 1, 1961, Jet Propulsion Laboratory.

23. "Permanent Satellite Base and Logistics Study," Vol. III, Human Engineering Study, Vought Astronautics, June 30, 1961, (Confidential).

24. "Permanent Satellite Base and Logistics Study, Vol. IV, Lunar Payload Design," American Machine & Foundry Co., June 30, 1961, (Secret).

25. "Permanent Satellite Base and Logistics Study, Vol. V, Geology and Environment," American Machine & Foundry Co., June 30, 1961, (Confidential).

26. "Permanent Satellite Base and Logistics Study (SR 17532), Vol. I, Part 1, Summary," Final Report, North American Aviation, Space and Information Systems Division, 30 June 1961.

27. "Physiological and Psychological Considerations for Manned Space Flight," CVA Report E9R-12349, Revised July 7, 1959, Chance Vought Aircraft, Dallas, Texas.

28. "Results of the First United States Manned Orbital Space Flight," NASA, February 20, 1962.

29. Roark, R. J., Formulas for Stress and Strain, 3rd Edition, McGraw-Hill, 1954.

30. Schneider, P. J., Conduction Heat Transfer, Addison-Wesley Publishing Company, 1955.

31. Seifert, Howard, Space Technology, John Wiley and Sons, Inc., New York, 1959.

32. Spady, Amos, Jr., "An Exploratory Investigation of Jet-Blast Effects on a Dust-Covered Surface at Low Ambient Pressure," NASA TN D-1017, February 1962.

33. Stone, Irving, "Surveyor Lunar Spacecraft Has Varied Approaches" Aviation Week, January 30, 1961.

34. Thompson, J. N. and Ripperger, E.A., "Cushioning For Aerial Delivery," Part III, Bul. #30, Shock, Vibration and Associated Environments, February, 1962, Off. of Sec. of Defense.

35. "Aviation Week and Space Technology", March 12, 1962, Pg. 183.

36. Hunsaker and Rightmire, Engineering Applications of Fluid Mechanics, McGraw - Hill Book Co. New York, 1947.

APPENDIX I

SPECIFIC ENERGY CAPACITY
OF METAL HONEYCOMBS

Problem: Establish the specific energy capacity of a Mar-Aging
Steel honeycomb structure.

Symbols (with typical units):

A = Actual cross-sectional Area of Metal (in^2)

C = Specific energy capacity of absorber (per Unit Weight) (ft.-lb./lb.)

f_A = Ratio of Metal Volume to Total Honeycomb Volume

p_{av} = Mean crushing stress (psi)

R = Ratio of cell wall thickness to cell diam.

t = Cell wall thickness (in)

ρ_h = Honeycomb density (lb.-sec.^{2}/in.^{4})

ρ_m = Material density (lb.-sec.^{2}/in.^{4})

ϵ = Peak strain

η := Efficiency

σ_{yp} = Tensile yield strength (psi)

q_{yp} = Shear strength (psi)

The following relation is taken from reference 22:

$$p_{av} = \sigma_{yp} \ R^2 \ (\frac{4.750}{K} + 14.314) + 1.155 \ R \ q_{yp}$$

where K is a factor determined by the deformation characteristics
and is about 0.4 for hexagonal cell metal honeycomb structures.

$$P_{av} = \left(40.5\,R + 1.155\,\frac{q_{yp}}{\sigma_{yp}}\right)\,R\,\sigma_{yp}$$

$$C = P_{av}\,\epsilon\,/\,\rho_{h}g \quad \text{(See Summary of Principal Equations, Appendix V)}$$

$$C = \frac{\epsilon}{\rho_{h}g}\,(40.5\,R + 1.155\,\frac{q_{yp}}{\sigma_{yp}})\,R\,\sigma_{yp}$$

Determination of $\rho_h g$ in terms of geometry and density of material for hexagonal cell honeycombs:

$$A = (b - 2a\,\cos\frac{\pi}{3})\,t + 2at$$

$$A = b + 2a\,(1 - \cos\frac{\pi}{3})\,t$$

$$A = (b + a)\,t$$

$$h = (a\,\sin\frac{\pi}{3}) + t$$

$$h = \frac{a}{2}\,\sqrt{3} + t$$

$$a = 2\,(h - T)/\,\sqrt{3}$$

$$b = 2a + 2a\,\cos\frac{\pi}{3} = 2\,a\,(1 + 1/2) = 3a$$

$$A = 4\,at$$

$$f_A = A/bh = \frac{4}{3}\,\frac{t}{h}$$

$$R = \frac{t}{2h}$$

$$f_A = \frac{8}{3}\,R$$

$$\rho_h = f_A\,\rho_m$$

$$\rho_h g = f_A\,(\rho_m g) = \frac{8}{3}\,R\,\rho_m g$$
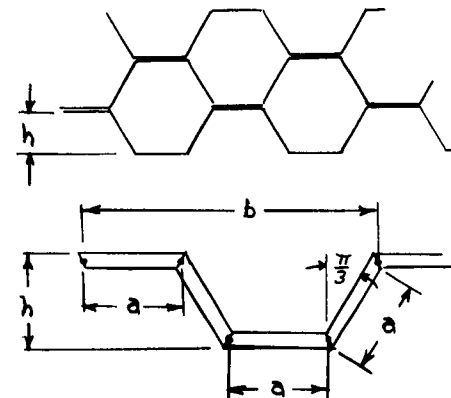
Specific energy capacity can be determined as follows:

$$C = \frac{\text{Average Force} \cdot \text{Stroke}}{\text{Weight Density} \cdot \text{Volume}}$$

$$C = \frac{p_{av} \cdot (Area) \cdot \epsilon \cdot (height)}{\rho_h \cdot (Area) \cdot (height)}$$

$$C = \frac{3}{8} \frac{\sigma_{yp} \epsilon}{\rho_m} \left(40.5 \, R + 1.155 \, \frac{q_{yp}}{\sigma_{yp}}\right)$$

Evaluating p_{av} and C based on 80% compression for Mar-Aging Steel:

$\rho_m = 0.283 \, \#/in^3$

$\epsilon = 0.8$

$\sigma_{yp} = 250,000$ psi

$q_{yp} = 0$ (this value is based on the recommendation of the author of reference 22 that the shear deformation mechanism was found not to be a significant factor for Mar-Aging Steel in work carried out by the author subsequent to the publication of reference 22.)

$$p_{av} = 10.1 \, R^2 \cdot 10^6 \text{ psi}$$

$$C = 894,000 \, R \text{ ft-lb/lb}$$

R	0.033	0.030	0.020	0.013	0.010
p_{av} (psi)	11,000	9,100	4,050	1,710	1,010
C (ft-lb/lb)	29,500	26,800	17,900	11,600	8,940

APPENDIX II

SPECIFIC ENERGY CAPACITY OF IDEAL GASES

Problem: Establish the specific energy capacity of an ideal gas where the gas is compressed adiabatically and then bled at constant pressure.

Symbols (with typical units):

E = Total energy dissipated (ft. -lb.)

E_c = Work done in compressing gas (ft. -lb.)

E_b = Work done in bleeding gas (ft. -lb.)

p = Gas pressure (psi)

W = Total weight of gas (lb.)

V = Total volume of gas (in^3)

m = Total mass of gas (lb. -sec.^{2}/in.)

T = Absolute temperature of gas (°Rankin)

R = Gas constant = $p V / (W T)$ (ft. / °Rankin)

C = Specific energy capacity of gas (per unit weight) (ft. -lb. /lb.)

Subscripts "o" and "c" denote conditions at begining and end of compression stroke, respectively.

$$E = E_c + E_b$$

$$E_c = - \int_{V_c}^{V_o} p \, dv$$

$$E_b = p_c V_c$$

$$E_c = - p_o V_o \int_{V = V_o}^{V = V_c} \left(\frac{V_o}{V} \right)^k d\left(\frac{V}{V_o} \right)$$

$$E_c = \frac{-p_o V_o}{1 - k} \left[\left(\frac{V}{V_o} \right)^{(1-k)} \right]_{\frac{V}{V_o} = 1}^{\frac{V}{V_o} = \frac{V_c}{V_o}} = \frac{p_o V_o}{1 - k} \left[1 - \left(\frac{V_c}{V_o} \right)^{(1-k)} \right]$$

bleed phase

compression phase $\left(p V^k = p_o V_o^k \right)$

64
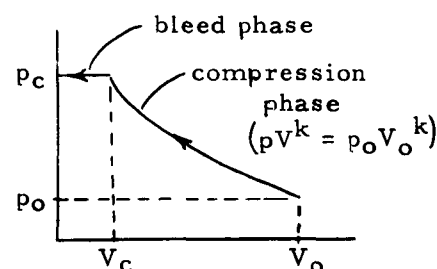
$$\frac{V_c}{V_o} = \left(\frac{p_o}{p_c}\right)^{\frac{1}{k}}$$

$$E_c = \frac{p_o V_o}{1-k}\left[1 - \left(\frac{p_o}{p_c}\right)^{1-k}\right] = \frac{p_o V_o}{k-1}\left[\left(\frac{p_c}{p_o}\right)^{\frac{k-1}{k}} - 1\right]$$

$$V_c = V_o\left(\frac{p_o}{p_c}\right)^{\frac{1}{k}} \qquad\qquad p_c = p_o\left(\frac{p_c}{p_o}\right)$$

$$p_c V_c = p_o V_o\left(\frac{p_c}{p_o}\right)^{\frac{k-1}{k}}$$

$$E = \frac{p_o V_o}{k-1}\left[k\left(\frac{p_c}{p_o}\right)^{\frac{k-1}{k}} - 1\right]$$

$$pV = W \cdot R \cdot T$$

$$W = \frac{pV}{RT} = \frac{p_o V_o}{RT}$$

$$C = \frac{RT}{k-1}\left[k\left(\frac{p_c}{p_o}\right)^{\frac{k-1}{k}} - 1\right]$$

For Air at approximate mean temp of 530°R:

$$R = 53.35 \text{ Ft/°R}, \quad k = 1.40$$

$$C = 2.5\left(53.35\frac{Ft}{°R}\right)(530°R)\left[1.4\left(\frac{p_c}{p_o}\right)^{0.286} - 1\right]$$

$$C = 70,700 \text{ ft}\left[1.4\left(\frac{p_c}{p_o}\right)^{0.286} - 1\right]$$

$\frac{p_c}{p_o}$	$\left(\frac{p_c}{p_o}\right)^{0.286}$	$1.40\left(\frac{p_c}{p_o}\right)^{0.286} - 1$	$C\left(\frac{ft-lb}{lb}\right)$
2	1.219	0.72	50,900
4	1.485	1.08	76,500
10	1.930	1.70	120,000

APPENDIX III

SPECIFIC ENERGY CAPACITY OF DUCTILE METALS

Problem: Establish the specific energy capacity of ideal elasto-
             plastic materials subject to gross plastic tensile strain.

Symbols (with typical units):

C =   Specific energy capacity of deformable element.   (ft. -lb. /lb.)

E_a = Energy absorbed in deforming element.   (ft. -lb.)

W =   Weight of Element.   (lb.)

A =   Cross-sectional area of element.   (in^2)

L =   Length of Element.   (in.)

ρg =   Weight density of Element.   ($\#/in^3$)

P =   Tensile Load at yield.   (lb.)

σ_{yp} = Tensile Yield Stress (psi)

δ =   Total deflection of deformable element. (in.)

δ_e = Elastic limit deflection of element. (in.)

ϵ =   Total Strain of element.

E =   Elastic Modulus of element.   (psi)

$$C = \frac{E_a}{W}$$

$$W = AL\,\rho g$$

$$E_a = P\left(\delta - \frac{\delta_e}{2}\right)$$

$$P = \sigma_{yp}A$$

$$\delta = \epsilon L$$

$$\delta_e = \frac{PL}{AE} = \frac{\sigma_{yp}}{E}\,L$$

$$C = \frac{\sigma_{yp}}{\rho g}\left(\epsilon - \frac{\sigma_{yp}}{2E}\right)$$
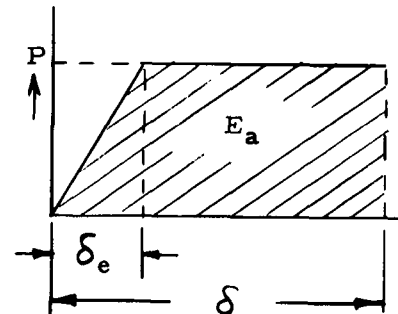
Based on values typically reported for rupture strain (% elongation) and yield stress, the following capacities can be established. See Section 4.1 for discussion of rupture strains.

Material	Steel ASTM-A7	Aluminum ASTM 3003	Aluminum ASTM 2024
σ_{yp} (10^3 psi)	45	10	25
ϵ (%)	20	25	15
ρg (lb/in^3)	0.282	0.0975	0.0975
E (10^6 psi)	29	10.0	10.6
C (ft-lb/lb)	2650	2130	3180

APPENDIX IV

SPECIFIC ENERGY CAPACITY OF FRICTION ABSORBERS

Problem: Establish order-of-magnitude values for specific energy capacity for coulomb friction energy absorption elements.

Symbols (with typical units):

K = Conductivity (BTU/hr-ft - °F)

c_p = Heat Capacity (BTU/lb - °F)

C = Specific energy capacity per unit weight (ft-lb/lb)

α = Thermal diffusivity (ft^2/hr)

t_1 = Surface temp. which is constant for $\theta > 0$ - °F

t_i = Initial temp. of unit (°F)

ℓ = Thickness of disc(ft.)

γ = Specific weight of unit (lb/ft^3)

θ = Instantaneous time (secs.)

$\vdash\Theta\dashv$ = Fourier Modulus = $\alpha\theta / \delta_1^2$

$\delta_1 = \ell/2$ (ft.)

Configuration of device

A satisfactory device to convert the kinetic energy of landing to thermal energy by means of coulomb friction is a series of discs pressed together in a stack. Alternate discs are keyed to a moving shaft while the others are held fixed. This arrangement is shown in the following diagram.
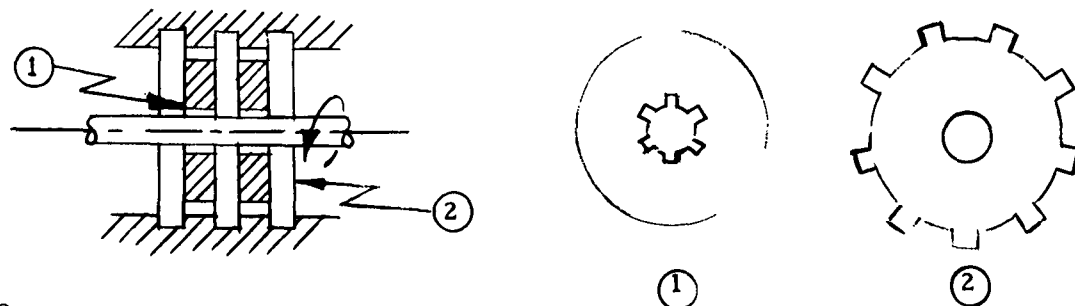
The temperature distribution in the individual plates must be evaluated in order to determine the size of the discs for materials of interest. It is necessary to make some assumptions about the system in order to reduce the complexity of the analysis.

Assumptions

1. The mating surfaces of the discs are at the same temperature.

2. All of the energy is absorbed by the discs.

3. The vehicle is decelerated at a constant rate.

4. The surface temperature of the discs is constant (see discussion below).

5. There is no radial heat flow.

Accounting for variable boundary temperature of the discs complicates evaluation of the heat flow into the dics considerable. Since it is desired that energy be absorbed at a nominally uniform rate, the boundary temperature may be expected to vary more or less uniformly from an initial value to a maximum value. It is assumed that the total heat flow into the discs under such conditions can be reasonably approximated by the heat flow associated with a constant boundary temperature equal to the mean value between initial and maximum boundary temperatures. The deriviation at the end of this appendix demonstrates that material strength is not a major factor in determining the weight of energy absorption elements and it is therefore assumed that the surface temperature of the discs can be raised to the value at which material strength is derated to 10% of nominal room temperature values.

The temperature at the center of a flat plate of thickness,   is given as a function of time by the following equation:

$$\frac{t - t_1}{t_j - t_1} = \frac{4}{\pi} \sum_{n=1}^{\infty} \frac{1}{n} \ (e)^{-\ (n\pi/2)^2 \theta} \sin \frac{n\pi}{2} \quad ; n = 1, 3, 5 \ldots$$

(See reference 30, page 235)

Deceleration time

θ = V/a = 35/10 (32.2) = <u>0. 109 sec.</u>

The thickness required for aluminum and steel to obtain a temperature at the center of the disc which is 95% that of the boundary temperature after 0.109 sec. have been determined as below. Any thickness values less than these will provide a thermal efficiency of virtually 100%. The values established are sufficiently thick so that this is not a significant design limitation.

Disc thickness for aluminum

Material: Al 2219 - T8

Let $\dfrac{t - t_1}{t_i - t_1} = 0.05$

From Figure 10-2, page 235 of reference 30.

$\theta = 1.38$

$\theta = \alpha \theta / \delta_1^2 ; \quad = K/c \gamma$

$\gamma = 0.10$ lb/in^3, K = 128 BTU/hr-ft-°F, c = 0.215 BTU/lb - °F

$\alpha = 128/0.215$ (0.10) (172.8) = 3.45 ft^2/hr.

$\theta = \dfrac{3.45 \ (0.109)}{(L/2)^2 \ (3600)} = 0.000418/\ell^2$

$\ell^2 = 0.00418/\theta = 0.000418/1.38 = 0.000308$

$\ell = 0.01752$ ft. = <u>0.21 in.</u>

Disc thickness for steel

Material: Alloy Steel

Let $\dfrac{t - t_1}{t_i - t_1} = 0.05$

From Figure 10-2, page 235 of reference 30.

$\theta = 1.38$

$\gamma = 0.283$ lb/in^3, K = 22.0 BTU/hr-ft-°F, c = 0.114 BTU/lb-°F

$$\theta = \alpha \theta / \delta_1^2; \quad = K/c$$

$$\alpha = 22/0.114 \, (0.283) \, (1728) = 0.396 \ ft^2/hr.$$

$$\theta = \frac{0.396 \, (0.109)}{(L/2)^2 \, (3600)} = \frac{0.0000481}{L^2}$$

$$\ell^2 = 0.0000481/\theta = 0.0000481/1.38 = 0.0000349$$

$$\ell = 0.0059 \ ft = \underline{0.076 \ in.}$$

Specific Energy capacity

Aluminum

$$E = W \ c_p \, (\ t) \qquad\qquad \text{Where} \quad n \quad \text{is approximately 1.0 for this unit.}$$

$$C = \frac{E}{W} = c_p \Delta t$$

$$t_i = 200 \ °F$$

$$t_{max} = 640 \ °F \ \text{(Temperature at which yield strength is 10\% of strength at room temperature)}$$

Average surface temperature

$$t_{avg} = (t_i + t_{max})/2 = 420 \ °F$$

$$C = 0.215 \, (420 - 200) \, (778) = \underline{36,800} \ ft\text{-}lb/lb$$

Steel

$$t_i = 200 \ °F$$

$$t_{max} = 1200 \ °F$$

Avg. surface temp.

$$t_{avg} = (t_i + t_{max})/2 = 700 \ °F$$

$$C = 0.114 \, (700 - 200) \, (778) - \underline{44,400} \ ft\text{-}lb/lb.$$

Proportioning the discs

The proportions of the disc are dependent on the amount of energy absorbed (E), Temperature increase (Δt), torque transmitted (T), and shear strength (S).

Volume (V) of material required

$$V = E/\{c_p \, (\Delta t) \eta \gamma\} = (R^2 - r^2) \pi L$$

Torque transmitted

$$T = SAr$$

The shear area (A) for the discs is only 1/2 of the total circumferential area available due to the splines required to lock the discs to the shaft. Further, the length of discs locked to the shaft is only 1/2 the total stack length.

$$A = \frac{1}{2} \left(2 \pi r \frac{\cdot}{2}\right) = \frac{1}{2} \pi r L$$

Combining the above equations

$$T/S = \frac{1}{2} \pi r^2 L$$

$$V = \pi r^2 L \left[(\frac{R}{r})^2 - 1\right]$$

$$V = \frac{2T}{S} \left[(\frac{R}{r})^2 - 1\right]$$

$$S = \frac{2T}{V} \left[\left(\frac{R}{r}\right)^2 - 1\right]$$

This last equation indicates that the strength of the material will not be a critical factor since the ratio of external to internal disc radii can be adjusted to accomodate available material strengths.

APPENDIX V

SIZING BULK ENERGY ABSORBERS

Problem: Determine proportions of bulk energy absorber required to accomodate specific alightment parameters.

Alightment Parameters (with typical units):

m = Vehicle mass (lb. -sec.^{2}/in.)

V = Impact Velocity (in. /sec.)

a = Peak deceleration (including gravity) (in. /sec^2)

η = Deceleration efficiency

δ = Deceleration Stroke (in.)

γ = ratio of local to earth gravity

Energy Absorber Parameters (with typical units):

C = Specific energy capacity (in. -lb. /lb.)

p = Peak crushing pressure (psi)

ρ_g = weight density (lb/in^3)

E = Total Energy Capacity (in. -lb.)

W = Total weight (lb.)

Vol = Total Volume (in^3)

A = Cross section area (in^2)

h = height (in.)

ϵ = energy absorbing strain

p_{av} = average crushing pressure (psi)

$\eta = p_{av}/p$

From the foregoing definitions and elementary mechanical properties, the following relations can be developed:

$$\delta = \epsilon h$$

$$Vol = Ah$$

$$W = \rho_g A h = \rho_g A \delta / \epsilon$$

$$p_{av} = \eta p$$

$$E = \eta m a \delta = p_{av} A \delta = CW$$

$$E = \frac{1}{2} m V^2 + m \gamma g \delta$$

$$\eta a \delta = \frac{1}{2} V^2 + \gamma_g \delta$$

$$\delta = \frac{1}{2} V^2 / (\eta a - \gamma_g)$$

$$E = \eta m a \delta = \frac{1}{2} m V^2 / \left(1 - \frac{\gamma_g}{\eta a}\right)$$

$$C = \frac{p_{av} A \delta}{W} = \frac{p_{av} \epsilon}{\rho_g}$$

Summary of Principal Equations

$$\delta = \frac{1}{2} V^2 / (\eta a - \gamma_g)$$

$$h = \delta / \epsilon$$

$$C = \epsilon p_{av} / \rho_g$$

$$W = \eta m a \delta / C = \left(\frac{m V^2}{2C}\right) / \left(1 - \frac{\gamma_g}{\eta a}\right)$$

$$W = \frac{m V^2}{2C} \quad @ \ \gamma_g \ll \eta a$$

$$A = \eta m a / p_{av} = \epsilon W / (\rho_g \delta)$$

Proportions for Mar-Aging Steel Honeycomb Absorber with Cell Wall Diam. ratio (R) = 0.013, force efficiency (η) = 0.9, and Strain (ϵ) = 0.8:

$mg = 10^5$ lb

$V = 35$ fps

$a = 10g$

$\gamma = 0.165$

$p_{av} = 1710$ psi

$\rho_g = \left(\dfrac{8}{3}\right) R \ (0.283 \ lb/in^3)$

$\left.\phantom{\begin{array}{c}x\\x\end{array}}\right\}$ See Appendix I

$\rho_g = 0.0098 \ lb/in^3$

$\delta = 25.8$ in.

$h = 32$ in.

$A = 526$ in.^{2}

$W = 166$ lb.

APPENDIX VI

WEIGHT ANALYSIS OF HYDRAULIC CYLINDER ABSORBERS

Problem: Determine the total weight of a hydraulic energy absorption
system for alightment.

Symbols (with typical units):

σ_c = Cylinder hoop stress (psi)

σ_e = End Cap Stress (psi)

W_c = Weight of Cylinder (lb.)

W_e = Weight of piston and end cap. (lb.)

W_o = Weight of oil (lb.)

W_p = Weight of piston rod (lb.)

A_p = Piston rod area (in^2)

E = Alightment energy (in. -lb.)

δ = Stroke of piston (in.)

F = Maximum piston force (lb.)

p = Maximum fluid pressure (psi)

η = Force efficiency of energy absorption system

ρ_g = Weight density of cylinder material (lb. /in^3)

α = Fluid weight density $\div$ ρ_g
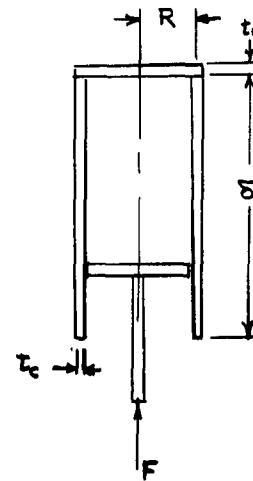
Cylinder stress, $\sigma_c = pR/t_c$ (Case 1, page 268, ref. 29)

End cap stress, $\sigma_e = (3/4)p(\frac{R}{t_e})^2$ (Case 6, page 195, ref. 29)

@ $\sigma_c = \sigma_e = \sigma$

$t_c = p\dfrac{R}{\sigma}, \quad t_e = \sqrt{(3/4p\ R^2/\sigma}$

$W_c = 2\pi R\ t_c\ \delta\ (\rho g)$

$W_e = 2\pi R^2\ t_e\ (\rho g)$

$W_p = A_p\ \delta\ (\rho g),$

$W_o = \alpha\ (\rho g)\ \pi R^2 \delta$

$F\quad = \pi R^2 p$

$E\quad = \eta F \delta$

$A_p\quad = F/\sigma$ (discounting buckling problems)

$P = \dfrac{F}{\pi R^2} = \dfrac{E}{\pi R^2 \eta \delta}$

$W_c = 2\ E\ (\rho g)/(\eta \sigma)$

$W_e = \dfrac{(\rho g)}{p}\sqrt{\dfrac{3}{\pi \sigma}}\ \left(\dfrac{E}{\eta \delta}\right)^3$

$W_p = F\delta(\rho g)/\sigma\ =\ E\,(\rho g)\,/\,(\eta \sigma)$

$W_o = \alpha(\rho g)\ E/(\eta p)$

$W_{total} = W_c + W_e + W_p + W_o$

Inspection of these weight formulae shows that the total weight is independent of the number of cylinders provided buckling is no problem. Cylinder weights for Tripod Alightment configuration are given below (It is probable that buckling problem will increase piston rod weight):

$\alpha = 0.115, \quad \eta = 0.85$

$\rho g = 0.283\ lb/in^3$

$\sigma = 60,000\ l.c.$

$E = \dfrac{1}{3}\ (1.9 \cdot 10^6\ ft\text{-}lb)$

Case I: $\delta = 27"$	Case II: $\delta = 54"$
$p = 5000$ PSI	$p = 5000$ PSI
$W_{tot} = 271$ lb/cylinder	$W_{tot} = 243$ lb/cylinder

APPENDIX VII

FUEL SAVINGS WITH ASSISTED TAKE-OFF

Problem: Determine the fuel savings associated with using the landing system as a catapult type engine in lieu of using rocket engines to impart the same value of energy to the vehicle assuming that the energy capacity of the catapult system is equal to the energy absorbed at alightment and that the launch acceleration rate is equal to the deceleration rate at alightment. Assume also that the acceleration rate is constant.

Symbols (with typical units):

W = vehicle weight (total) (lb.)

w_r = weight of fuel consumed by rocket engine (lb.)

w_c = weight of fuel consumed by catapult engine (lb.)

e = specific chemical energy of fuel (per unit weight) (ft.-lb./lb.)

η_r = rocket engine combustion efficiency

η_c = catapult engine efficiency

E = alightment (& launch) energy (ft.-lb.)

V = alightment velocity (ft./sec.)

T = acceleration thrust (lb.)

a = acceleration magnitude (ft./sec.^{2})

s = acceleration stroke (ft.)

t = duration of acceleration (sec.)

γ = ratio of local gravity to earth gravity

$I = T\,t/w_r = \sqrt{2\,\eta_r\,e/g}$ = Specific impulse of rocket engine (lb.-sec./lb.)

$$\eta_r = I^2 g/(2_e)$$

$$T = \frac{W}{g} \gamma \; g = \frac{W}{g} \; a$$

$$V = at$$

$$V^2 = 2\,a\,s$$

$$w_r = T \left(t/I\right)$$

$$w_r = \frac{W}{g} \; (a + \gamma g) \left(\frac{V}{a}\right) \Big/ \sqrt{2\,\eta_r e/g}$$

$$w_r = W \; V \; (1 + \frac{\gamma g}{a}) \Big/ \sqrt{2\,\eta_r\,eg}$$

$$a = V^2/2\,s$$

$$w_r = W \cdot V \; (1 + \frac{2\gamma g s}{V^2}) \Big/ \sqrt{2\,\eta_r\,eg}$$

$$E = \eta_c \, e \, w_c$$

$$E = T \cdot s$$

$$E = \frac{W}{g} \left(a + \gamma g\,s\right)$$

$$E = \frac{W}{g} \left(\frac{V^2}{2} + \gamma_{gs}\right)$$

$$w_c = \frac{W}{\eta_c e} \left(\frac{V^2}{2g}\right)\left(1 + \frac{2\gamma gs}{V^2}\right)$$

$$@ \begin{cases} W = 10^5 \text{ lb.} \\ V = 35 \text{ ft/sec} \\ \gamma = 0.165 \\ e = 4.5 \left(10^6\right)\text{ft} \; (H_2 + O_2) \\ I = 340 \text{ sec.} \\ \eta_r = 0.1 \;\; \text{(typical for gun)} \end{cases} \Big\} \text{ ref. 36}$$

$$\eta_r = 0.41$$

$$\frac{2\gamma_g}{V^2} = \left(7.22 \times 10^{-4}\right) s \left(\frac{1}{\text{in}}\right)$$

$$\sqrt{2\,\eta_r\,e\,g} = 10{,}780 \text{ ft/sec}$$

$$w_r = 325\,\# \,(1 + 7.22 \times 10^{-4})\, s \left(\frac{1}{\text{in}}\right)$$

$$w_c = 4.23\,\# \,(1 + 7.22 \times 10^{-4})\, s \left(\frac{1}{\text{in}}\right)$$

s (in)	27	54	108
$\left\{1 + \left(\frac{7.22}{10^4}\right)\right\} s$ (in.)	1.0195	1.039	1.078
w_r (lb)	331	338	350
w_c (lb)	4.3	4.4	4.6
$(w_r - w_c)$ (lb)	327	334	345

80

APPENDIX VIII

SURFACE CONTACTOR STRESS ANALYSIS

Problem: Determine the configuration and sizes required for the surface contactors.

Symbols (with typical units):

τ = Stress, shear (psi)

σ = Stress, tensile (psi)

F = Impact force (lb.)

ν = Poisson's ratio

R = Outside radius of plate being analyzed (in.)

r_o = Radius of load application (in.)

t = thickness of plate being analyzed (in.)

p = pressure acting on lunar surface (psi)

n = number of ribs

I = moment of inertia (in^4)

A = Area (in^2)

w = weight of surface contactor components (lb.)

ρg = weight density $(lb. /in^3)$

Material: 18 NiCoMo (300) Mar-Aging Steel

σ_{allow} = 175, 000 psi

τ_{allow} = 0. 6 σ_{allow} = 105, 000 psi

ν = 0. 26, m = $1/\nu$ = 3. 85, ρg = 0. 283 lb/in^3

$p_{avg} = 200$ psi

For a triangular pressure distribution

$$P_1 = 2\, P_{avg} = 400 \text{ psi}$$
$$P_2 = 0.75\, p_1 = 300 \text{ psi}$$
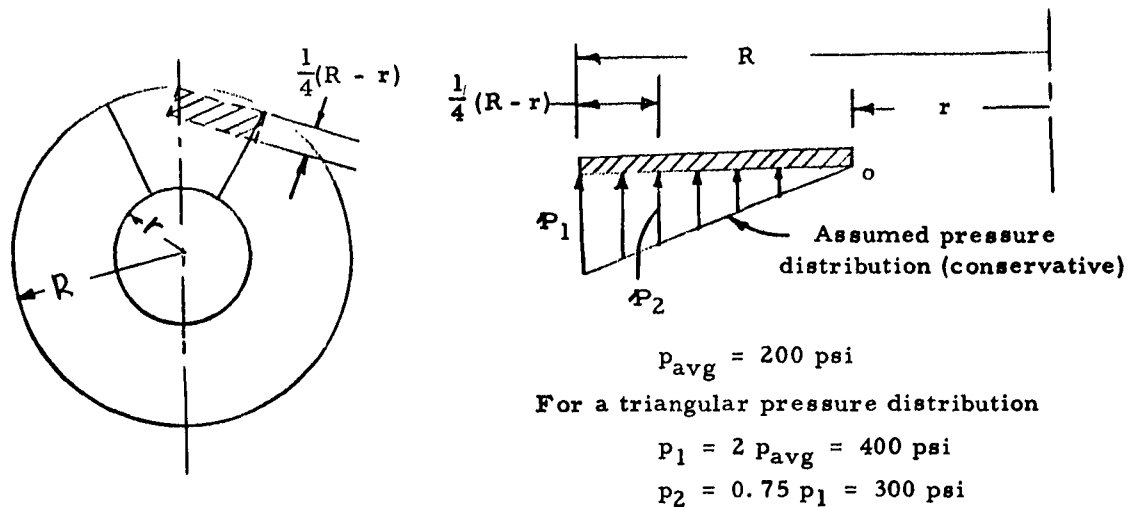
The average pressure acting over the shaded strip in the above diagram is $p = (300 + 400)/2 = 350$ PSI.
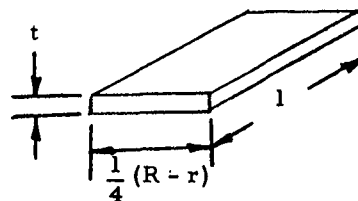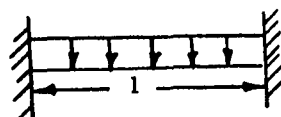
$l = 2\pi R/n$ $A = 1/4\,(R-r)\quad = 1/4\,(R-r)\,(2\,R)/n$

$\nabla = M/Z\ = 1/12\ pA\ l/Z$

$Z = (1/4)(R-r)\ t^2/6$

$$\nabla = \frac{4\,p\,A\pi R}{(R-r)\,t^2\,n} \qquad = \qquad \frac{2\,\pi^2\,p\,R^2}{t^2\,n^2}$$

$$t^2\,n^2 = 2\pi^2\,p\,R^2/\nabla$$

$P = 400$ psi

83
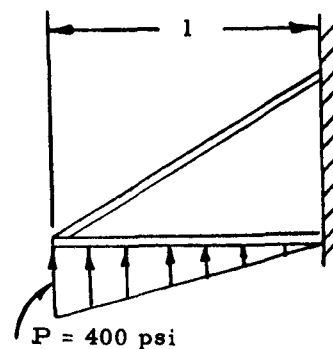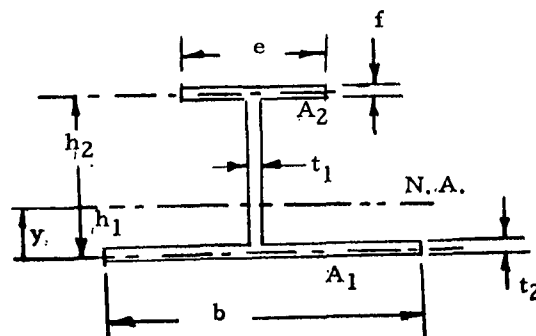
3. Rib

The rib consists of a web made of sheet steel and a top flange plate. The web is made triangular in shape along the length of the rib to eliminate material from regions which are not highly stressed. The rib is analyzed as a beam fixed at one end with the portion of the outer plate stiffened by the rib forming the lower flange. It is assumed that all of the bending load is taken by the flanges and all of the shear load is resisted by the web.

a. Web

$$b = \pi (R + r) / n \qquad F = pb (R-r)$$

$$A = (3/2) \, F / \tau \qquad \text{(For a rectangular section)}$$

$$A = t_1 (h_1 + h_2)$$

$$t_1 = (3/2) \frac{P \pi (R^2 - r^2)}{\tau \, n \, (h_1 + h_2)}$$

where n = number of ribs.

b. Upper Flange

$$\tau = Mh_2/I \qquad M = 2/3 \, (pb) \, (R-r)1$$

$$I = A_1 h_1^2 + A_2 h_2^2 \qquad B = 2 \pi r/n \quad \text{(Conservative)}$$

$$\frac{h_1}{h_2} = \frac{A_2}{A_1} \qquad A_1 = bt_2$$

$$h_2 = \frac{A_1 \, (h_1 + h_2)}{\left[\frac{M}{\tau} + A_1 \, (h_1 + h_2) \right]}$$

$$A_2 = \frac{h_1}{h_2} \qquad A_1 = ef$$

84

4. Upper Support Ring

$$\nabla = pR/t$$
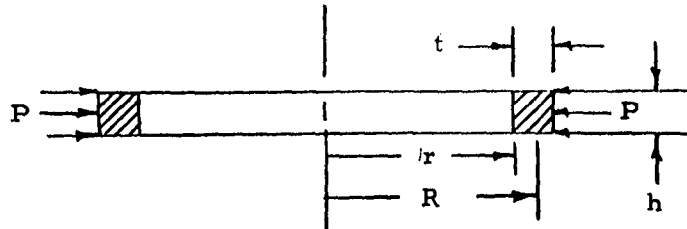
$$\nabla = \frac{F\ (r + t/2)}{2\ \ (r+t)\,h\,t}$$

$$R = r + t/2$$

$$p = F/A = F/2\pi\ (r+t)\,h$$

where F is the force transmitted from the upper flange of the rib.

from which the dimensions t and h can be determined.

5. Support Tube
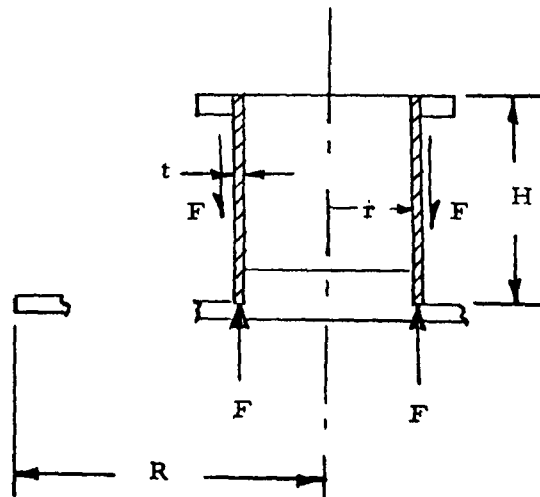
The tube resists the shear from the webs.

$$F = p\,\pi\,(R^2 - r^2)$$

$$A = F/\nabla$$

$$A = 2\pi\,r\,t$$

$$t = \frac{F}{2\,\pi\,r\,\nabla}$$

SUMMARY OF RESULTS

UNIT	TRIPOD Weight - lb.	QUADRIPOD Weight - lb.
Center Plate	62. 1	47. 2
Outer Plate	137. 5	45. 6
Ribs	40. 1	14. 2
Upper Support Ring	6. 2	4. 2
Support Tube	2. 2	1. 2
Total for One Unit	248. 1	112. 4
Total	744. 3	449. 6

APPENDIX IX

STABILITY ANALYSIS

Problem: For the mission parameters of Section 2, determine the horizontal "reach" required to prevent upset for a rigid undercarriage and for a self-aligning undercarriage.

Symbols (with typical units):

γ = Ratio of local gravity to earth gravity

V_h = Horizontal velocity (ft. /sec.)

α = Inclination angle of surface (radians)

b = Height of obstacle (ft.)

r = Reach (ft.)

L = Increase in c.g. height during tipping. (ft.)

β = Initial vehicle tilt (radians)

Upset will not occur if the horizontal kinetic energy of the vehicle at touchdown is exceeded by the increase in potential energy of the vehicle as it moves from its initial contact status to its incipient upset status.

For a rigid system:

@ $\sin \alpha = \alpha$

$\sin \beta = \beta$

$$m \, \gamma \, gL = (1/2) m \, V_h^2$$

$$\sqrt{V_h^2 + (a_i r)^2} = h + b + L + (a_1 + a_2) \, r \alpha + a_2 r \, \beta$$

$$\delta_1 = b + L = b + \frac{V_h^2}{2 \gamma g}$$

@ $a_o = a_1 + a_2$

$$h^2 + a_1^2 \, r^2 = \left[h + \delta_1 + (a_o \alpha + a_2 \beta) \, r \right]^2$$

$$h^2 + a_1^2 \, r^2 = h^2 + 2 h \delta_1 + \delta_1^2 + 2 (h + \delta_1) (a_o \alpha + a_2 \beta) + (a_o \alpha + a_2 \beta)^2 \, r^2$$
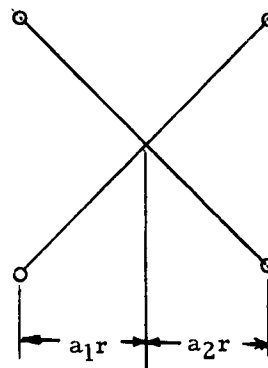
$$\psi = a_o \alpha + a_2 \beta$$

$$r^2 \left[a_1^2 - \psi^2 \right] - r \left[2 (h + \delta_1) \psi \right] - \delta (2h + \delta_1) = 0$$

$$r = \frac{(h + \delta_1) \psi \pm \sqrt{h^2 \psi^2 + \delta (2h + \delta_1) \, a_1^2}}{(a_1^2 - \psi^2)}$$

$V_h = 3.5 \text{ ft/sec}$ $\qquad\qquad$ $b = 1 \text{ foot}$

$\gamma = 0.165$ $\qquad\qquad$ $\alpha = 3° = 0.0523$

$h = 35 \text{ feet}$ $\qquad\qquad$ $\beta = 1° = 0.0174$

$$\delta_1 = 1 \text{ ft.} + \frac{12.25 \text{ ft.}}{0.165(32.2)} = 2.15 \text{ ft.}$$

$$\psi = 0.0174 \, (3 \, a_1 + 4 \, a_2)$$

88
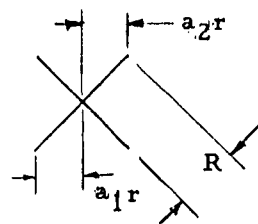
Case I	Case II
$a_1 = 1, \quad a_2 = 1$	$a_1 = 1, \quad a_2 = 2$
$\psi = 0.1218$	$\psi = 0.1914$
$r = 17.95$ ft.	$r = 22.06$ ft.
$R = r\sqrt{2} \doteq 25$ ft.	$a_2 r = 2r = 44$ ft.
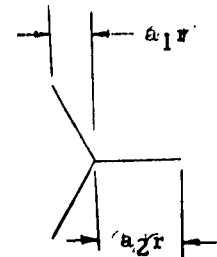
For Self-Aligning System:

Assuming effect of alignment stroke on
c.g. height has negigible infuence on
stability and $\sin\beta = \beta$:

$$L + h(1 - \beta^2) + r\beta = \sqrt{r^2 + h^2}$$

$$\left[L + h(1 - B^2)\right]^2 + r\left\{2\beta\left[L + h(1 - \beta^2)\right]\right\}\ldots$$

$$- r^2(1 - B^2) - h^2 = 0$$

@ $\beta^2 \ll 1$

$$\delta_2 = h + L = h + \frac{V_h^2}{2\gamma g}$$

$$r^2 - r(2\beta\delta_2) - L(h + \delta_2)$$

$$r = \beta\delta_2 \pm \sqrt{(\beta\delta_2)^2 + L(h + \delta_2)}$$

@ $\begin{cases} V_h = 3.5 \text{ ft/sec} \\ \gamma = 0.165 \end{cases}$

$L = 1.15$ ft.

$(\Delta r / \Delta h) = -.14$

$(\Delta r / \Delta \beta) = 0.7$ ft/degree
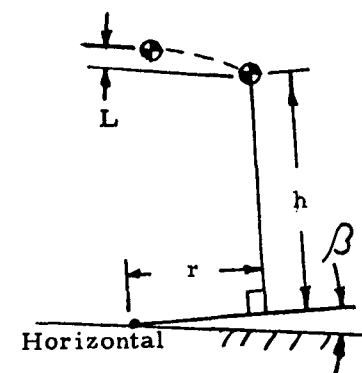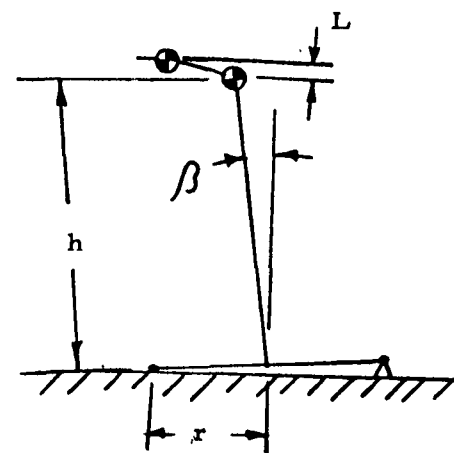
β (deg)	1°	1°	2°
h (ft)	36	35	35
δ_2 (ft)	36.15	37.15	37.15
r (ft)	9.84	9.70	10.4

Testing Tolerable Velocity sensitivity to changing β:

$$r\,\beta = \sqrt{r^2 + h^2} - h - L$$

$$\beta = \sqrt{(h/r)^2 + 1} - \frac{h}{r} - \frac{L}{r}$$

$$\frac{\partial B}{\partial V_h} = -\frac{\partial L}{r\,\partial V_h} = -\frac{V_h}{r\,\gamma\,g}$$

$$@ \begin{cases} \gamma = 0.165 \\ V_h = 3.5 \text{ ft/sec} \\ r = 9.70 \text{ ft.} \end{cases}$$

$$\frac{\partial V_h}{\partial B} = \frac{r\,\gamma\,g}{V_h} = 0.26 \text{ fps/degree}$$

90

DURATION OF TIPPING MOTION

Problem: Perform an approximate "inverted" pendulum analysis to determine the time from touchdown to upset for the "borderline" upset case.

$$mR^2 \ddot{\theta} - m\gamma_g R \theta = 0$$

$$\ddot{\theta} - b^2 \theta = 0$$

$$b = \left| \sqrt{\frac{\gamma_g}{R}} \right|$$

$$\theta = A_1 \cosh(bt) + A_2 \sinh(bt)$$

$$\dot{\theta} = b \left[A_1 \sinh(bt) + A_2 \cosh(bt) \right]$$

To just produce upset:

$$(1/2) m V^2 = m \gamma_g h_o$$

$$V = \left| \sqrt{2 \gamma_g h_o} \right|$$

@ $h \ll R$

$$\cos \theta = \frac{R - h}{R}$$

$$\theta \approx \sin \theta = \sqrt{1 - \cos^2 \theta} \rightarrow \sqrt{2 \frac{h}{R}}$$

@ $t = o$; $\cosh(bt) = 1$ $\theta = \left| \sqrt{2 h_o / R} \right|$

$\sinh(bt) = 0$ $\dot{\theta} = -V/R$

$$A_1 = \theta = \left| \sqrt{2 h_o / R} \right|$$

$$A_2 = \dot{\theta}/b = -V/Rb = -\left| \sqrt{2 h_o / R} \right|$$

Symbols:

t = time (sec)

Geometric symbols per sketch:
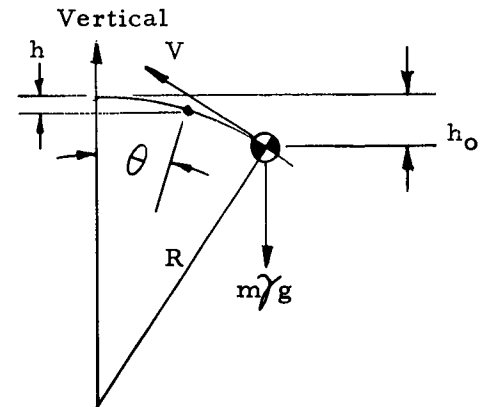
91

@ $t \gtreqless 0$

$$\theta = \left| \sqrt{2\,h_o/R} \right| \left[\cosh(bt) - \sinh(bt) \right] = \left| \sqrt{2\,h_\theta/R} \right| e^{-bt}$$

$$\theta = \left| \sqrt{2\,h/R} \right|$$

$$e^{bt} = \sqrt{h_o/h}$$

$$2\,bt = \ln(h_o/h)$$

$$t = (1/2b)\ln(h_o/h)$$

@ $h = 0,\ t = \infty$

@ $\begin{cases} h = h_o/10 \\ \gamma = 0.165 \\ R = \sqrt{(35ft)^2 + (9.7\ ft)^2} = 36.3\ ft \quad \text{(see Table, Appendix IX)} \end{cases}$

$$1/2\,b = \sqrt{\dfrac{R}{4\gamma g}} = 1.31\ sec$$

$$t = 3.0\ sec.$$

APPENDIX XI

EFFECTS OF UNBALANCE OF
ENERGY ABSORBERS ON TIPPING

Problem: What amount of tilting occurs during landing due to an unbalance of the force characteristics of the energy absorbers.

Symbols (with typical units):

a = Vertical deceleration (ft. /sec.)

F = Force acting on vehicle due to energy absorbers (lb.)

h = Height of vehicle c. g. (ft.)

I = Moment of inertia of vehicle about point at which vertical axis of vehicle intersects bottom of vehicle. (lb. -ft. -sec^2)

m = Mass of vehicle (lb. -sec^2/ft.)

r = Vehicle reach (ft.)

T = Torque (ft. -lb.)

t = Time (sec.)

V = Horizontal velocity of c. g. due to tipping (ft. /sec.)

α = Tangential acceleration during tipping (radians/sec^2)

ω = Angular velocity during tipping (radians/sec.)

θ = Vehicle rotation during tipping (radians)

δ_h = Horizontal movement of c. g. due to tipping (ft.)

$$\omega = \alpha t$$

$$\theta = \frac{1}{2}\alpha t^2$$

$$\alpha = T/I$$

$$T = (F_1 - F_2) r$$

$$F_1 + F_2 = ma$$

$$\text{Let } A = F_2/F_1$$

$$T = F_1 (1 - A) r$$

$$ma = F_1 (1 + A)$$

$$I \approx mh^2$$

$$\alpha = \frac{T}{I} = \frac{F_1 (1-A)r}{mh^2} = \frac{a (1-A)r}{(1+A) h^2}$$

$$\alpha = \frac{ar}{h^2} \left[\frac{1 - A}{1 + A} \right]$$

$$V = \omega h = \alpha \cdot t \cdot h$$

$$\delta_h = \omega h \left(\frac{t}{2} \right)$$

$$@ \begin{cases} A = 9/10 \\ a = 10g \\ r = 10 \text{ ft.} \\ h = 35 \text{ ft.} \\ t = 0.1 \text{ sec.} \end{cases}$$

$$V = 0.48 \text{ ft/sec}$$

$$\delta_h = 0.29 \text{ in.}$$
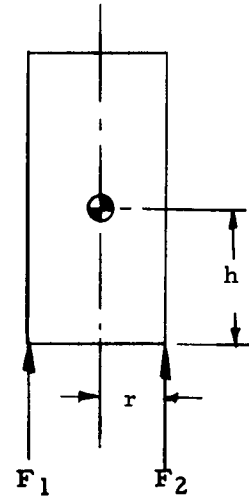
APPENDIX XII

SELF - ENERGIZING LOCK

Problem: Establish criteria for a self-energizing lock.

Symbols (with typical units):

F, N = Normal Forces (lb.)

μ = Coefficient of Friction

θ = Wedge Angle (radians)

Far Sliding Wedge:
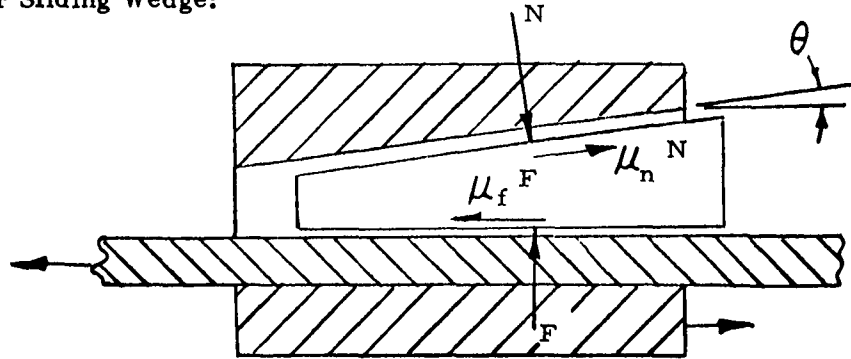
For equilibrium of the wedge:

$$F = N \cos \theta - \mu_n N \sin \theta$$

Lock is self-energizing when $\mu_f F \gtrsim N \sin \theta + \mu_n N \cos \theta$

Combining above equations

$$\mu_f = \frac{N (\sin \theta + \mu_n \cos \theta)}{N (\cos \theta - \mu_n \sin \theta}$$

$$\mu_f = \frac{\sin \theta + \mu_n \cos \theta}{\cos \theta - \mu_n \sin \theta}$$

For small values of θ:

$$\mu_f = \frac{\theta + \mu_n (1)}{1 - \mu_n \theta} = \frac{\theta + \mu_n}{1} = \theta + \mu_n$$

For "Roller" Wedge:
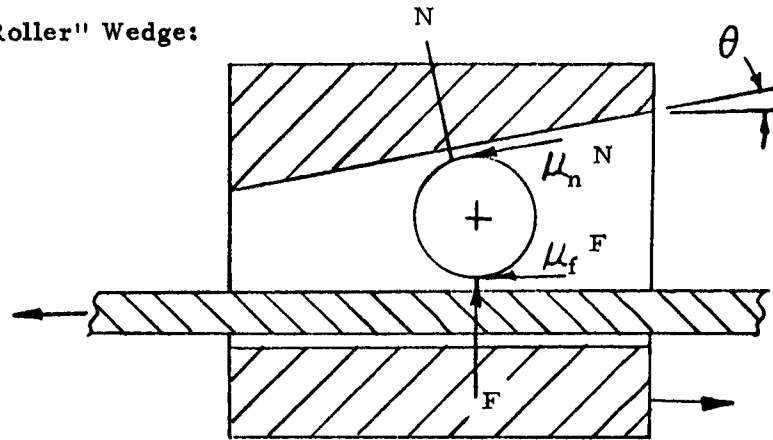
Assuming rolling friction is negligible lock will be self-energizing if μ_f and μ_n are each equal to or less than the minimum value required to prevent slippage.

Far equilibrium of the roller:

$$\mu_n N = \mu_f F$$

$$N \sin \theta = \mu_n N \cos \theta + \mu_f F$$

$$N \cos \theta + \mu_n N \sin \theta = F$$

Combining above equations

$$\sin \theta = \mu_n \cos \theta + \mu_n$$

$$\mu_n = \sin \theta / (1 + \cos \theta)$$

$$\mu_f = \mu_n \frac{N}{F} = \mu_n / (\mu_n \sin \theta + \cos \theta)$$

For small values of θ

$$\mu_n = \mu_f = \frac{\theta}{2}$$

APPENDIX XIII

ALIGNMENT STROKE REQUIREMENTS

Problem: Determine surface contactor displacement requirements for the
quadripod and tripod self-aligning landing systems under the
following conditions (assume an equalizing differential connection
of the lock trip line).

The following surface conditions were used to ascertain the maximum
stroke required during the aligning phase of the landing for the quadripod
and tripod configurations:

1) 3° slope plus a 1 foot obstacle under one contactor.

2) 3° slope plus a 1 foot obstacle under two adjacent contactors.

3) 3° slope plus a 1 foot obstacle under two opposite contactors for
the quadripod configuration and a 1 foot obstacle under one of
two pads on upper portion of slope for the tripod configuration.

In all cases, a nominal displacement criterion is given by the
expression:

$$\sum x_n = 0$$

where x_n is the displacement of strut n having a datum which is the hori-
zontal plane in which all surface contactors can lie when the trip line is
taught. A positive stroke indicates a direction down from the datum.

The maximum stroke requirement found for a given surface contactor
in the following analysis will be the same for all surface contactors since the
landing orientation cannot be predicted.

QUADRIPOD CONFIGURATION

Surface Condition 1
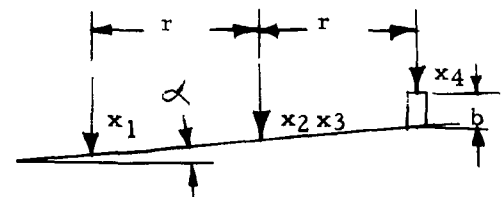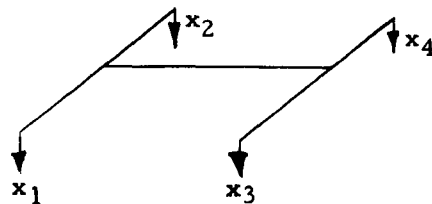
<u>Aligning Conditions</u>   (Conditions required to keep vehicle in pre-alightment
                                            attitude)

$x_2 = x_3$

$x_2 + r\alpha = x_1$

$x_2 - r\alpha = x_4 + b$

By combining these equations with the self aligning criteria the required
stroke for each strut can be determined.

<u>Required Stroke of Each Strut</u>

$x_1 = r\alpha + \dfrac{b}{4}$ $x_3 = \dfrac{b}{4}$

$x_2 = \dfrac{b}{4}$ $x_4 = -(r\alpha + \dfrac{3b}{4})$

@ r = 153 in.

   b = 12" (1' obstacle)

   $\alpha = \pm 3° = \pm 0.0523$

then:

   $x_1 = 9.58", -3.58"$

   $x_2 = x_3 = 3.00"$

   $x_4 = -15.58, -2.42"$

<div align="center">Surface Condition 2</div>

<u>Aligning Conditions</u>

$x_1 = x_2$

$x_3 = x_4$

$x_1 - x_3 = \dfrac{2r}{2} + b$

<u>Required Stroke of Each Strut</u>

$x_1 = x_2 = \left(\dfrac{r\alpha}{2} + \dfrac{b}{2}\right)$

$x_3 = x_4 = -x_1 = -\left(\dfrac{r\alpha}{\sqrt{2}} + \dfrac{b}{2}\right)$

98

@ $r = 153'$

$\alpha = \pm 0.0523$

$r\alpha = 6.58''$

$b = 12''$

then:

$x_1 = x_2 = 10.65'', 1.35''$

$x_3 = x_4 = -10.65'', -1.35''$

Surface Condition 3

Aligning Conditions

$x_2 = x_3$

$x_1 - 2r\alpha = x_4$

$x_1 - r\alpha - b = x_2$

Required Stroke of Each Strut

$x_1 = r\alpha + \dfrac{b}{2}$ $\qquad\qquad x_3 = -\dfrac{b}{2}$

$x_2 = -\dfrac{b}{2}$ $\qquad\qquad x_4 = -r\alpha + \dfrac{b}{2}$

@ $b = 12''$

$\alpha = \pm 3° = \pm 0.0523$

$r = 153''$

$r\alpha = 6.58''$

then:

$x_1 = 12.58''$ or $-0.58''$

$x_2 = x_3 = 6''$

$x_4 = 12.58''$ or $-0.58''$

SUMMARY

Maximum positive stroke = 12.58 in.

Maximum negative stroke = 15.58 in.
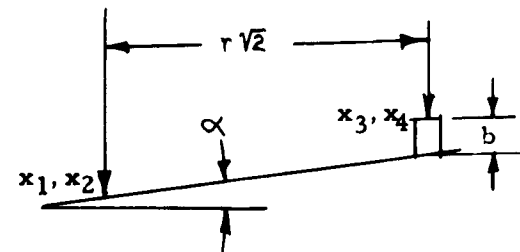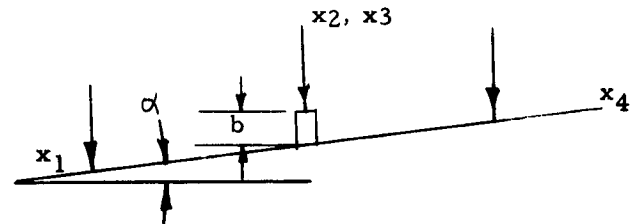
Total stroke = 28.16 in.

99

TRIPOD CONFIGURATION

Surface Condition 1

Aligning Conditions

$$x_2 = x_3$$

$$x_2 = x_1 + b + 3/2\, r\alpha$$

Required Stroke of Each Strut

$$x_1 = -\left(r\alpha + \frac{2b}{3}\right)$$

$$x_2 = x_3 = \frac{r\alpha}{2} + \frac{b}{3}$$

@ $r = 18.2' = 218''$

$\quad \alpha = \pm 0.0523$

$\quad r\alpha = \pm 11.4''$

then::

$\quad x_1 = -19.4'', +3.4''$

$\quad x_2 = x_3 = +9.7'', -1.7''$
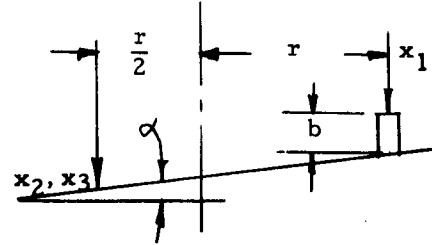
Surface Condition 2

Aligning Conditions

$$x_1 = x_3 + b + \frac{3}{2} r\alpha$$

$$x_2 = x_3$$

Required Stroke of Each Strut

$$x_1 = r\alpha + \frac{2b}{3}$$

$$x_2 = x_3 = -\left(\frac{r\alpha}{2} + \frac{b}{3}\right)$$

@ $b = 12''$

$\quad \alpha = \pm 3° = \pm 0.0523$

$\quad r\alpha = \pm 11.4''$

100
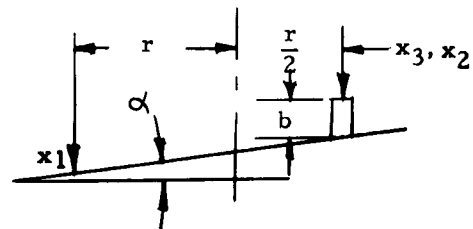
Then:

$$x_1 = +19.4''; \; -3.4$$

$$x_2 = x_3 = -9.7; \; +3.4$$

Surface Condition 3

Aligning Conditions

$$x_1 = x_3 + b + (3/2) r \alpha$$

$$x_2 = x_3 + b$$

Required Stroke for Each Strut

$$x_1 = r\alpha + \frac{2b}{3}$$

$$x_2 = -\frac{r\alpha}{2} + \frac{2b}{3}$$

$$x_3 = -\left[\frac{r\alpha}{2} + \frac{b}{3}\right]$$

@ $b = 12''$

$\alpha = 3° = \pm 0.0523$

$r = 218''$

$r\alpha = \pm 11.4''$

Then:

$$x_1 = -3.4''; \; + 19.4''$$

$$x_2 = +13.7''; \; +2.3''$$

$$x_3 = -9.7''; \; + 1.7''$$

SUMMARY

Maximum positive stroke	=	19.4	in.
Maximum negative stroke	=	19.4	in.
Total Stroke	=	38.8	in.
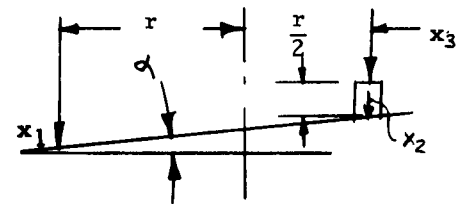
UNDERCARRIAGE STRUCTURAL ANALYSIS

Problem: Perform sample size and weight calculations for a support structure suit-
able for a 100,000 lb. vehicle with a self-aligning tripod alightment system
having a horizontal radius of 18.2 feet to the surface contactor. Assume
Aluminum structural materials with an allowable tensile stress of 60,000
psi, and allowable shear stress of 36,000 psi per Section 3.

$$P_V = 11 \times (100,000 \text{lb}) \times (\tfrac{1}{3}) = 367,000 \text{ lb (per Section 2.3.1)}$$

$$P_R = 0.2 \, P_V = 73,400 \text{ lb.}$$

$$P_T = 0.1 \, P_V = 36,700 \text{ lb.}$$

2.3' dimension based on clearance
requirements per Section 2.3.3 and
Table 1 and alightment stroke of
19.4 per Appendix XIII.
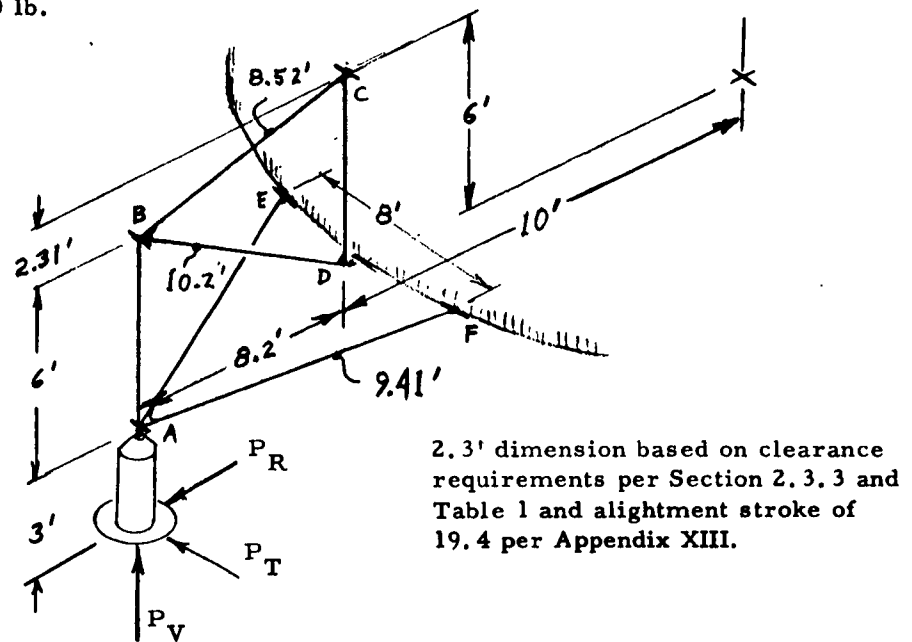
Resultant Axial Loads:

Load applied to member AB	367,000 lb.	Compression
Load applied to member BC	587,000 lb.	Compression
Load applied to member CD	238,000 lb.	Compression
Tension applied to member BD	580,000 lb.	Tension
Tension applied to member AF	43,300 lb.	Tension or Compression

Loads in member AE same as in member AF.

Resultant Moments on Member AF (or AE)

$$\text{Torsion Load} = \tfrac{1}{2} \ (36,700 \text{ lb}) (3 \text{ ft}) \ \left(\tfrac{8.2}{8.52}\right) \times \left(\tfrac{8.52}{9.41}\right) = 48,000 \text{ ft-lb.}$$

$$\text{Bending Moment} \begin{cases} = \tfrac{1}{2} (36,700) (3 \text{ ft}) \left(\tfrac{2.31}{8.52}\right) = 14,900 \text{ ft-lb in A-E-F Plane.} \\ = \tfrac{1}{2} (36,700) (3 \text{ ft}) \left(\tfrac{8.20}{8.52}\right)\left(\tfrac{4.00}{9.41}\right) = 22,500 \text{ ft-lb in} \perp \text{ Plane} \end{cases}$$

General Symbols

E = Elastic Modulus (= 10^7 psi for aluminum)

A = Cross sectional Area of Member (in^2)

I = Area Moment of Inertia of Member (in^4)

c = Distance from centroid to extreme fiber (in)

r = Radius of Gyration of Member (in)

P = Applied Force (lb)

M = Applied moment (in-lb)

T = Applied Torsion (in-lb)

f = Applied stress (psi)

F = Allowable stress (psi)

L = Length of member (in)

W = Weight of member (lb)

w = Specific weight of Aluminum $(0.101\ lb/in^3)$

Member in Simple Tension

Member BD

P = 580,000#

L = 124 in.

For 9" dia tube with (3/8)" wall

A = 10.16 in^2

Tensile Stress

$$f = \frac{P}{A} = 57,000 \text{ psi} \quad < F$$

Therefore, above tube is satisfactory

W - wAL = 127 lb.

Member in Simple Compression

Member BC

$P = 587,000$ lb.

$L = 102.2$ in.

For 8 inch diam tube with (1/2)" wall

$A = 11.78$ in^2

$r = 2.66$ in.

$f = P/A = 50,000$ psi. $< F = 60,000$ psi

Critical P for Buckling $= P_{cr}$

$$P_{cr} = A \cdot E \cdot (\frac{r}{L})^2 = 785,000 \text{ lb} > P$$

Therefore, above tube is satisfactory

$W = wAL = 121$ lb.

Member CD

$P = 238,000$ lb

$L = 72''$

For 6" diam tube with $(\frac{1}{4})$" wall

$A = 4.52$ in^2

$r = 2.03$ in.

$f = 52,600$ psi $< F$

$P_{cr} = 356,000$ psi $> P$

Therefore, above tube is satisfactory

$W = 32.9$ lb

Member with Axial and Transverse Loads

Member AB

Maximum $M = (73,400 \text{ lb}) \times (36 \text{ in})$

Maximum $M = 2.26 \times 10^6$ in-lb.

For 9" square tube with (3/4)" wall:

$I = 282$ in^4

$A = 24.8$ in^2

Maximum $f = \dfrac{P}{A} + \dfrac{Mc}{I}$

Maximum $f = 57,800$ psi F

Therefore, above tube is satisfactory

$W = wAL = 180$ lb (72" length AB, only)

Member with Compression, Torsion and Bending Loads

Member AF

$L = 113$ in

Design Criteria per MIL-HDBK-5 Section 2.53

$$\frac{f_c}{\bar{F}_c} + \sqrt{\left(\frac{f_b}{F_b}\right)^2 + \left(\frac{f_s}{F_s}\right)^2} \leqq 1$$

where subscripts c, b, and s denote stresses due to compression, bending and shear, respectively.

For 7" diam.tube with (3/8)" wall

I (area) $= 43.0$ in^4

I (polar) $= 95.9$ in^4

$A = 7.8$ in^2

397,000 lb
A 36,600 lb
72"
30,300 lb
B
110,000 lb
36"
73,400 lb
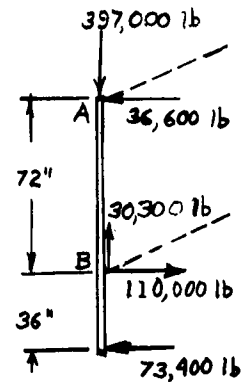
Compression Stress (Axial Load = 43,300 lb)

$$f_c = \frac{P}{A} = 5,500 \text{ psi}$$

Bending Stress

$$M_{max} = \sqrt{(14.9)^2 + (22.5)^2} \times 10^3 \text{ ft-lb} - 32,400 \text{ ft-lb}$$

$$f_b = \frac{M_{max} \cdot c}{I \text{ (area)}} = 32,700 \text{ psi}$$

Shear Stress (due to torsion load)

$$f_s = \frac{Tc}{I \text{ (polar)}} = 21,000 \text{ psi}$$

Checking design criteria

$$\frac{f_c}{F_c} + \sqrt{(\frac{f_b}{F_b})^2 + (\frac{f_s}{F_s})^2} = \frac{5.5}{60} + \sqrt{(\frac{32.7}{60})^2 + (\frac{21}{36})^2} = 0.875 < 1$$

Therefore, above tube is satisfactory

$$W = wAL = 89.0 \text{ lb.}$$

APPENDIX XV

FUEL REQUIREMENTS FOR LUNAR LAUNCH

Problem: Determine the ratio of fuel mass to capsule mass necessary to accelerate a capsule from the lunar surface to a velocity at the end of the propulsion phase sufficient for escape of the capsule from the lunar field of gravity. Assume that the thrust and fuel consumption rates are constant during the propulsion phase and that the change in lunar gravity during that phase is negligible. The thrust value shall be equal to the maximum value allowable for the capsule.

Symbols (with typical units):

r = radius distance from center of moon (ft.) * +

v = rate of change of r (ft./sec.)   *

t = time elapsed from launch ignition (sec.) *

g = acceleration due to gravity at earth = 32. 2 ft. /sec^2

A = ratio of maximum capsule acceleration to gravity at earth surface

m_c = capsule mass (lb. -sec^2/ft.)

m_f = mass of fuel at launch ignition (lb. -sec^2/ft.)

$m = m_c + m_f$ = total vehicle mass at launch ignition (lb. -sec^2/ft.)

$F = m_f/m_c$ = ratio of fuel mass to capsule mass

$q = m_f/t_b$ = fuel consumption rate (lb. -sec^2/ft. -sec.)

$T = m_c A_g$ = Thrust (lb.)

$I = Tt_b/m_f g$ = Specific Impulse of fuel (lb. -sec. /lb.)

γ = ratio of gravity at lunar surface of gravity at earth surface

* Subscript "b" denotes status at end of propulsion phase (burnout)

\+ Subscript "s" denotes condition at lunar surface

Mass at any instance during propulsion phase $= (m - qt)$

$(m - qt)\, dv/dt = T - (m-qt)\, \gamma g$

$$dv = \int_o^t \left[\frac{T}{m-qt} - \gamma g \right] dt$$

$$v = - \left(\frac{T}{q}\right) \times \ln\left(1 - \frac{q}{m} t\right) - \gamma g\, t$$

$$r - r_s = \int_o^t v\, dt$$

$$r = \left(\frac{Tm}{q^2}\right) \left\{ \left(1 - \frac{q}{m} t\right) \left[\ln\left(1 - \frac{q}{m} t\right) - 1 \right] + 1 \right\} - \gamma g \frac{t^2}{2} + r_s$$

$$q = \frac{mf}{t_b} = \frac{T}{tb} = \frac{T}{Ig} = \frac{mcA}{I}$$

$$t_b = FI/A$$

$$\frac{T}{q} = Ig$$

$$\frac{Tm}{q^2} = \left(\frac{T}{q}\right)\left(\frac{m}{q}\right) = \frac{Ig\, m}{m_c A/I} = \frac{I^2 g}{A}\ (I + F)$$

At Burnout:

$t = t_b$

$$\left(1 - \frac{q}{m} t\right) = \left(1 - \frac{mf}{m}\right) = \frac{mc}{mc+mf} = \frac{1}{1 + F}$$

$$V_b = -I g \cdot \ln\left[\frac{1}{1 + F}\right] - Ig\, \frac{F\gamma}{A}$$

$$V_b = Ig \left[\ln(1+F) - \frac{\gamma}{A} F \right]$$

$$r_b = \frac{I^2 g}{A} (1+F) \left\{ \frac{1}{1+F}\left[\ln\left(\frac{1}{1+F}\right) - 1 \right] + 1 \right\} - \frac{\gamma g}{2} \frac{F^2 I^2}{A^2} + r_s$$

$$r_b = \frac{I^2 g}{2 A} \left\{ 2 A \left[F - \ln(1+F) \right] - \gamma F^2 + \frac{2A^2}{g I^2} r_s \right\}$$

The energy available for lunar escape at burnout is equal to the kinetic energy of the capsule at burnout velocity and the amount of energy required is equal to the integral of the mutual attractive force with respect to the distance traveled integrated over the range from burnout radius to infinity.

$$\frac{1}{2} M_c V_b^2 = \int_{r_b}^{\infty} \left[\frac{\gamma_g\, r\, s^2\, m_c}{r^2} \right] \, dr$$

$$V_b^2 = \frac{2\, \gamma_g\, r s^2}{r_b}$$

Substituting for r_b

$$V_b^2 = \frac{(2A^2)\ 2\,\gamma_g\ r s^2}{I^2 g\ \left\{ 2A \left[F - 1n\ (1+F) \right] - \gamma F^2 + \frac{2A^2}{gI^2}\ r_s \right\}}$$

$$(V_b)_1 = \left(\frac{2A\, r_s}{I}\right) \Big/ \sqrt{\left(\frac{2M}{\gamma}\right) \left[F - 1n\ (1+F) \right] - F^2 + \frac{2}{\gamma_g}\ \left(\frac{A}{I}\right)^2 r_s}$$

$$(V_b)_2 = Ig \left[1n(1+F) - \frac{\gamma}{A}\ F \right]$$

A valid solution for F is one which provides equal values of $(V_b)_1$ and $(V_b)_2$. The transcendental nature of the expressions indicates iterative solution procedures.

For Lunar Surface $\qquad\qquad \gamma = 0.165$
$\qquad\qquad\qquad\qquad\qquad r_s = 1080$ miles

Some calculated values for representative A and I values are given below (200 sec is a low specific impulse value, taken low to compensate for engine weight):

I (sec)	A	F	V_b (fps)	t_b (sec)
200	40	2.23	7490	11.2
200	20	2.26	7480	23
200	10	2.29	7420	46
250	10	1.58	7410	40
300	10	1.19	7390	36

BALLAST REQUIREMENT FOR DROP TESTS
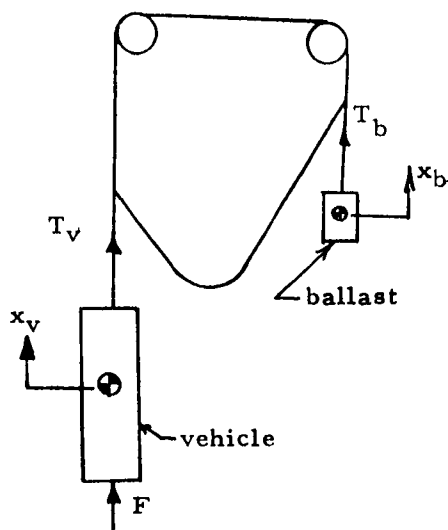
m_c = Chain and cable mass (lb. $-\sec^2$/ft.)

m_v = Model vehicle mass (lb. $-\sec^2$/ft.)

m_b = ballast mass (lb. $-\sec^2$/ft.)

s = scale factor $\left(\dfrac{\text{model length}}{\text{real length}}\right)$

U = weight unbalance (lb.)

a = acceleration (ft. /$\sec^2$)

g = earth gravity = 32. 2 ft. /$\sec^2$

Eqs. of motion:

$$F + T_v - m_v g = m_v \ddot{x}_v = - m_v a$$

$$T_b - m_b g = m_b \ddot{x}_b = m_b a$$

$$T_v - T_b = m_c \ddot{x}_b = m_c a$$

$$F = m_v (g-a) - T_v = m_v (g-a) - T_b$$

$$F = m_v (g-a) - m_c a - m_b (g + a)$$

$$F = (m_v - m_b) g - (m_v + m_b + m_c) a$$

@ $F = 0$; $a = a_o$

$$m_b = m_v \left(\frac{g - a_o}{g + a_o}\right) - m_c \left(\frac{a_o}{g + a_o}\right)$$

$$m_v - m_b = m_v \left(1 - \frac{g - a_o}{g + a_o}\right) + m_c \left(\frac{a_o}{g + a_o}\right) = \left(\frac{a_o}{g + a_o}\right) \cdot (2 m_v + m_c)$$

$$m_b = \left\{ m_v \left[(g + a_o) - 2 a_o\right] - m_c a_o \right\} / (g + a_o)$$

110

$$m_b = m_v \left(\frac{g - a_0}{g + a_0}\right) \ -m_c \left(\frac{a_0}{g + a_0}\right)$$

@. $a_0 = \gamma_s g$

$$m_b = m_v \left(\frac{1 - \gamma_s}{1 + \gamma_s}\right) \ - m_c \left(\frac{\gamma_s}{1 + \gamma_s}\right)$$

$$m_b = m_v \left(\frac{1}{1 + \gamma_s}\right) \ - (m_v + m_c) \left(\frac{\gamma_s}{1 + \gamma_s}\right)$$

$$m_b + m_b \gamma_s = m_v - (m_v + m_c) \gamma_s$$

$$U = (m_v - m_b) g = (m_v + m_c + m_b) \gamma_s g$$

$$m_v + m_c + m_b = m_v \left[\left(\frac{1 - \gamma_s}{1 + \gamma_s}\right) + \left(\frac{1 + s}{1 + s}\right) \right] + m_c \left[\left(\frac{1 + s}{1 + s}\right) - \left(\frac{s}{1 + s}\right) \right]$$

$$m_v + m_c + m_b = (2 m_v + m_c)/ (1 + \gamma_s)$$

$$U = (2 m_v + m_c) g \left(\frac{\gamma_s}{1 + \gamma_s}\right)$$

APPENDIX XVII

EVALUATION OF UPSET TESTS

Problem: Establish appropriate energy balance relationships to evaluate correlation between observed test data and analytical, system performance prediction methods.

Assuming that upsetting motion commences <u>after</u> the vertical impact motion has been arrested, the total energy of the system is the kinetic energy associated with the horizontal motion of the test mass relative to the alightment platform. During an alightment action which just produces an incipient upset status, all this energy will be transferred to increase the potential energy of the test apparatus or will be consumed in system friction. There are two ways in which the system potential energy can vary in an alightment action. The potential energy level can increase due to the lift of the vehicle c.g. associated with upsetting motion, operating against the test unbalance. The potential energy level can decrease (for a given vehicle elevation) due to the drop of the ballast which occurs as the suspension trolley moves along the slightly canted "trapeze" bar in the direction of alightment platform motion. During an upsetting motion, the support chain is driven a distance equal to the sum of the vehicle c.g. lift and the ballast drop. This motion, operating against the chain and pulley friction, consumes energy as does the horizontal motion of the trolley operating against the trolley bearing friction.

Let the appropriate physical quantities be indicated by the symbols indicated in the sketch or defined below:

E_h = Horizontal Kinetic Energy (in. -lb.)

E_L = Increase in system P.E. due to vehicle c.g. lift (in. -lb.)

E_b = <u>In</u>crease in system P.E. due to ballast drop (in. -lb.)

E_c = Friction energy consumed in driving chain and pulley (in. -lb.)

E_t = Friction energy consumed in driving trolley (in. -lb.)

X_L = Lift of vehicle c.g. (in.)

X_b = drop of ballast (in.)

X_t = horizontal trolley displacement (in.)

$\mathcal{M}_t$ = trolley friction coefficient

ψ = Angle of trapeze cant (radians)

V_h = horizontal alightment velocity (in./sec.)

W_v = weight of vehicle and attached mass subject to horizontal motion. (lb)

W_b = ballast weight (lb.)

U = vertical unbalance force (lb.)

F_c = chain and pulley friction force (lb.)

$X_L = l_u - l_o$

$l_o = r \quad + (h + \Delta h)(1 - \beta^2)$

$l_u = \sqrt{r^2 + \{h + \Delta h + r\,(\alpha - B)\}^2}$

The following relationships are applicable:

$E_h = E_L + E_b + E_c + E_t$

$E_L = U \cdot X_L$

$E_b = - W_b\, X_b$

$E_c = F_c\,(X_L + X_b)$

$E_t = \mathcal{M}_t W_b\, X_t$

$E_h = W_v\, V_h^2 / (2g)$

$X_b = \psi \cdot X_t$
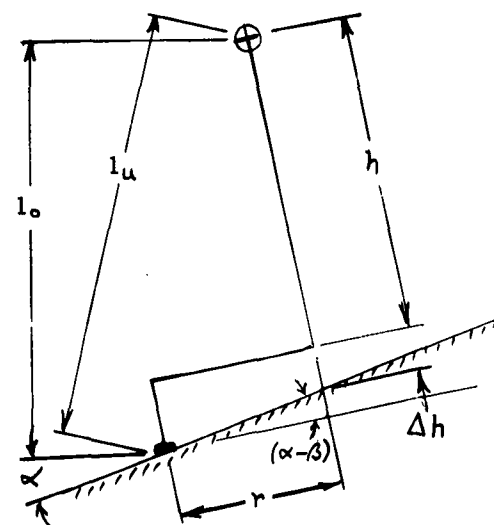
$$(U + F_c) \, X_L + (F_c - W_b) \, X_b + \mathcal{M}_t W_b \, X_t - W_v \, V_h^2/(2g) = 0$$

$$(U + F_c) \, X_L + \left[\psi F_c + (\mathcal{M}_t - \psi) \, W_b \right] X_t - W_v \, V_h^2/(2g) = 0$$

@$\mathcal{M}_t = \psi/2$, what is X_t?

$$X_t = \frac{W_v \, V_h^2/(2g) - (U + F_c) \, X_L}{F_c - W_b \psi/2}$$

$$X_t = \frac{2 (U + F_c) \, X_L - W_v \, V_h^2/g}{\psi (W_b - 2 F_c)}$$

@ $r = 10.5$ in.

$h = 32.0$ in.

$\Delta h = 2.13$ in.

$\alpha = 6.2° = 0.109$

$\left. \right\}$ measured test values

$X_L = 1.08" \ @ \ B = 3°$

$X_L = 1.22" \ @ \ B = 2°$

$X_L = 1.53" \ @ \ B = 0°$

@ $W_v = 31.5$ lb.

$W_b = 28.9$ lb.

$F_c = 10$ oz.

$U = 18$ oz.

$\psi = 1/48$

$V_h = 3.6$ in/sec

$\left. \right\}$ measured test values

$X_t = 6.1 \, X_L - 2.0$ in.

$X_t = 4.6" \ @ \ B = 3°$

$X_t = 5.4" \ @ \ B = 2°$

Inspection shows that if $\mathcal{M}_t$ were changed to zero, X_t would be halved.

114

APPENDIX XVIII

SKETCHES OF TEST APPARATUS

$\frac{1}{2}''$ Chain

24"

48"

Main Ballast

Secondary Ballast

Test Model
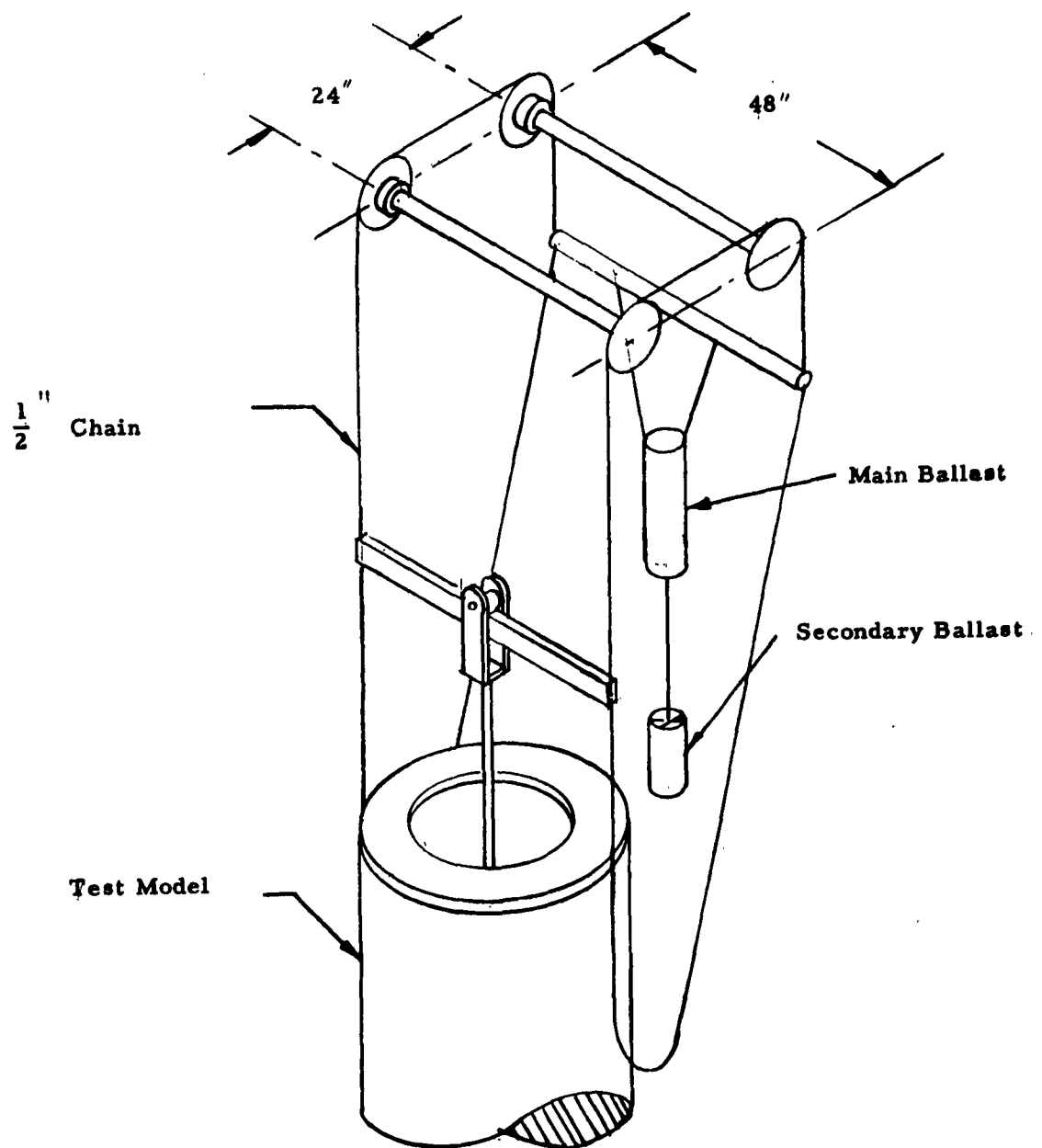
Figure 17 Test Vehicle Suspension Rig.

Half Round

$\frac{1}{4}$"

4' x 8'

Boston Gear
Ratiomotor
MB 5832S
$(\frac{1}{20}$ hp., 53.9 rpm. $)$

Drive Chain

2" x 4"

Scale 16:1

Figure 18 Alighment Platform

117
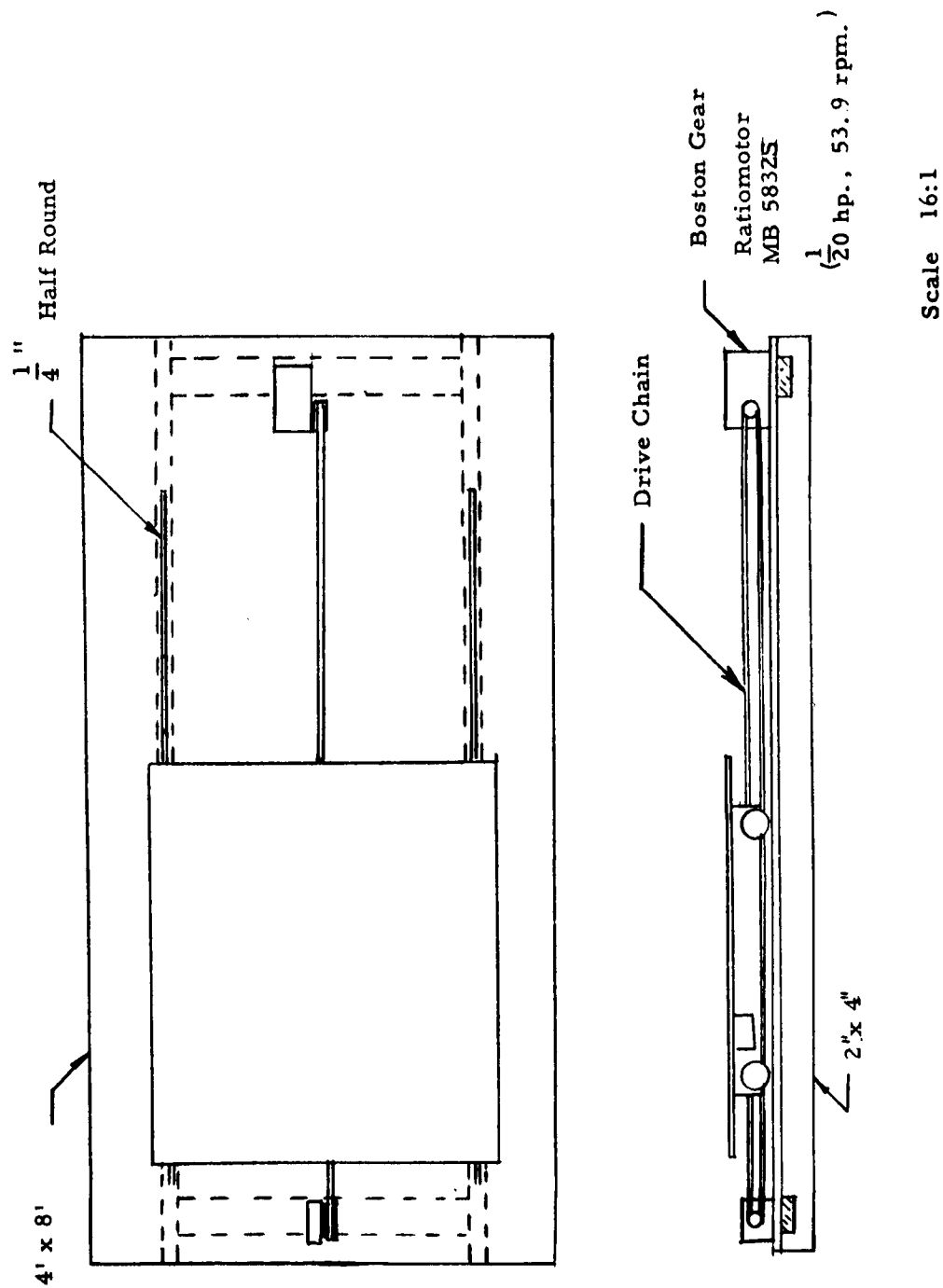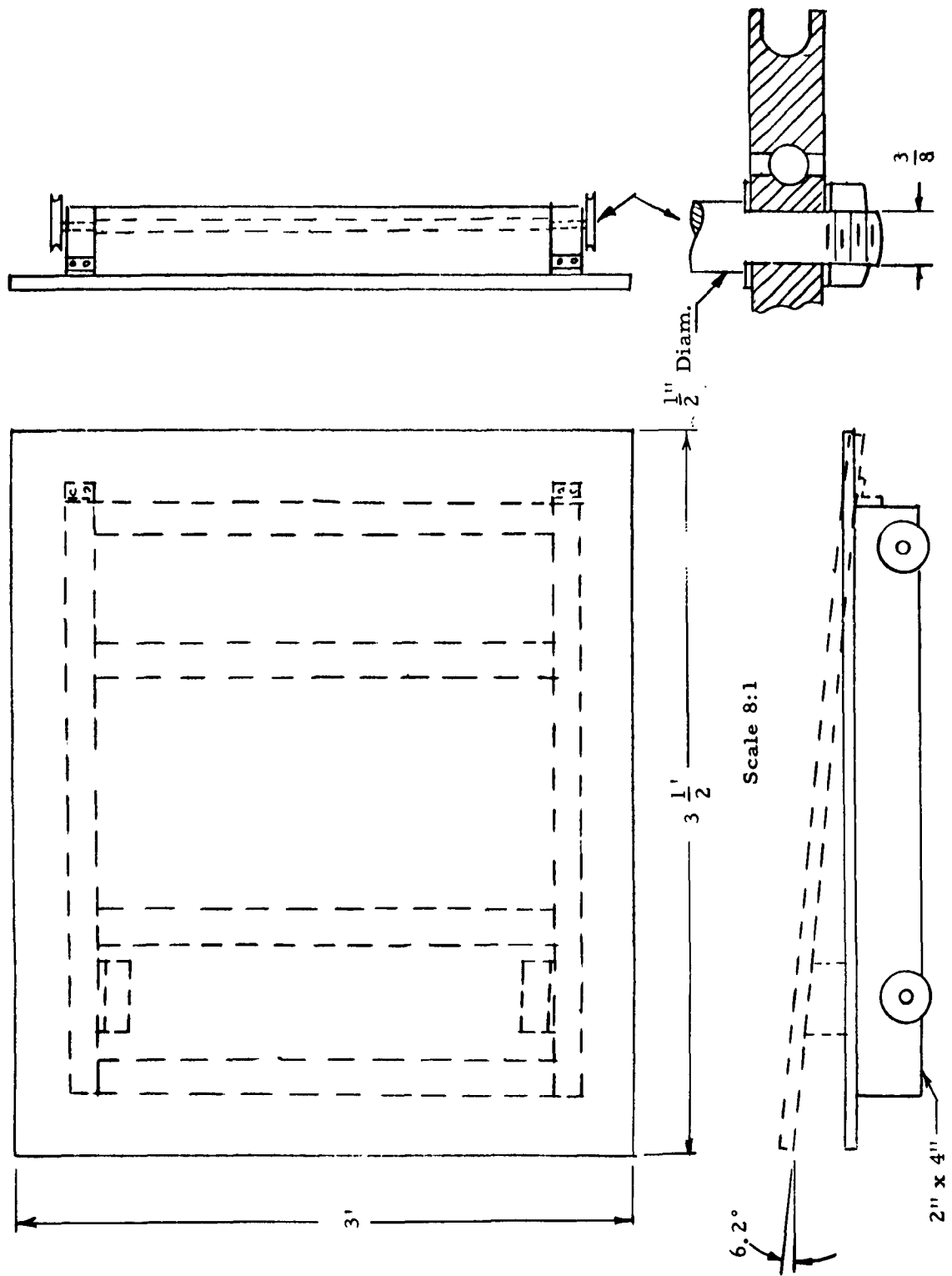
Figure 19, Horizontal Velocity Cart

3'

$3\frac{1}{2}'$

$1\frac{1}{2}''$ Diam.

$\frac{3}{8}$

Scale 8:1

6.2°

2" x 4"

118

Two Fiber Tubes
Approx 20" Diam
by 72" Total Length

Spherical Bushing

Three Thumb Nuts to
Provide Lateral Adjustment
of Spherical Bushing Position

Threaded to Provide Vertical
Adjustment of Spherical Bushing
Position

Four Alightment Strut Mechanisms
Equally Spaced.
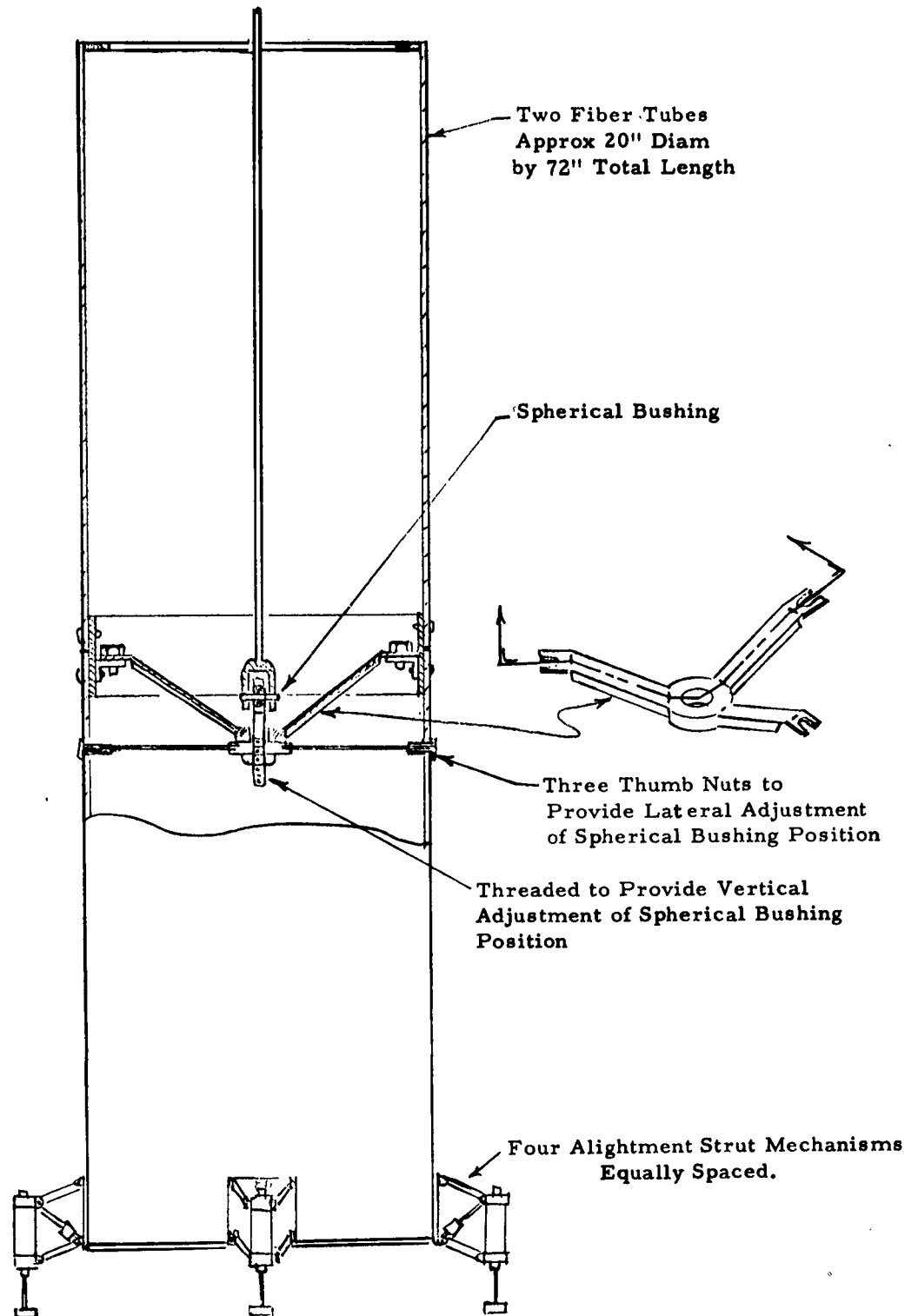
Figure 20   Test Vehicle

119
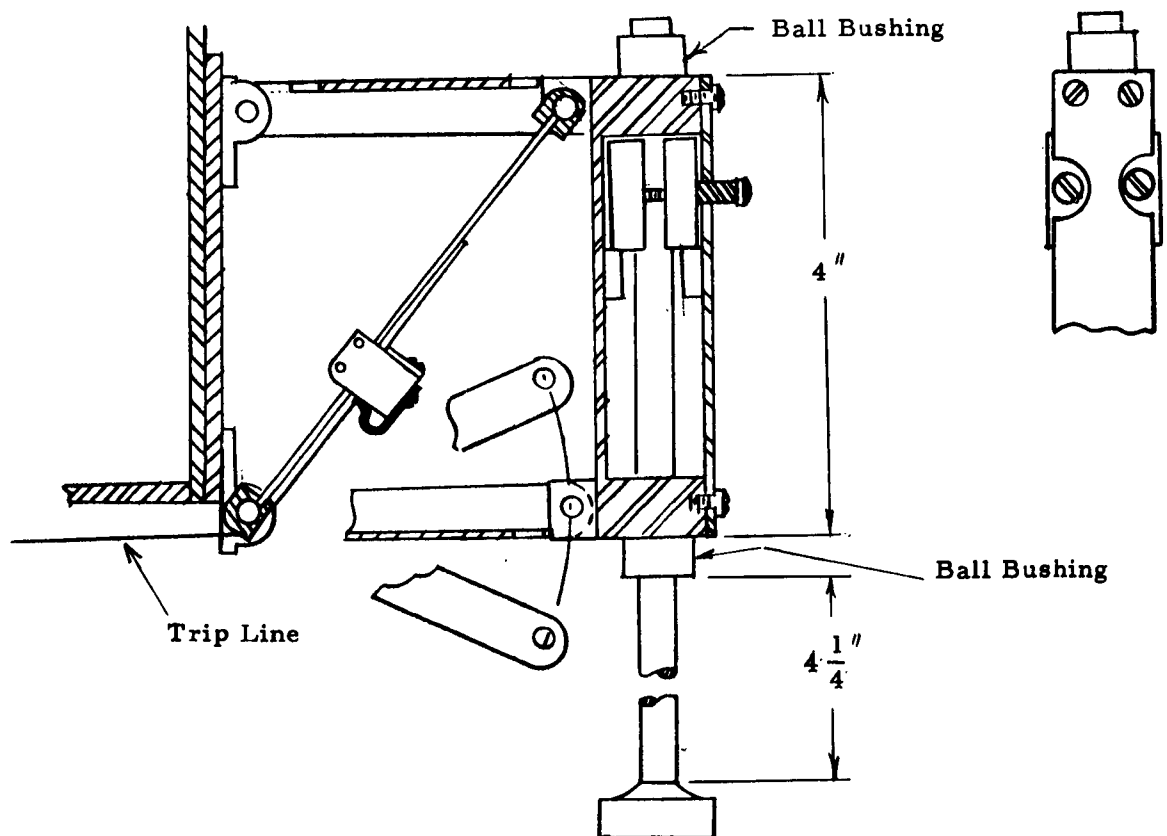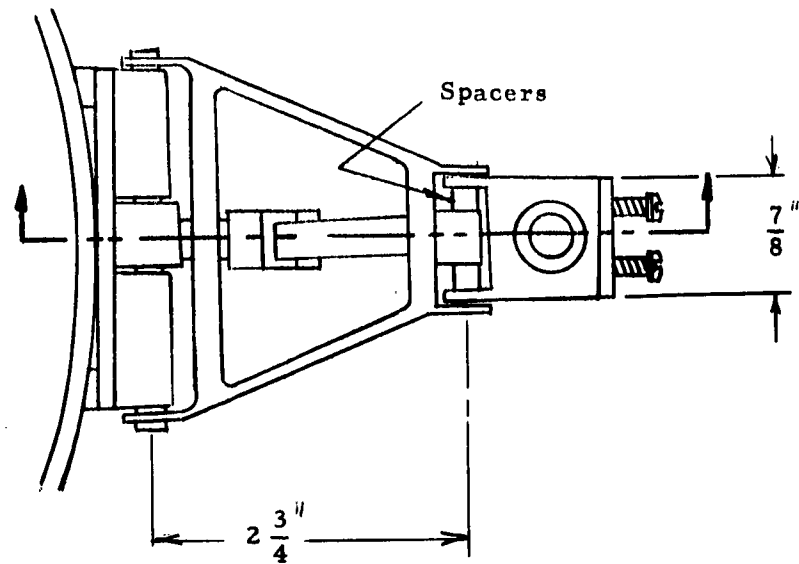
Figure 21 Alightment Strut and Mechanism

Isometric of
Principal Parts

Bonded
Connection

$\frac{7}{16}$" Nominal

"Flat"
Spring

$\frac{1}{16}$" Dowel
(Six places)

$\frac{1}{16}$"

$3\frac{3}{8}$" Nominal

Hole For Trip Line
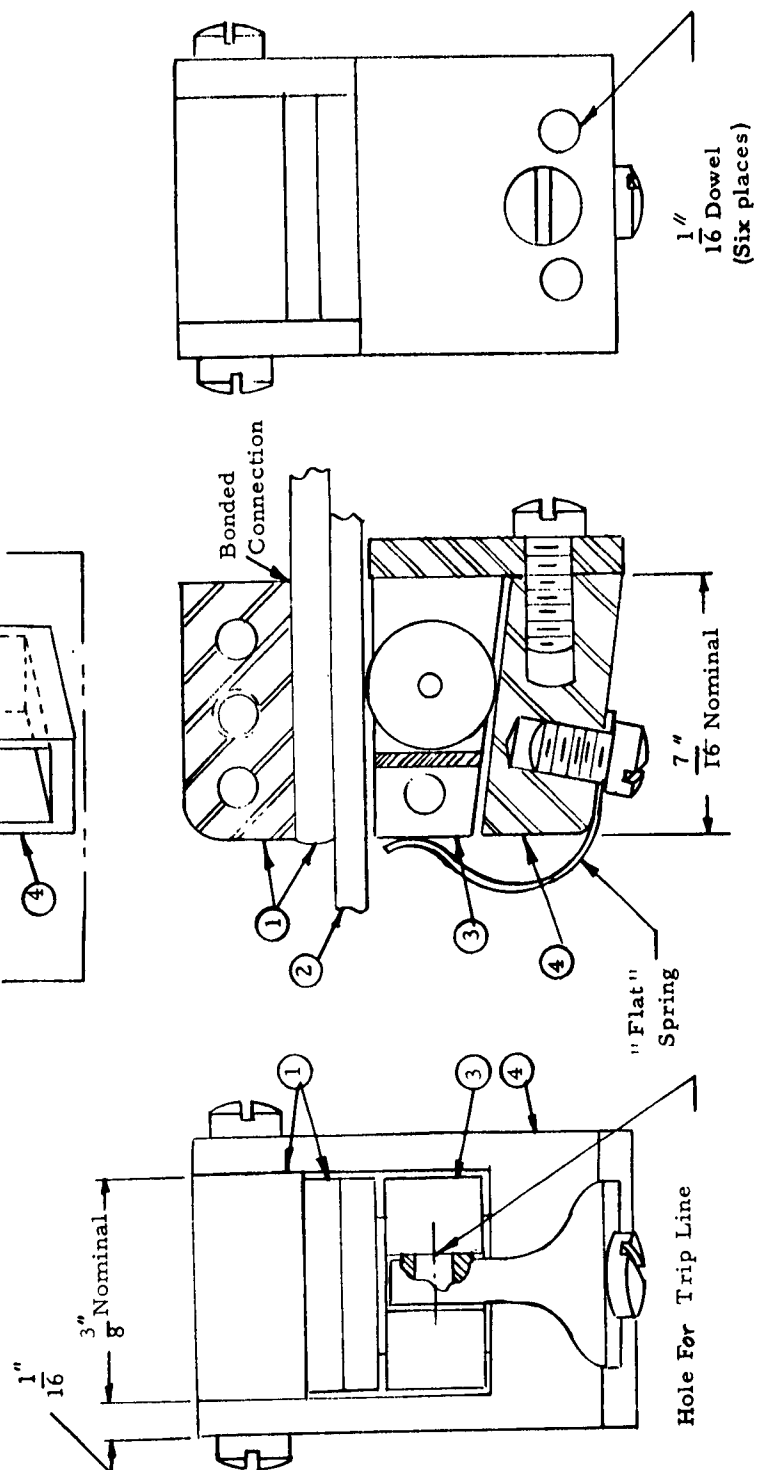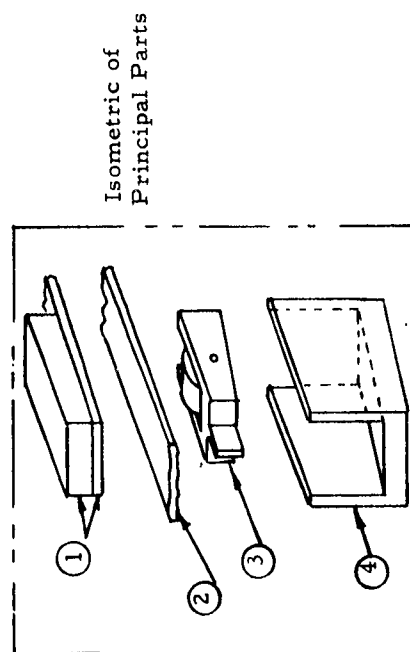
Figure 22 Self-Energizing Lock Assembly
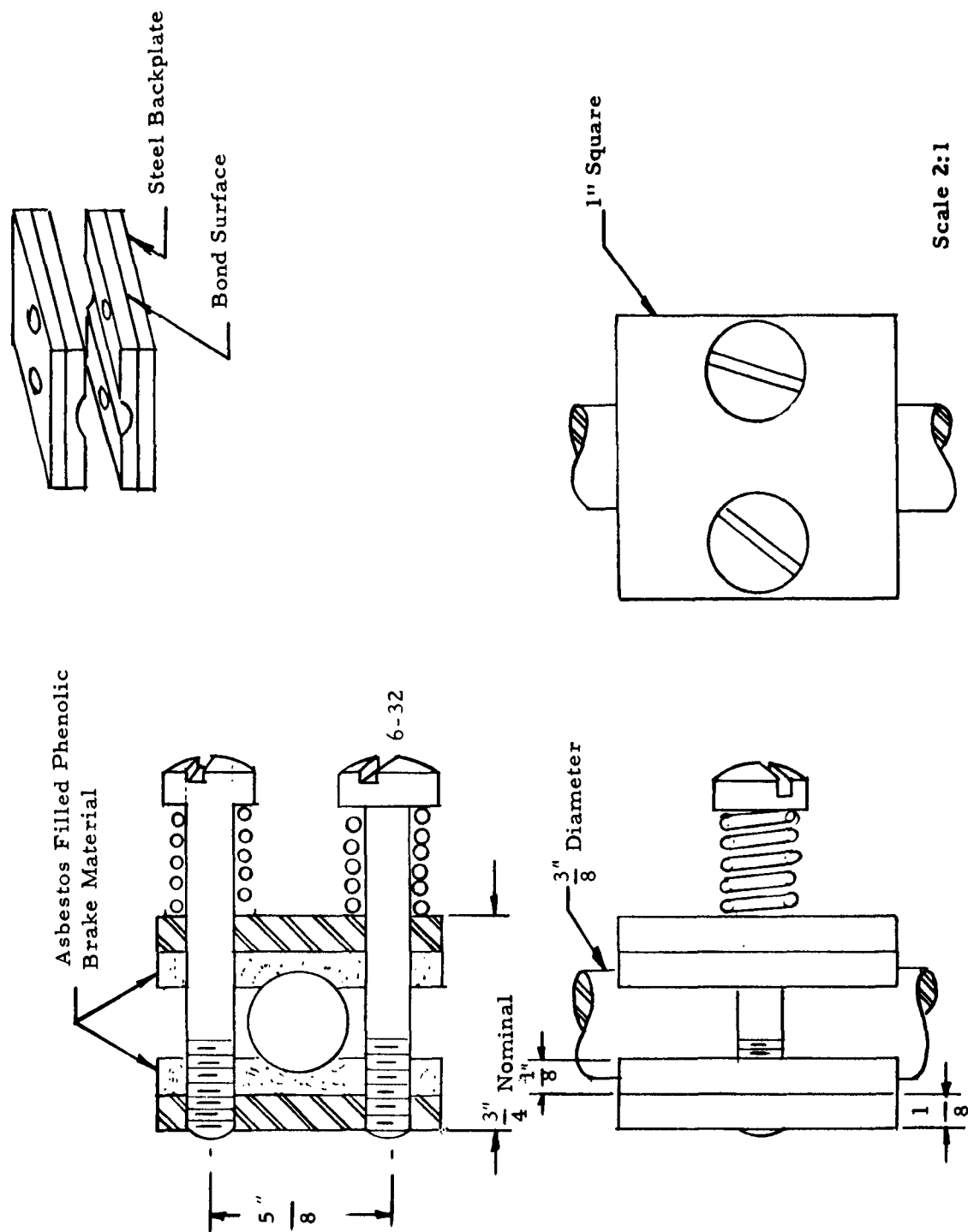
121

Figure 23 Energy Absorber

Scale 2:1

122

Figure 24. Strut Support Arm

123
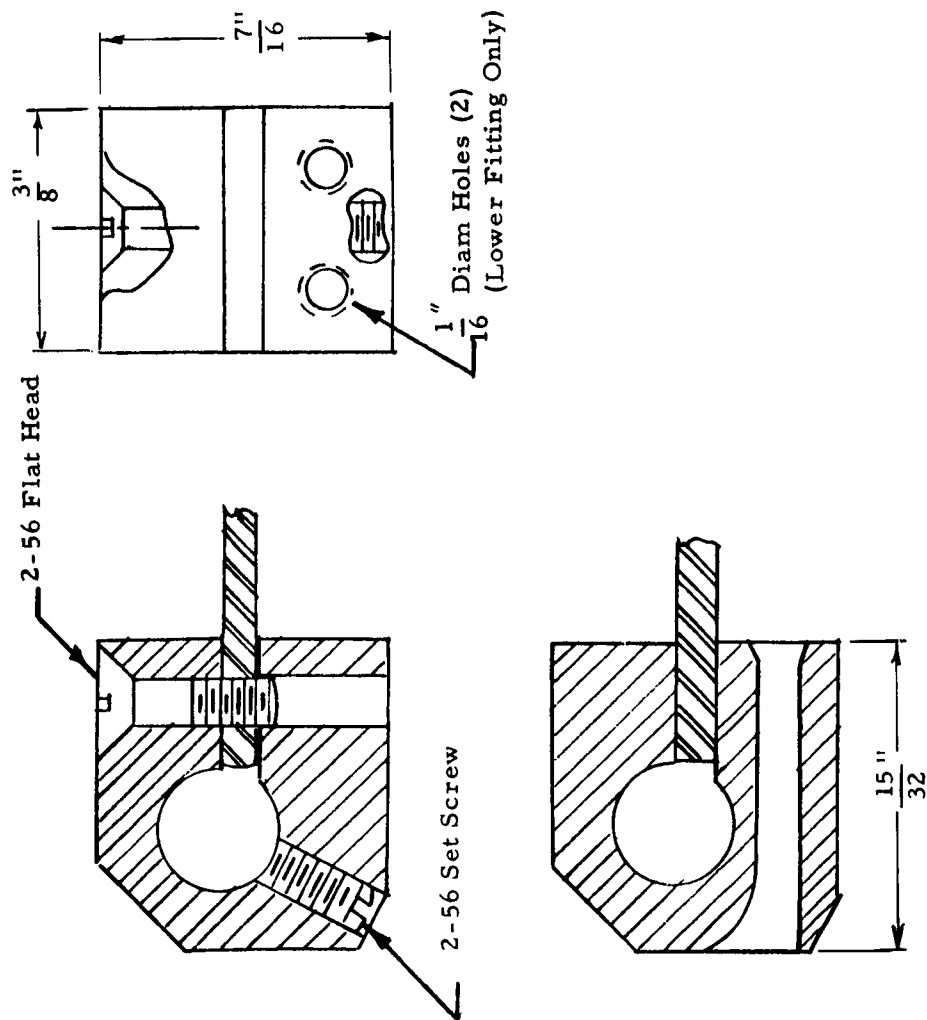
Figure 25 Diagonal End Fitting

7"/16

3"/8

1"/16 Diam Holes (2) (Lower Fitting Only)

2-56 Flat Head

2-56 Set Screw

15"/32

124

APPENDIX XIX

PHOTOGRAPHS OF TEST APPARTUS
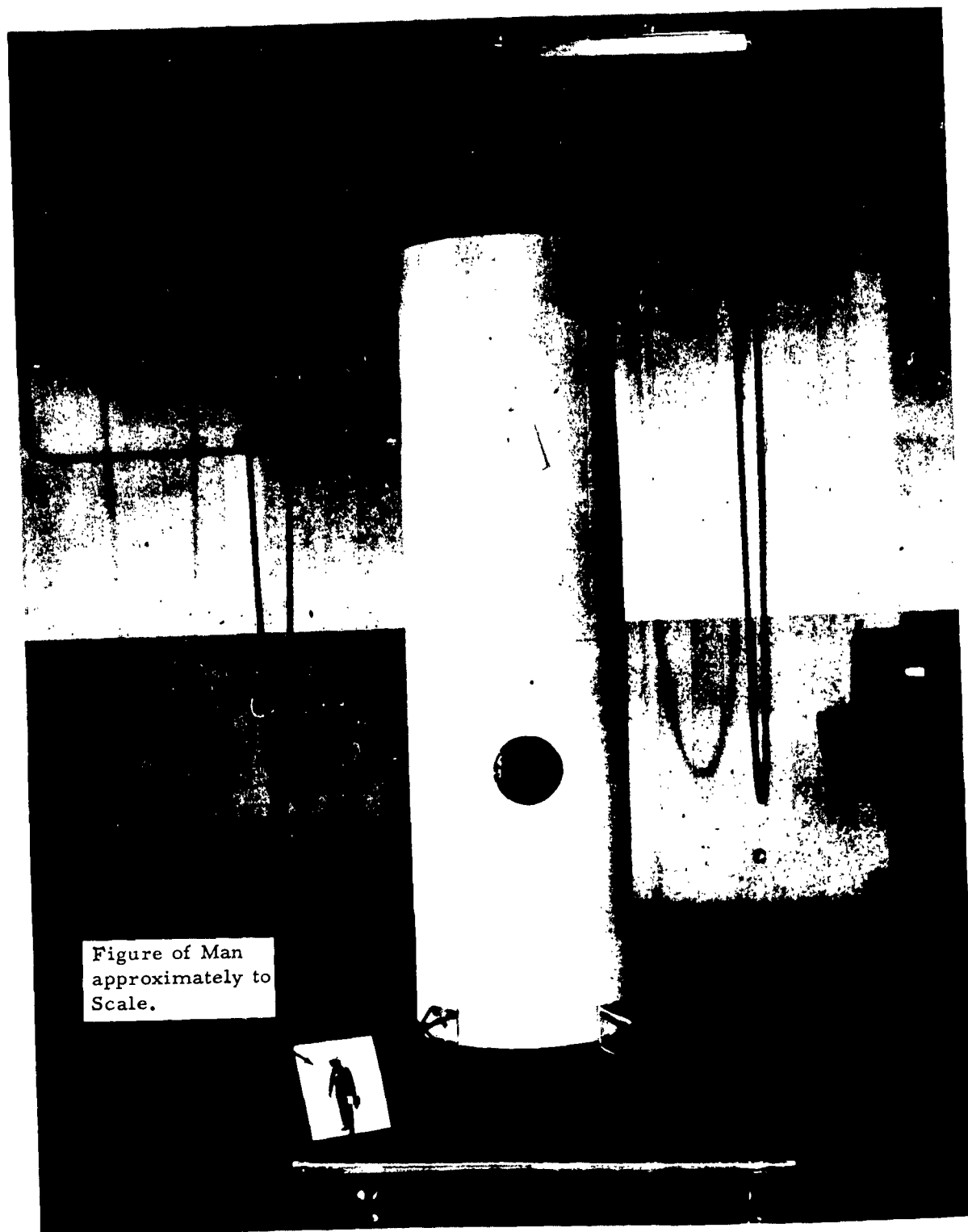
Figure of Man
approximately to
Scale.

Figure 26 Vehicle in Touchdown Status

Displacement Sensing Switch

Ballast Support Bar
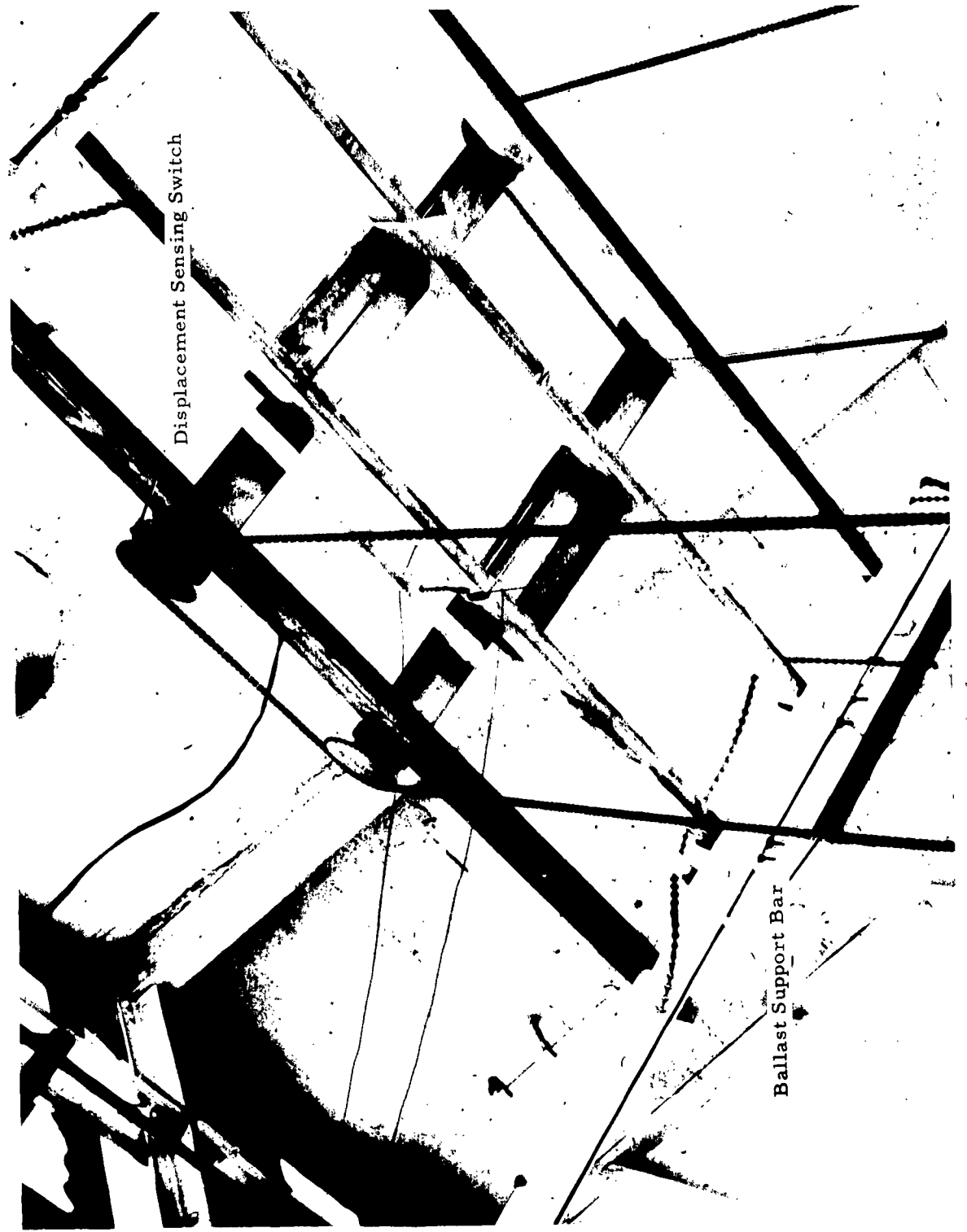
Figure 27   Pulley Suspension System
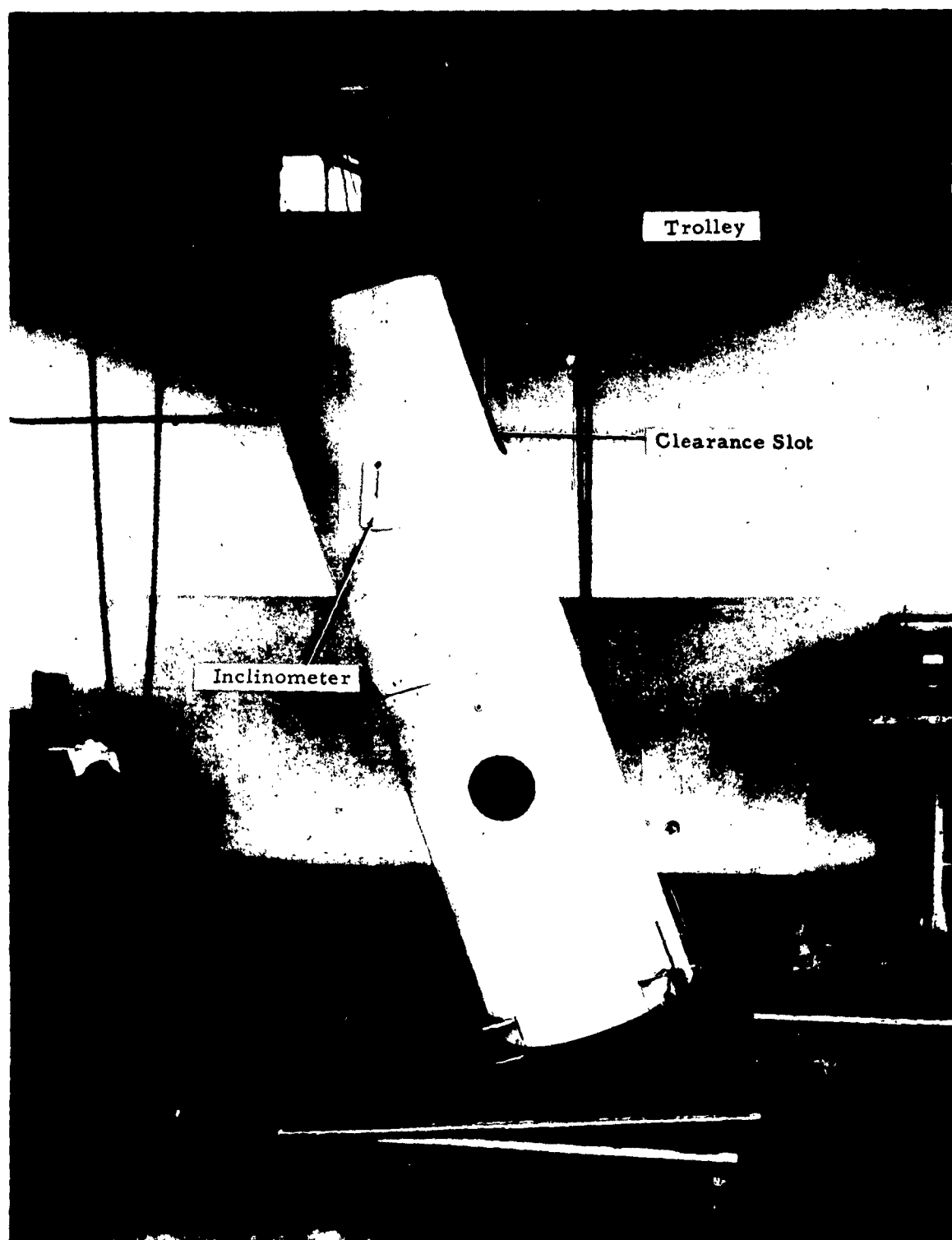
Figure 28.   Vehicle in Upset Position
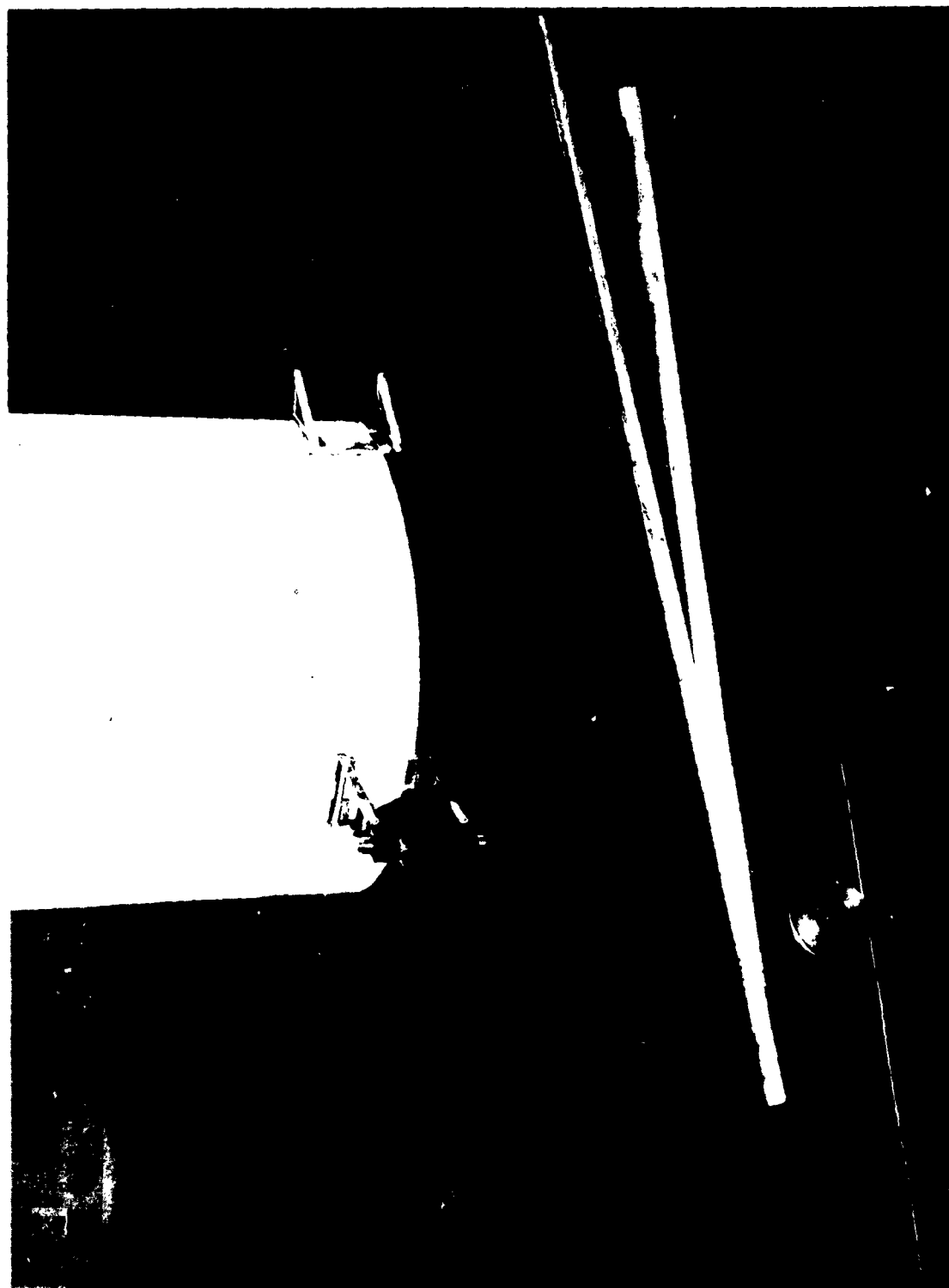
Figure 29. Alightment System in Actuated Position
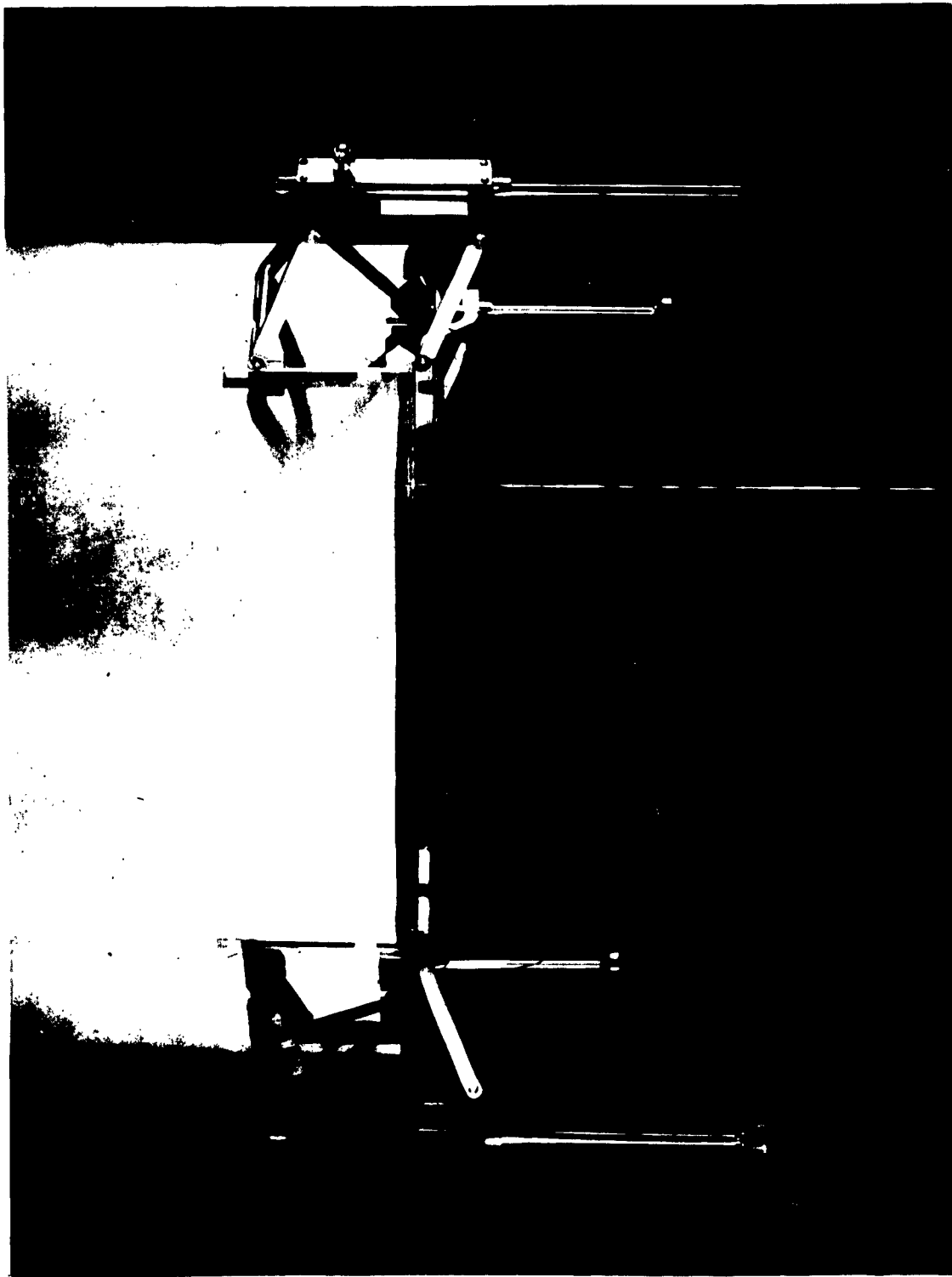
Figure 30. Pre-Touchdown Attitude of Alightment System

Ball Bushing

Self-Energizing
Lock Ass'y

Adjusting Screws

Stops

"A Frame" Support Arm

Ball Bushing

Actuating Rod

Surface Contactor
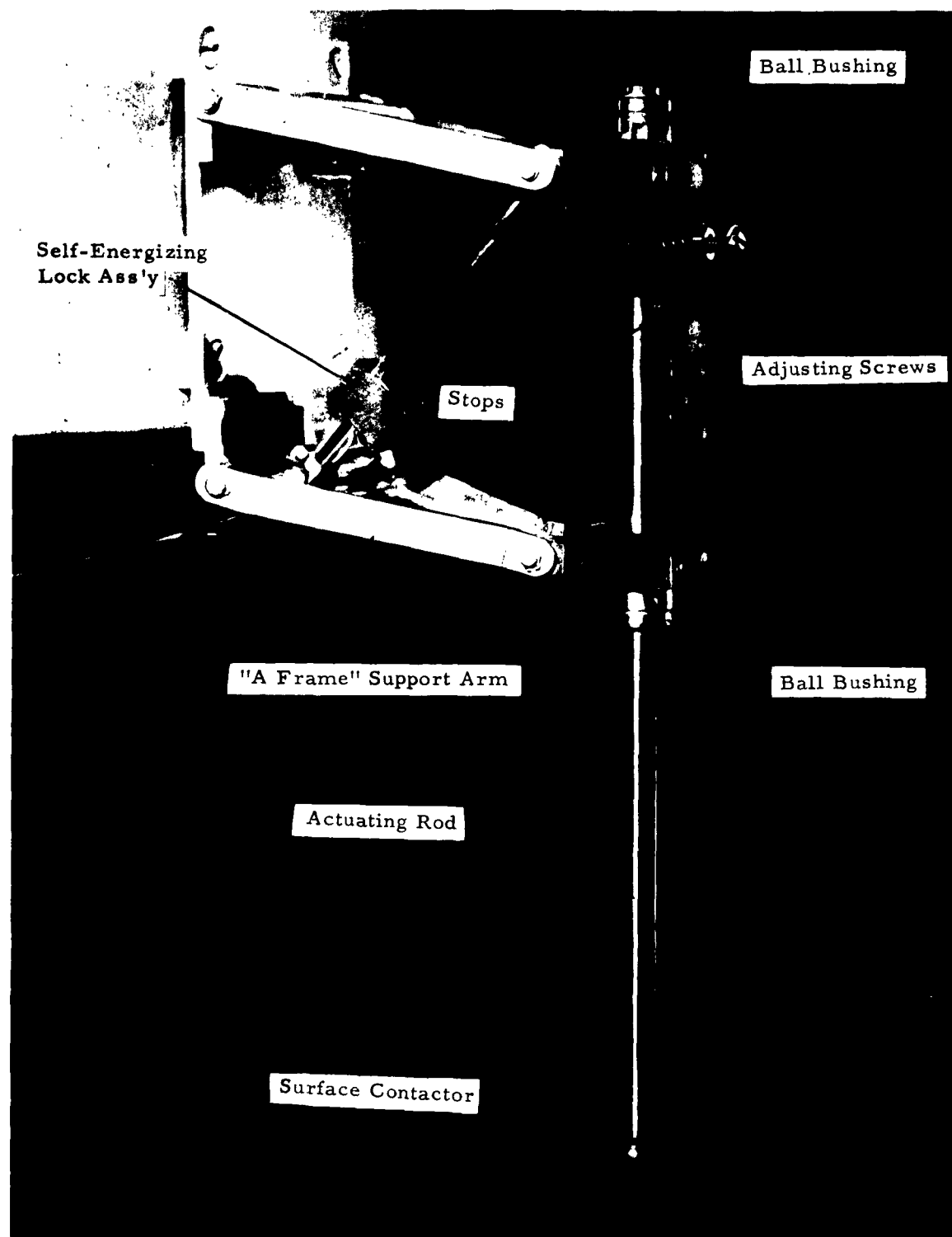
Figure 31. Alightment Strut
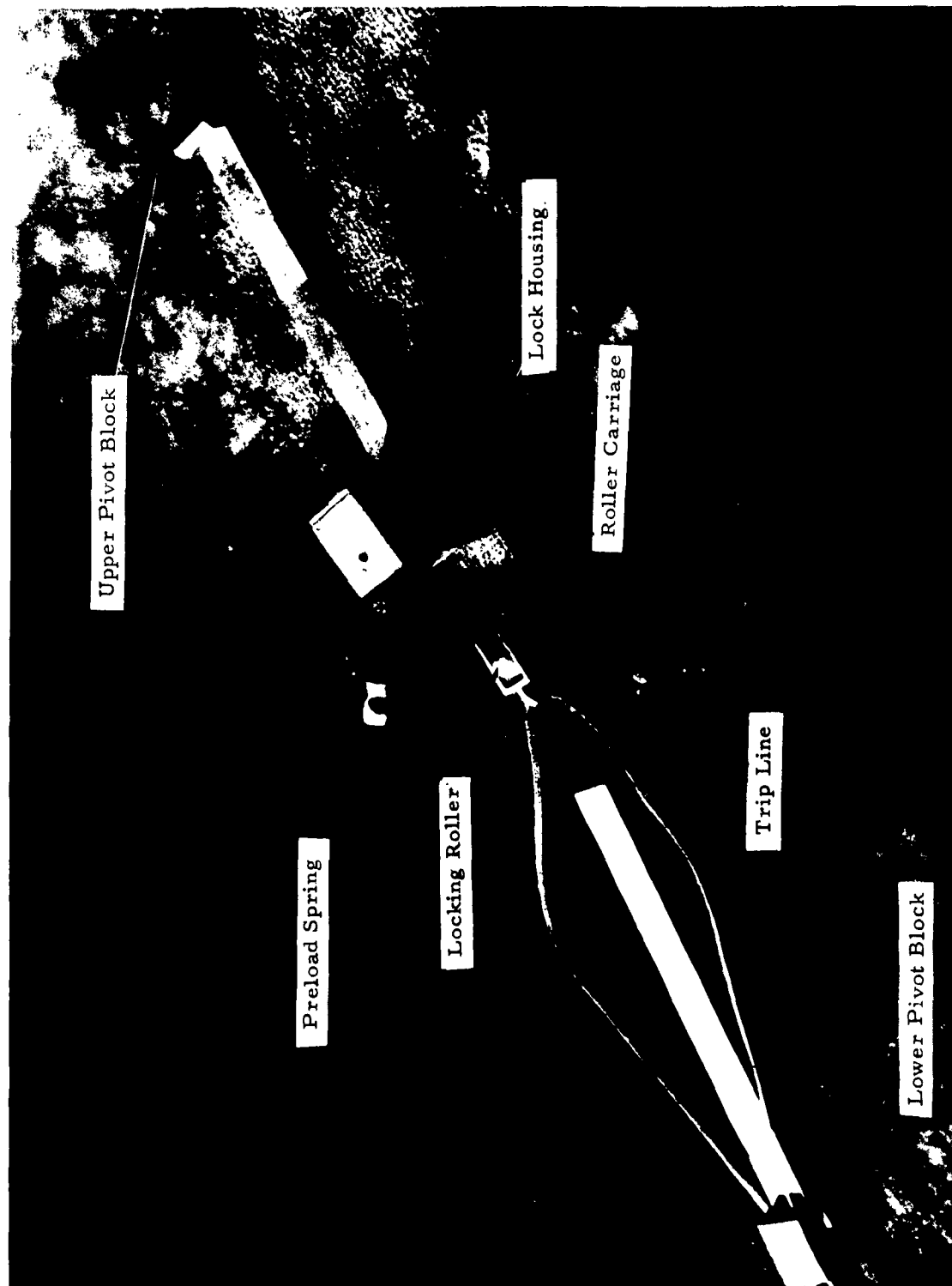
Figure 32 Self-Energizing Lock Disassembled
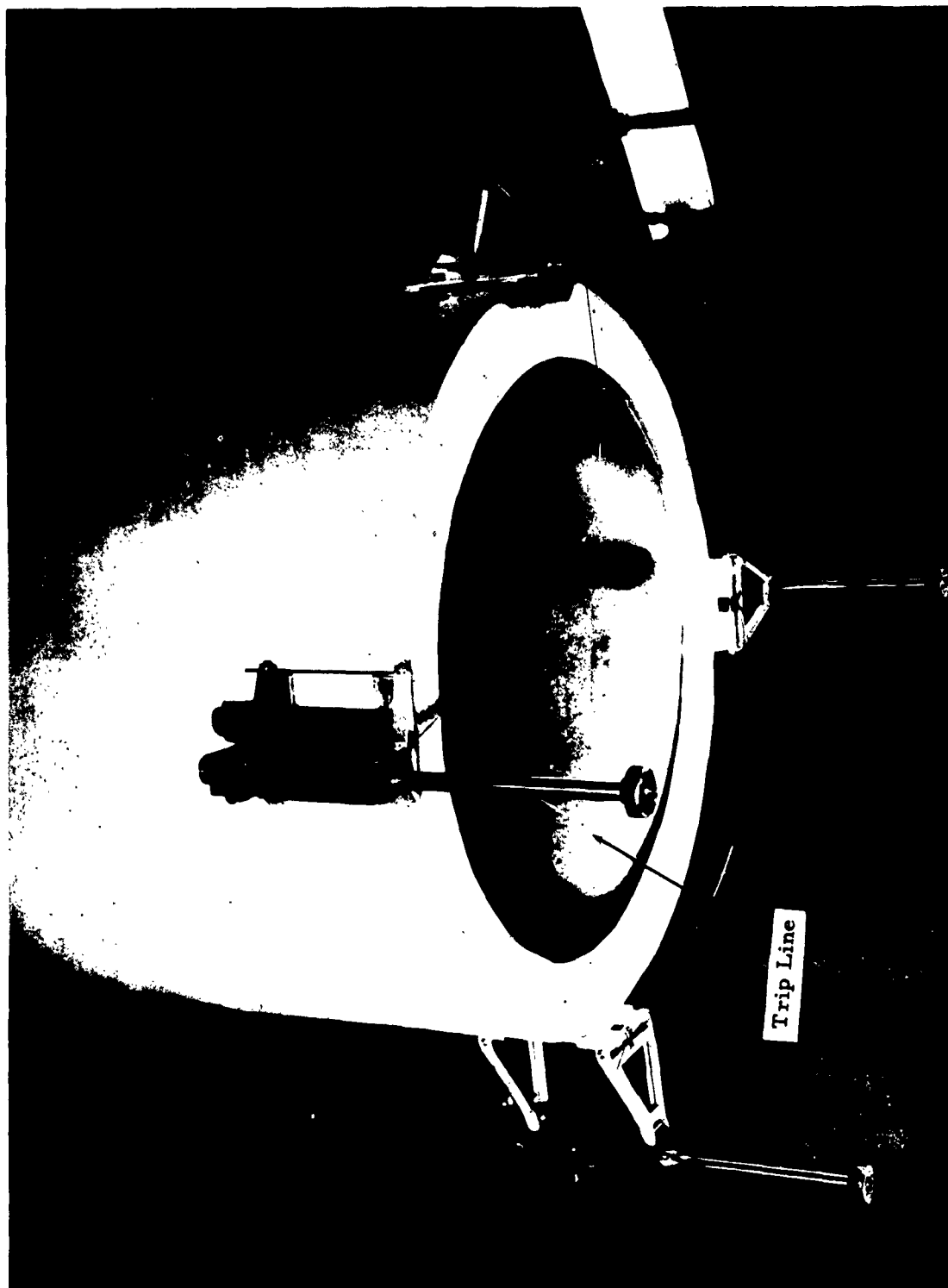
Figure 33 Lock Trip Line Arrangement (Slack Status)

Trip Line
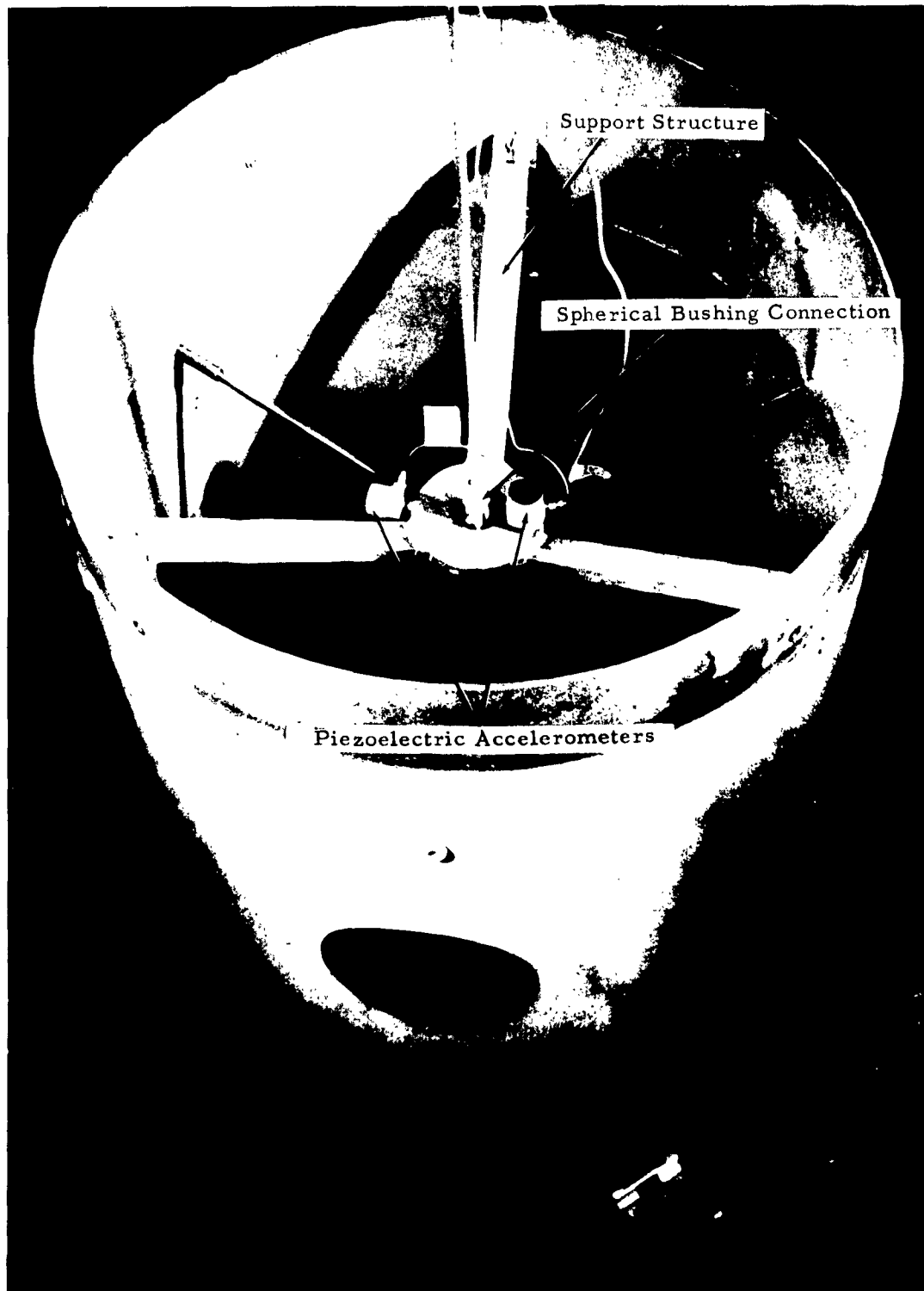
Figure 34   Vehicle Suspension Arrangement
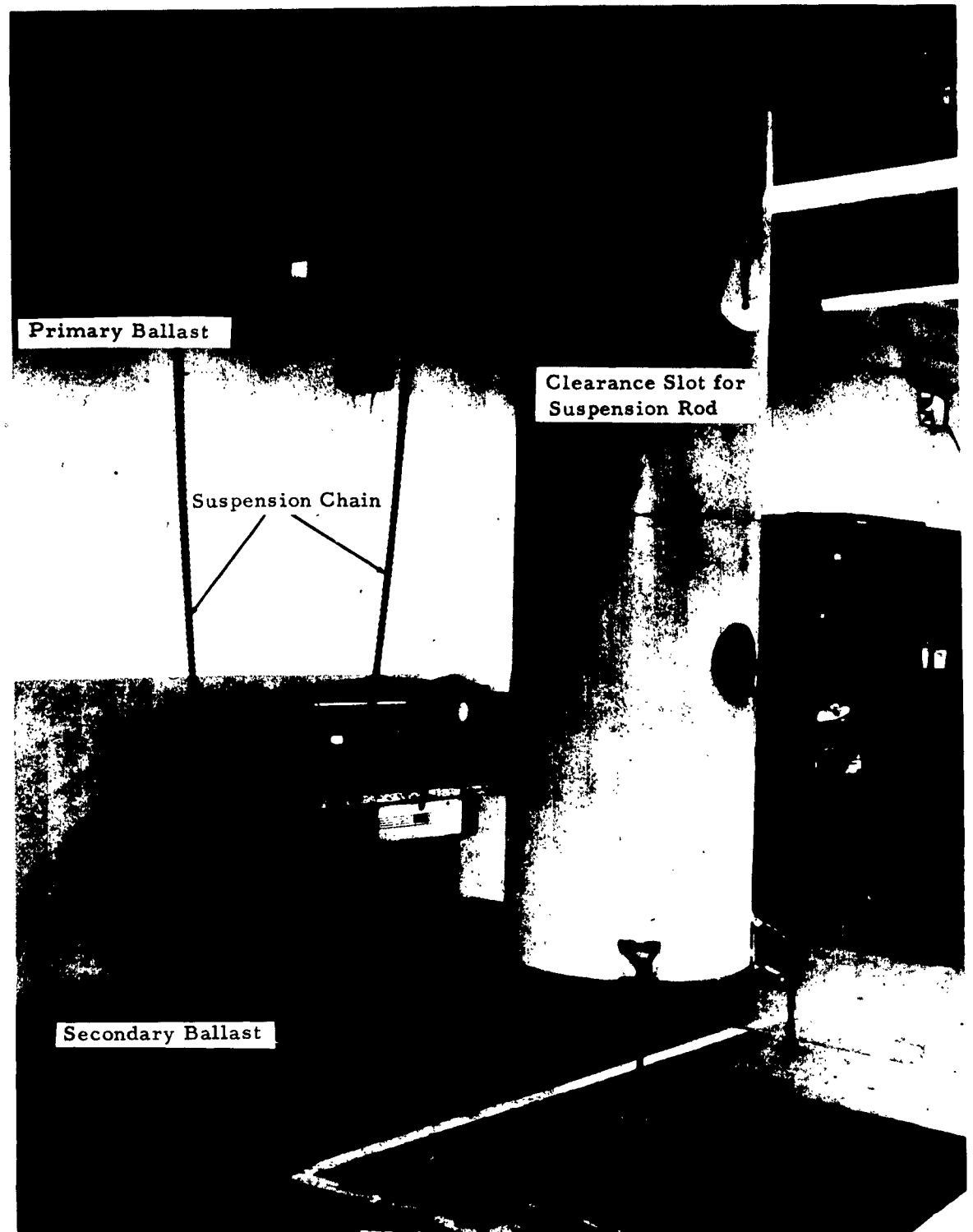
Figure 35   Vehicle During Drop Test

135

APPENDIX XX

TYPICAL ACCELEROMETER RECORDING

Figure 36   Accelerometer Recording – Run No. 3

Aeronautical Systems Division, Dir/Aeromechanics
Flight Dynamics Lab, Wright Patterson AFB, Ohio
Rpt. No. ASD-TDR-63-454, LUNAR ALIGHTMENT
SYSTEMS INVESTIGATION, Final Report, May 63,
150 Pg. incl. illus., tables refs.

UNCLASSIFIED Report

Mission parameters are estimated for manned
lunar alightment. Undercarriage concepts are
developed which provide for alightment on unpre-
pared lunar surfaces and provide the necessary
support for subsequent launch from the lunar sur-
face. A novel concept is described which places
steel honeycomb energy absorption elements at
the ends of four self-aligning strut mechanisms.

(over)

The self-aligning feature, which is applicable to
any number of surface contactors, results in an
alightment system whose bulk and weight are a small
fraction of the comparable quantities for systems
using fixed undercarriages. It has been found that
the incorporation of auxiliary launch engines in the
alightment system to utilize salvaged alightment
energy or chemical fuels offers no advantage. An-
alytical background material is reported and an ex-
perimental program which verified the feasibility
of the self-aligning feature is described.

Aeronautical Systems Division, Dir/Aeromechanics
Flight Dynamics Lab, Wright Patterson AFB, Ohio
Rpt. No. ASD-TDR-63-454, LUNAR ALIGHTMENT
SYSTEMS INVESTIGATION, Final Report, May 63,
150 Pg. incl. illus., tables refs.

UNCLASSIFIED Report

Mission parameters are estimated for manned
lunar alightment. Undercarriage concepts are
developed which provide for alightment on unpre-
pared lunar surfaces and provide the necessary
support for subsequent launch from the lunar sur-
face. A novel concept is described which places
steel honeycomb energy absorption elements at
the ends of four self-aligning strut mechanisms.

(over)

The self-aligning feature, which is applicable to
any number of surface contactors, results in an
alightment system whose bulk and weight are a small
fraction of the comparable quantities for systems
using fixed undercarriages. It has been found that
the incorporation of auxiliary launch engines in the
alightment system to utilize salvaged alightment
energy or chemical fuels offers no advantage. An-
alytical background material is reported and an ex-
perimental program which verified the feasibility
of the self-aligning feature is described.